รายงานวิจัยฉบับสมบูรณ์

โครงการ

การเลือกเกิดปฏิกิริยาออกซิเดชันของเอธิลีนบนฐานรองรับที่มีตัวเร่งปฏิกิริยาเป็นโลหะเงินและโลหะผสมเงิน-ทอง

(Selective Oxidation of Ethylene over Supported Ag and Bimetallic Au-Ag Catalysts)

โดย

นาย ศิริพงษ์ โรจน์ลือชัย

รศ.ดร. สุเมธ ชวเดช

Prof. Johannes W. Schwank

31 สิงหาคม 2545

สัญญาเลขที่ BGJ/9/2543

รายงานวิจัยฉบับสมบูรณ์

โครงการ

การเลือกเกิดปฏิกิริยาออกซิเดชันของเอธิลีนบนฐานรองรับที่มีตัวเร่งปฏิกิริยาเป็นโลหะเงินและโลหะผสมเงิน-ทอง

(Selective Oxidation of Ethylene over Supported Ag and Bimetallic Au-Ag Catalysts)

โดย

นาย ศิริพงษ์ โรจน์ลือชัย*

รศ.ดร. สุเมธ ชวเดช*

Prof. Johannes W. Schwank**

* วิทยาลัยปิโตรเลียมและปิโตรเคมี จุฬาลงกรณ์มหาวิทยาลัย

** Department of Chemical Engineering, The University of Michigan

สนับสนุนโดยสำนักงานกองทุนสนับสนุนการวิจัย

Abstract

Project Code : BGJ43-8-0009

Project Title : Selective Oxidation of Ethylene over Supported Ag and Bimetallic Au-Ag Catalysts

Investigator : Mr. Siriphong Roatluechai
The Petroleum and Petrochemical College, Chulalongkorn University

E-mail Address : siriphong@rocketmail.com

Project Period : 2 Years (1 September 2000 - 31 August 2002)

Silver-based catalyst is currently used for production of ethylene oxide since it provides both adequate activity and selectivity. Under the normal production conditions, the selectivity of epoxidation reaction is relatively low resulted from the low oxygen surface coverage. In practice, a small amount of halogenated hydrocarbon is added to the gas stream for inhibiting deep oxidation. Therefore, it is desirable to find an alternative to replace this toxic compound. The objectives of this research were to study the effect of gold as promoter on silver catalyst over Degussa C Al_2O_3 and also to investigate the effect of supports which was TiO_2. Catalyst activity experiments for ethylene epoxidation were carried out by using a differential reactor. For 13.18% Ag on Degussa C Al_2O_3 gave the optimum ethylene epoxidation. An addition of 0.54% gold on 13.18% Ag/Al_2O_3 maximized the activity with the ethylene oxide selectivity up to 90%. In contrast, Ag on TiO_2 was poor catalysts for ethylene epoxdation. As expected, Au/TiO_2 gave a good trend for ethylene epoxidation but still obtained a lower yield than Ag/Al_2O_3. Among the prepared catalysts in this research, Au-Ag on Al_2O_3 is the best catalyst for ethylene epoxidation.

Keywords : Ethylene oxide/Ethylene oxidation/silver/gold/Al_2O_3 /TiO_2 / CeO_2

บทคัดย่อ

รหัสโครงการ : BGJ43-8-0009

ชื่อโครงการ : การเลือกเกิดปฏิกิริยาออกซิเดชันของเอธิลีนบนฐานรองรับที่มีตัวเร่งปฏิกิริยาเป็นโลหะเงินและโลหะผสมเงิน-ทอง

ชื่อนักวิจัย : นายศิริพงษ์ โรจน์ลือชัย
วิทยาลัยปิโตรเลียมและปิโตรเคมี จุฬาลงกรณ์มหาวิทยาลัย

E-mail Address : siriphong@rocketmail.com

ระยะเวลาโครงการ : 2 ปี (1 กันยายน 2543 - 31 สิงหาคม 2545)

ในปัจจุบันตัวเร่งปฏิกิริยาโลหะเงินถูกใช้สำหรับการผลิตเอธิลีนออกไซด์ เพราะให้ทั้งความสามารถเกิดปฏิกิริยาและการเลือกเกิดปฏิกิริยาที่สูงเพียงพอ ภายใต้สภาวะของการผลิตตามปกติ การเลือกเกิดปฏิกิริยาอีพอกซิเดชันค่อนข้างต่ำอันเนื่องจากมีออกซิเจนปกคลุมบนพื้นผิวตัวเร่งปฏิกิริยาน้อย ในทางปฏิบัติการเติมสารฮาโลจิเนทไฮโดรคาร์บอนจำนวนเล็กน้อยในสารตั้งต้นเพื่อยับยั้งปฏิกิริยาการเผาไหม้ ดังนั้นจึงเป็นสิ่งจำเป็นในการหาทางเลือกอื่นเพื่อทดแทนสารประกอบที่เป็นพิษนี้ วัตถุประสงค์ของการวิจัยนี้ คือการศึกษาผลของการใช้ทองเป็นตัวส่งเสริมบนตัวเร่งปฏิกิริยาโลหะเงินบนฐานรองรับ อลูมินา (Degussa C Al_2O_3) และศึกษาผลของการเปลี่ยนฐานรองรับอื่นๆ เช่น ไททาเนีย (TiO_2) ในงานวิจัยนี้ได้ทำการทดลองศึกษาความสามารถของตัวเร่งปฏิกิริยาสำหรับเอธิลีนอีพอกซิเดชัน โดยใช้เตาปฏิกรแบบดิฟเฟอเรลเชียล สำหรับผลการทดลองของ Ag/Degussa C Al_2O_3 พบว่าปริมาณโลหะเงินที่เหมาะสมที่สุดคือ 13.18% โดยน้ำหนัก สำหรับปฏิกิริยาอีพอกซิเดชันของเอธิลีน การเติมโลหะทองบนตัวเร่งปฏิกิริยาโลหะเงิน พบว่า 0.54% ของทองบน 13.18% Ag/Al_2O_3 สามารถให้เกิดการเลือกเกิดปฏิกิริยาสูงสุดได้ถึง 90% ในทางกลับกันผลของการศึกษาแสดงให้เห็นว่าโลหะเงินบนฐานรองรับไทเทเนียในการเป็นตัวเร่งปฏิกิริยาที่ไม่ดีสำหรับปฏิกิริยาอีพอกซิเดชัน แต่ พบว่า Au/TiO_2 ให้แนวโน้มที่ดีในการเป็นตัวเร่งปฏิกิริยาของปฏิกิริยาเอธีลีนอีพอกซิเดชัน โดยสรุปจากผลการทดลองทั้งหมดในงานวิจัยนี้สำหรับตัวเร่งปฏิกิริยาที่เตรียมได้ พบว่า Au-Ag $/Al_2O_3$ เป็นตัวเร่งปฏิกิริยาที่ดีที่สุดสำหรับปฏิกิริยาอีพอกซิเดชัน

คำหลัก : เอธิลีนออกไซด์/ เอธิลีน ออกซิเดชัน/ เงิน/ ทอง/ อลูมินา/ ไทเทเนีย

ACKNOWLEDGEMENTS

First of all, I would like to gratefully acknowledge The Thailand Research Fund under The Royal Golden Jubilee Ph.D Program for supporting scholarship and Basic Research Grant for Royal Golden Jubilee Program for partial research expense.

Moreover, I would like to express my gratitude to my US advisor, Prof. Johannes W. Schwank who gave me a lot of suggestion and support during the time that I did some part of my research at The University of Michigan in 2000-2001 and Dr.Corinna Wauchope and Dr.John Mansfield who advised and trained me to use TEM, XPS and SEM at Electron Microbeam Analysis Laboratory (EMAL).

I am very grateful to my Thai advisor, Assoc. Prof. Sumaeth Chavadej, as well as Assist. Prof. Vissanu Meeyoo who always encouraged me and gave valuable suggestions and comments for my research work over the Ph.D program. I would like to acknowledge Mahanakorn University, especially Dr.Vissanu's lab, to allow me to use mass spectroscopy.

Furthermore, I would like to acknowledge Kokes Awards for providing me financial support and accommodation for me to attend the 17th North America Catalysis Society Meeting on June 3-8, 2001 at Toronto, Ontario, Canada.

Also, I would like to thank all PPC staffs for their contributions, especially C.P.O. Poon Arjpru for and Mr. Sanit Prinakorn for experimental setup.

I would like to thank my Ph.D. friends for help and friendship especially, Apanee Luengnaruemitchai, Punjaporn Trakultamupatam, Chalothorn Soponvuttikul, Siriporn Jongpatwut, Jiraporn leerat and Korada Supat. Moreover, I would like to extend my thanks to M.S. friends (class in 1997-2000) at PPC and also Thai students and Nguyen Anh Duc at the University of Michigan for their sincere friendship and kind assistance. In addition, students in class 1997-2001, especially catalysis groups for their help are also acknowledged. I deeply appreciate for their kindness and love.

Last but not least, I wish to extend my grateful thanks to my family for their love, encouragement, and understanding.

Finally, I would like to dedicate this dissertation to my family and Buddha.

TABLE OF CONTENTS

CHAPTER **PAGE**

CHAPTER **PAGE**

LIST OF TABLES

LIST OF FIGURES

FIGURE **PAGE**

FIGURE **PAGE**

FIGURE **PAGE**

ABBREVIATIONS

AAS	=	Atomic Adsorption Spectrophotoscopy
BE	=	Binding Energy
DRIFTS	=	Diffuse Reflection Infrared Fourier Transform Spectroscopy
EDS	=	Energy Dispersive Spectroscopy
FT-IR	=	Fourier Transform Infrared Ray
SEM	=	Scanning Electron Microscopy
STEM	=	Scanning Transmission Electron Microscopy
TEM	=	Transmission Electron Microscopy
TPD	=	Temperature Programmed Desorption
XPS	=	X-Ray Photoelectron Spectroscopy
XRD	=	X-Ray Diffraction

CHAPTER I
INTRODUCTION

1.1 Statement of Problem

The selective oxidation of ethylene depends on the choice of the catalytic system and the reaction conditions. Silver-based catalysts are commonly employed for the production of ethylene oxide since they give both adequate activity and selectivity. The unique epoxidation activity of silver has been attributed to its ability to adsorb oxygen not only on its surface but also to incorporate oxygen into the subsurface of silver. This subsurface oxygen in silver, which has low bond strength, is believed to be a key factor in imparting the high selectivity for epoxidation of ethylene. It has also been known that a significant subsurface oxygen concentration in silver with low bond strength (13 kJ/mole) can only be achieved when the silver surface has an oxygen coverage of more than 50 %. At lower oxygen surface coverage, the oxygen bond strength increases to 63 kJ/mole and the catalyst loses its high epoxidation selectivity.

Unfortunately, at typical operational conditions of the industrial ethylene epoxidation process (~550 K), oxygen surface coverage of silver becomes small. This low oxygen surface coverage limits the selectivity of epoxide formation. One strategy to increase the oxygen surface coverage is to lower the operational temperature but then the catalytic activity becomes too low for a practical process. In practice, a small amount of halogenated hydrocarbons such as vinyl chloride or 1, 2 dichloroethane is added to the gas stream as a moderator to inhibit CO_2 formation, thereby increasing the selectivity at a slight sacrifice of conversion.

1.2 Purpose of Research

Silver catalysts are known as highly selective catalysts for ethylene epoxidation. Small amounts of promoters and modifiers can improve the activity of ethylene and the selectivity towards ethylene oxide. The promoters and modifiers, such as alkali earth metal, and chloride, appears to exert a synergistic effect (Karavasilis *et al.,* 1996). The presence of a small amount of metal promoter acts to stabilize silver against sintering (Matar *et al.,* 1989). The role of modifiers can be explained in terms of electronic interactions between the silver crystallite and the support. It has been known that the presence of atomic oxygen favors complete oxidation while molecular oxygen enhances ethylene oxide formation. Chlorine containing modifiers are believed to not only change the relative concentrations of atomic and molecular oxygen, but also to increase the probability of molecular oxygen to give ethylene oxide (Matar *et al.,* 1989). In addition, on pure metallic Au, molecular oxygen does not adsorb. Atomic oxygen, on the other hand, will adsorb. On supported Au, especially when Au is present in a state of high dispersion, oxygen will adsorb at temperature of about 200°C, and very high activity for oxygen transfer has been adsorbed even at room temperature, for example in the oxidation of CO of CO_2. Given these unusual oxygen transfer properties of gold, it appears interesting to explore how adding small amount of gold to silver would change its activity and selectivity for epoxidation of ethylene.

1.3 Objectives

In this research, the objectives were as follows:

1. to conduct a fundamental study of the effect of gold addition to silver on the activity and selectivity of the ethylene oxidation reaction;
2. to investigate the effect of different support materials (high suface area, non porous alumina and titania) on the selectivity of Ag in ethylene oxidation;
3. to study the activity of gold on titania.

Karavasilis, C., S. Bebelis, and C. G. Vayenas, "In situ controlled promotion of catalyst surfaces via NEMCA: The effect of Na on the Ag-catalyzed ethylene epoxidation in the presence of chlorine moderators", Journal of Catalysis 160, 205-213 (1996).

Matar, S., M. J. Mirbach, and H. A. Tayim, Catalysis in petrochemical processes, pp. ix, 200, Kluwer Academic Publishers, Dordrecht ; Boston, 1989.

CHAPTER II
LITERATURE SURVEY

2.1 Epoxidation

2.1.1 General

Ethylene oxide is mainly used as chemical intermediate to produce various consumer products. Almost 60% of ethylene oxide is converted to ethylene glycol which is used as anti-freeze reagent and in the manufacture of polyesters. Additionally, ethylene oxide is used for the production of ethoxylates, which are surface-active agents used in the detergent, textile, and paint industries.

Other derivatives are glycol ethers, which are widely used in brake fluids; ethoxylates in detergent formulations; as a solvent for paints and lacquers; an extractant of sulphur compounds from refinery gases, and ethanolamines used in textiles finishing and detergents. di and triethylene glycols, polyols and choline chloride are also synthesized from ethylene oxide. Ethylene oxide is also an excellent disinfectant, fumigant and sterilizing agent (Wells, 1991).

In 1859, Wultz developed the chlorohydrin process involving the addition of hypochlorous acid to ethylene followed by dehydrochlorination. In 1931 a patent was issued to Lefort for direct oxidation of ethylene to ethylene oxide using a silver catalyst. Currently, around 98% of ethylene oxide capacity in the world is based on this route. In many plants, oxygen is favored over air because it is more economic and allows higher productivity and pollution problems caused by vent gases such as dichloroethane are markedly reduced.

The primary and secondary reactions which take place during the oxidation of ethylene are (Dumas and Bulani, 1974):

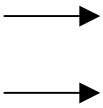

Both reactions are exothermic reactions and carbon dioxide and water are the undesired products formed from the complete oxidation of both ethylene oxide and ethylene. The deep oxidation reaction releases a large amount of heat. Thus, attempts have been made to minimize the deep oxidation reaction (Dumas and Bulani, 1974 and Matar *et al.,* 1989).

Pena *et al.* (1998) studied the ethylene oxidation in different membrane reactors which were PBMR-O(oxygen as permeate with ethylene flowing over the catalyst bed) and PBMR-E (ethylene as permeate with oxygen flowing over the catalyst bed), and compared the performance of the membrane reactors will that of fixed bed reactors (FBR). The study of FBR showed that a high oxygen/ethylene ratio increased the ethylene oxide selectivity. The behavior of the membrane reactors was different depending on the configuration, with the PBMR-O exhibiting smaller and the PBMR-E gave larger ethylene oxide selectivity, as compared to the FBR. It was found that the selectivity of EO increased above that of the FBR with residence time of both reactants for both configurations of the membrane reactor. It was found that high oxygen/ethylene ratio favored ethylene oxide selectivity for the all addition of different levels of dichloroethane in the feed and the performance was in the order PBMR-E>FBR>PBMR-O. An increase in dichloroethane concentration in the inlet stream increased the ethylene oxide selectivity to values exceeding 80% for low ethylene conversions. The addition of ethane was controlling the amount of chlorine adsorbed on the catalyst surface. High levels of dichloroethane resulted in detectable catalyst deactivation after a few hours on stream. The optimum level of dichloroethane was found to be 1-2 ppm (Lafarga and Varma, 2000).

The model of the intrinsic reaction kinetics in plug flow behavior over the packed bed catalyst and the dusty gas model (DGM) for membrane transport were used to show that the imposed pressure gradient resulted in predominantly flow through the membrane, which inhibits back diffusion of components from the catalyst bed. The variables studied included reaction temperature and inlet reactant concentrations. The model results, as also demonstrated experimentally, confirmed that the PBMR-E was the best

configuration, followed by the conventional fixed-bed reactor(FBR) and the PBMR-O, respectively (Al-Juaied *et al.,* 2001).

2.1.2 Oxygen Adsorption

In the late 1980s, Campbell (1985) studied the kinetics of selective ethylene oxidation catalyzed by a clean Ag(111) surface compared to Ag(110) and supported Ag catalyst. The results showed that the activity of Ag (111) in epoxidation was about half that of Ag(110), but about 50 times higher than the reported results for the high surface area Ag catalysts. The steady-state coverage of atomically adsorbed oxygen was a factor of about 18 lower on Ag (111) than on Ag(110). These results are consistent with a mechanism whereby molecularly adsorbed O_2 and ethylene are combined to form an intermediate in the rate-determining step. This intermediate then rapidly branches into ethylene epoxide or CO_2 pathways.

In contrast, there are three groups suggesting that atomically adsorbed oxygen is the active species for epoxidation. In the absence of promoters and moderators, Grant *et al.* (1985) proposed that chemisorbed atomic oxygen reacts with adsorbed ethylene to yield both ethylene and (CO_2 and H_2O). Chemisorbed dioxygen appears to play no direct role in either of these reactions; the presence of subsurface oxygen is necessary for selective oxidation but not for total oxidation. van Santen *et al.* (1986) studied the reaction mechanism of ethylene epoxidation using $^{16}O_2$ and $^{18}O_2$. The results showed that under the conditions where $^{18}O_2$ equilibration in the gas phase was slow, ethylene initially reacted more rapidly with preadsorbed atomic oxygen than with molecular oxygen adsorbed in the precursor state if O_{ads}/Ag_s was unity. Nevertheless, with oxygen preadsorbed with $O_{ads}/Ag_s < 0.5$ and pretreated such that the oxygen atoms resided below the surface, it was concluded that subsurface oxygen atoms became incorporated in to the epoxide upon exchange with adsorbed oxygen surface atoms. Thus oxygen atoms that have been dissociated during adsorption of oxygen are incorporated into the epoxide. Carterand *et al.* (1988) theoretically explained the mechanism using ab

initio theoretical estimates. This mechanism proposed that a *surface atomic oxyradical anion* was the active oxygen species for forming epoxide.

Nakatsuji *et al.* (1997) studied the partial oxidation of ethylene to ethylene oxide catalyzed by silver by ab-initio Hartee-Fock and MP2 methods using the dipped adcluster model(DAM). They explained that the active species was the superoxide O_2^- which is molecularly adsorbed in the bend end-on geometry on the silver surface. Ethylene reacted with the terminal oxygen atom and the reaction proceeded smoothly without a large energy barrier to yield ethylene oxide.

Bukhtiyarov *et al.* (1994) showed that the treatment with a mixture of C_2H_4 and O_2 could activate a clean silver foil surface for ethylene oxide formation. They proposed that the catalytic surface center to be active for ethylene epoxidation must contain two adsorbed oxygen states with different ionicities of the Ag-O bond. The "ionic" oxygen [Eb(O 1s) = 528.4 eV] produces the sites of Ag^+ ions for ethylene adsorption, while the "covalent" oxygen [Eb(O 1s) = 530.5 eV] incorporates in the ethylene molecule, forming ethylene oxide.

Oxygen adsorption on supported silver depending on the cluster sizes was studied by XPS and TPD using a model carbon-supported silver catalyst (Bukhtiyarov and Kaichev, 2000). It was shown that the electrophyric oxygen active in ethylene epoxidation was produced on the small silver clusters ($\leq$ 100 Å) more effectively than on the bulk metal due to formation of subsurface oxygen. Enlargement of the silver particles decreased the amount of subsurface oxygen and results in the appearance of nucleophilic oxygen. These results were used in an attempt to explain the particle size effect in ethylene epoxidation over Ag/Al_2O_3 catalysts.

In temperature-programmed desorption (TPD) experiments, there were three adsorbed oxygen species observed (Kondarides and Verykios, 1993). First, a weakly adsorbed species (desorbed below 150°C) was related to the 10.5 kCal/mol adsorption process and assigned to molecularly adsorbed oxygen. Second, the desorption peak at 285°C was related to a nearby nonactivated process and is ascribed to atomic oxygen, probably multicoordinated on the

surface. Third, high temperature (300-400°C) feature, desorbing above 400°C is related to the highly activated process of 24 kcal/mol and attributed to desorption of subsurface oxygen.

2.1.3 Effect of Promoters

Presently, the catalysts used in commercial processes for ethylene oxide are metallic silver on the low surface area inert supports. Electronegative moderators have been found to be necessary for improving the selectivity of ethylene oxide. A large amount of moderators, however, can destroy the catalyst activity. The moderators, which are known to improve the selectivity of silver are Cl, Br, I, S, Se, Te, P and Bi. Chlorine is the most commonly used moderator added in the form of organic chlorides such as 1, 2-ethylene dichloride with low concentration of a few parts per million. The role of the moderator is thought to change not only the relative concentrations of atomic and molecular oxygen, but also to increase the probability for molecular oxygen to give ethylene oxide. Moreover, the role of promoters is also significant to stabilize silver against sintering (Matar *et al.,* 1989).

Campbell *et al.* (1985) studied the selectivity of ethylene oxide as a function of chlorinated hydrocarbons added to the reactant feeds. The results showed that the activation energies were varied with chlorine coverage (θ_{Cl}) and correlated with the electronic effects of θ_{Cl} upon desorption energies for molecularly adsorbed O_2 and ethylene. However, these reaction rates had no relationship to the large increase in selectivity appearing when $\theta_{Cl} > 0.4$. It was concluded that an increase in selectivity was governed by the ensemble effect, while CO_2 production required more free Ag atoms than epoxide production did.

Yeung *et al.* (1998) studied the ethylene epoxidation reaction network on a Ag/α-Al_2O_3 catalyst in the presence of 1,2-dichloroethane (DCE) using a single-pellet reactor. The results showed that the selectivity of ethylene oxide and the ethylene conversion decreased with increasing the width of the active layer and placing the Dirac-type active layer which was a catalyst pellet with a narrow active layer at subsurface locations. Nevertheless, addition of

DCE promoted the catalyst selectivity for ethylene oxidation reaction, but inhibited the overall reaction.

Yong *et al.* (1990) studied the epoxidation of ethylene over silver catalysts in the presence of added carbon monoxide and hydrogen. The addition of carbon monoxide and hydrogen in the feed stream led to incomplete oxidation and inhibited ethylene oxidation by direct competition for the silver surface. Ethylene conversion and ethylene oxide selectivity were reduced under the ethylene-rich condition. Moreover, for long periods (more than 10 h) and the presence of carbon monoxide in the feed stream, it was observed that ethylene conversion fell steadily while the ethylene oxide selectivity rose. The effect was very similar to the case of 1, 2-dichloroethane at the ppm level in the feed stream. In addition, comparing oxygen and nitrous oxide as oxidants, it was found that the ethylene oxide selectivity was declined to 14% at 240°C with nitrous oxide. Activation energies for ethylene conversion to all products were similar for the two oxidants but the rate was found to be approximately six times higher with oxygen than nitrous oxide (Yong and Cant, 1989).

Rhenium has also been used as promoter for ethylene epoxidation over silver catalysts (Jun *et al.,* 1992). It was found that both the conversion of ethylene and the selectivity of ethylene oxide could be improved by the use of a rhenium-modified silver catalyst. The effect of rhenium is to weaken the silver-oxygen bond, and to reduce the electron density of the adsorbed oxygen, which could be the reason for the enhancement of the selectivity of ethylene oxide.

Cesium is another metal used as a promoter. It has been found that the fresh catalyst with Cs promoter has fairly uniform coating of Ag over the planar α-alumina surface (Minahan and Hoflund, 1996a, 1996b, 1996c). For high surface area α-alumina, addition of cesium contributes to the neutralization of surface acidity which promotes complete combustion (Mao and Vannice, 1995). Moreover, Cs likely stabilizes the defects on the Ag surface, where electrophilic oxygen is probably localized. On the other hand, it can decrease the concentration of nucleophelic oxygen (surface Ag_2O), which is responsible for the deep oxidation of C_2H_4 (Goncharova *et al.,* 1995).

Various Cs oxides formed on the Ag (111) and Ag(110) single crystals depending on cesium coverage and oxygen pressure have been identified by XPS and TPD. The results were shown the existence of few Cs oxides with various stoichiometry: from suboxide, Cs_{2+x}, to superoxide, Cs_2O_4. The spectroscopic characteristics of two of them (suboxide and peroxide) are also observed for Cs-promoted Ag/Al_2O_3 catalysts suggesting their existence in real catalytic conditions. Their roles in silver-catalyzed ethylene epoxidation are different: peroxide seems to suppress the total oxidation, while promotion of ethylene epoxidation can be suggested for the suboxide.comparison (Podgornov *et al.,* 2000).

The effect of non-Faradaic electrochemical modification in catalytic activity was investigated during ethylene epoxidation on Ag films deposited on β-Al_2O_3, a Na^+ conductor (Dumas and Bulani, 1974). It was found that sodium coverage (θ_{Na}) up to 0.03 could enhance the rate of epoxidation without a significant effect on the rate of complete oxidation. The maximum selectivity of ethylene oxide (88%) was obtained for $\theta_{Na} = 0.03$ and 1 ppm dichloroethane. The results indicate that the chlorine atoms can replace strongly adsorbed oxygen atoms, and that chlorine adsorption consequently weakens the bond strength of the coadsorbed oxygen by withdrawal of electrons from the silver atoms and by creation of sites for the adsorption of weakly bound electrophilic oxygen which interacts with the double bond of ethylene molecules producing C_2H_2O. In contrast, the presence of sodium on the silver surface seems to stabilize the adsorbed chlorine via the formation of a silver-oxychloride surface complex (Karavasilis *et al.,* 1996).

Kondarides and Verykios (1996) conducted a study to investigate the effect of alloying silver with gold on the oxygen adsorption characteristics of silver using microgravimetric and temperature desorption techniques. Gold was chosen due to its ability to form solid solutions with silver at any composition and because of its inertness toward oxygen adsorption and ethylene oxidation. The results confirmed the presence of three adsorbed species of oxygen at elevated temperatures, namely molecular, atomic and subsurface. They also concluded that alloying Ag with Au influenced the bond strengths with the silver surface, which resulted in modifying the relative population of the adsorbed species. In the oxidation of ethylene, Geenen *et al.*

(1982) exhibited that the selectivity to ethylene oxide decreased sharply with increasing gold content of Ag-Au alloy on α-alumina support. On gold rich alloys no ethylene oxide was formed, the only products being carbon dioxide and water. The reason is that the reaction of ethylene with O_2^- results only in ethylene oxide if the adsorbed complex is sterically hindered by adjacent adsorbed species, such as O^{2-} or Cl^-, such that abstraction of hydrogen from the ethylene molecule in the way depicted above cannot occur. In the case of the alloys, the O_2^- species are seperated from one another and hence the adsorbed ethylene complex will react to form carbon dioxide and water.

2.2 Support Materials

2.2.1 Alumina Support

The effect of support materials such as Ag/η-Al_2O_3, Ag/TiO_2, Ag/a-Al_2O_3 and Ag/SiO_2 was investigated by Seyedmonir *et al.*(1990). Commercial α-alumina is a unique support material for silver because it facilitates the highly selective ethylene epoxidation. This is attributed to its inertness for isomerization of ethylene oxide to acetaldehyde. High silver loadings on the low surface area α-alumina (surface area <1 m^2g^{-1}) are typically used for commercial ethylene oxidation catalysts, in which silver is in poor dispersion. Mao *et al.* (1995) used high surface area (HSA) α-alumina (about 100 m^2g^{-1}) as support. The results showed that (HAS) α-alumina was a poor support for ethylene epoxidation due to the formation of small nanoparticles of Ag. The reaction rate increased with increasing surface area but the selectivity was poor. Therefore, it is interesting to prepare Ag catalyst on a high surface area alumina that permits to stabilize Ag in form of larger particles. In this study, fumed alumina of Degussa C having a surface area of 98 m^2/g was used as support for Ag. This support is a non porous material, and it was hoped that it should be to deposit Ag in large particle size on this support.

2.2.2 Titania Support

Supported metal catalysts are undoubtedly one of the major areas of research in heterogeneous catalysis. The study of well-known strong metal-support interaction (SMSIs) when the support is a reducible oxide has recived a lot of attention. The reason was the migration of reduced support particles onto the surface of metallic particles. The formation of a suboxide of the support was facilitated by the reduction being induced by the metallic particles (Holgado *et al.,* 1998). It has been known that group VIII noble metals supported on TiO_2 exhibits a strong metal-support interaction effect. Shastri *et al.* (1984) studied the behavior of gold supported on TiO_2. The results showed that TiO_2 played a special role compared to other typical catalyst support materials. It could stabilize high dispersion of Au up to 700° C. It was explained that this phenomenon did not appear to be due to the SMSI effect. While a temperature of 700°C was sufficient to accomplish the complete phase transformation of anatase to rutile in the blank TiO_2, no transformation occurred under the identical conditions on TiO_2 impregnated with Au.

2.3 Silver Catalysts

Silver is a uniquely effective catalyst for the industrial important epoxidation of ethylene. The ethylene epoxidation over silver catalyst has been intensively investigated due to two main reasons. First, there is no thermodynamic limit for further increasing selectivity to ethylene oxide and, second, there are still some fundamental questions concerning the mechanism of the reaction that remain unanswered. It has been proposed that the mechanistic steps may involve oxygen adsorption on the Ag surface, reaction of the adsorbed oxygen species with ethylene, and formation of intermediates on the surface (Minahan and Hoflund, 1996c).

The effect of crystallite size of silver on the activity and selectivity was studied by Wu et *al.* (1975). The activities per unit surface area for ethylene oxide formation and for carbon dioxide formation decreased with increasing crystallite size, but not at the same rate. The ethylene oxide selectivity was nearly zero for 20 Å

silver particles and gradually increased to 60% for 500 Å silver particles. Two types of active site are believed to be formed by adsorption of oxygen at steps and faces of the silver crystals, and reaction occurs between ethylene and atomic or molecular oxygen competitively adsorbed on these sites.

Verykios *et al.* (1980) studied the kinetic effect of total surface, average silver crystallite size, and silver crystallite morphology of supported silver catalysts on the epoxidation reaction. They found that the specific activity and selectivity of the catalysts were a strong function of the total surface area. The specific rates to ethylene oxide and to carbon dioxide and water formation exhibited strong structure sensitivity with minimum rates at silver crystallite sizes in the range of 500-700 Å. The changes in specific activity and selectivity appeared to be related to changes in the morphology as well as the size of the silver crystallites. Furthermore, they explained that crystallite size effects can be significant in small crystallites in which the surface atoms constitute a significant fraction of the total number of atoms in the crystal. Otherwise, edge and corner atoms constitute a significant fraction of the total number of surface atoms in small crystal (Smeltzer *et al.,* 1956). It is expected that edge and corner atoms exert different catalytic activities because they have a different coordination number than other surface atoms. Binding energies between surface atoms and between bulks atoms are different; for small crystallites such differences can be expected to depend on the size of the crystallites. These differences can influence the bonding energy with an adsorbed molecule and affect the specific catalytic activity.

Lee *et al.* (1989) proposed that the influence of metal crystallite size on the kinetic parameters was also found to depend on the carrier employed. Thus, the specific activity of $Ag/\alpha\text{-}Al_2O_3$ was found to exhibit a maximum at an average crystallite size of approximately 400Å while that of Ag/SiO_2 increased with crystallite size and appeared to level off at an average crystallite size of approximately 500 Å.

Comparably high selectivity can be attained over both large and small Ag crystallites although the ethylene dichloride levels for optimum values appear to differ, with larger crystallites requiring higher ethylene dichloride concentrations.

The lower TOF values on the Ag/SiO_2 catalysts are compensated by their much higher dispersions and these SiO_2 supported catalysts also show much greater resistance to sintering. A comparison with literature results indicates that in the absence of moderators a 1000-fold decrease in TOF occurs as Ag crystallite size decreases to 3 nm from that in bulk samples; however, structure sensitivity cannot be unequivocally claimed because of the unknown role of adsorbed oxygen on these small particles (Seyedmonir *et al.,* 1990).

2.4 Gold Catalyst

Gold is unique among metallic elements because of its resistance to oxidation and corrosion. In addition to its inert property to any chemical reactions, gold has very low affinity for gas adsorption. Moreover, it was found that molecular oxygen was chemisorbed on gold powder over the wide temperature range, with two distinct maixma at – 50°C and at 200°C (Schwank, 1983).

Kondarides *et al.* (1996) studied the effect of adding gold into silver catalysts on oxygen adsorption. The results confirmed the presence of three absorbed oxygen of atomic oxygen, molecular oxygen and subsurface oxygen at elevated temperatures and showed that alloying Ag with Au influenced the bond strengths with silver surface and, thus, modified the relative population of the adsorbed species.

Regarding to literature survey articles, researchers are focused on the advances in the catalysis research of Au catalyst for many reactions such as propylene epoxidation, CO oxidation, photocatalytic reaction and other reactions.

2.4.1 Epoxidation of Propylene

Hayashi and co-workers (1998) studied the vapor phase epoxidation of propylene over Au/TiO_2 in the presence of oxygen and hydrogen. They found that it produced propylene oxide with selectivity higher than 90% and the propylene

conversions of 1-2% at temperatures of 303-393 K when gold was deposited on TiO_2 by deposition-precipitation techniques as hemispherical particles with diameters smaller than 4.0 nm. Moreover, the reaction rate was independent on the concentration of propylene and increased linearly with increasing concentration of O_2 and H_2. Therefore, the results suggested that propylene adsorbed on gold surface might react with oxygen species formed at the perimeter interface between the gold particles and the TiO_2 support through the reaction of oxygen with hydrogen. In addition, it was observed that gold particles larger than 2.0 nm in diameter produced propylene oxide, where as smaller gold particles yielded propane.

Due to the deactivation of Au/TiO_2 catalysts**,** adding silica to the titania support can induce a longer life time of the catalyst. In 1999, Nijhuis *et al.* modified the titania support by dispersing SiO_2 on TiO_2 (TS-1). It was found that Au on TS-1 was more resistant to deactivation and able to give slightly higher yields of propylene oxide. The maximum propylene oxide yield obtained with this type of catalyst remained low (less than 2%). These low yields might be a result of oligomerization of propene oxide occurring on the catalyst when the propylene oxide partial pressure becomes too high.

The presence of hydrogen was crucial for the activity of the catalyst, most likely because the hydroperoxide-like compound formed on the gold particles is transferred via a spillover mechanism to the titanium atoms. This hydroperoxide on titanium was expected to be the species reacting with propene to produce propylene oxide (Nijhuis *et al.,* 1999).

Furthermore, Uphade and co-workers (2000) employed Au/Ti-MCM-41 (Ti/Si = 3/100) to study the effect of an addition of CsCl onto this catalysts on the gas phase epoxidation of propane using H_2 and O_2. They obtained 92% propylene oxide selectivity at the reaction temperature of 100°C after 60 min of reaction. The presence of CsCl with this catalyst reduced H_2 consumption by about 90% and improved the propylene oxide selectivity up to 97% at a propene conversion of 1.7%. It was reported that agglomeration of gold particles was caused by Cl^- anions. The mean diameter of Au particles, 2.2 nm, in Au/Ti-MCM-41 increased to about 10 – 20 nm and some clusters were even larger than 50 nm in size due to the direct contact between chloride and Au particles.

Mul and co-workers (2001) reported that irreversible adsorption of propylene oxide was observed on both a 1 wt% Au/TiO_2 and a 1 wt% $Au/TiO_2/SiO_2$ catalyst, and the reaction yielded bidentate propoxy moieties. The spectroscopic evidence for oligomerization or dimerization of propylene oxide was not found. Similar propoxy species were observed after prolonged exposure of the catalysts to a propene/oxygen/hydrogen mixture. Additionally, formate and acetate species were formed exclusively on the Au/TiO_2 catalyst after exposure to the reacting mixture at 400 K or decomposition of the adsorbed bidentate propoxy species in a hydrogen/oxygen mixture. Supporting Au and TiO_2 on SiO_2 apparently reduces the activity toward C-C bond breaking. Based on the spectroscopic results, deactivation of Au/TiO_2 catalyst likely related to the irreversible adsorption of a propoxy species on the activation of Ti site. On the TiO_2/SiO_2 catalyst, the acidic Ti sites that cause ring opening of propylene oxide are apparently not located near the active epoxidation center. Thus, no deactivation of dispersed Ti catalyst showed the formation of acetone and propanal. However these side products initially remained adsorbed on the catalyst surface under reaction conditions, maintaining a gas phase selectivity of 99%.

Stangland *et al.* (2000) characterized the two most effective propylene oxide catalysts, which were deposition-precipitation of gold onto titania-modified silica and silica-supported Au-Ti nanoclusters with a 200:1 gold to titanium ratio. The propylene oxide TOFs (turnover frequency) for Au/TiO_2 catalysts exhibited a relatively small spread at 373 K, but varied over 4 orders of magnitude as temperatures approached 473 K. The amount and phase of titania in contact with gold, influencing the number and type of Au-Ti contacts, is important in maximizing PO formation and limiting both oxidative cracking of PO to ethanal and CO_2 and propylene oxide isomerization reaction. A D_2 kinetic isotope effect observed for propylene oxide formation supports the idea that hydroperoxy intermediates are produced from H_2 and O_2 over catalyst's surface.

Zwijnenburg *et al.* (2002) prepared bimetallic Au catalyst by adding Pt or Pd on $Au/TiO_2/SiO_2$ with deposition-precipitation techniques. The results for Pd-Au catalysts indicated that although Pd seems well dispersed over support, hydrogenation of propene to unwanted propane occurred. This is probably due to the

presence of monometallic Pd particles. Moreover, results for Pt showed an increase in the hydrogen and oxygen efficiency, combined with a stable yield in propylene oxide. Hydrogenation of propene occurs at higher temperatures, but can be prevented by operating below 373 K.

2.4.2 CO Oxidation

The oxidation of CO is a typical reaction for which Au catalysts are extraordinarily active at room temperature and more active than other noble metal catalysts at temperature below 400 K. For this oxidation reaction, Au/TiO_2 has been intensively studied. This is because neither Au nor TiO_2 alone is active for CO oxidation but their combination generates surprisingly high catalyst activity. The following are literature articles relating to Au catalysts.

Haruta and co-workers (1993) prepared highly dispersed gold catalysts via co-precipitation and deposition-precipitation. They proposed that the small gold particles are hemispherical in shape and stabilized by epitaxial contact, dislocations, or contact with amorphous oxide layer. Among the gold catalysts supported on TiO_2 α-Fe_2O_3, and Co_3O_4, the turnover frequencies for CO oxidation per surface gold atom were almost independent on the kind of support oxides used and they increased sharply with a decrease in diameter of gold particles below 4 nm. Small gold particles not only provide the sites for the reversible adsorption of CO but also appreciably increase the amount of oxygen adsorbed on the support oxide. Based on the TPD and FT-IR data, the mechanism was proposed in which CO adsorbed on gold particles migrated toward the perimeter on support oxides and there it reacts with adsorbed oxygen to form bidentate carbonate species (Haruta *et al.,* 1993).

Adsorption of CO on pre-oxidized Au/TiO_2 at 253-303 K took place mainly as reversible Langmuir-type chemisorption. A large portion of CO was found to be adsorbed on TiO_2 support, which contributes to the reversible part of chemisorption. The irreversible part of CO adsorption, which was about 10% of the total amount of adsorbed CO, was related to CO_2 formation on the surface of gold particles and the accumulation of carbonate-like species on the surface of TiO_2 (Iizuka *et al.,* 1997). Adsorption of CO and CO_2 occurred almost instantaneously and

reversibly on preoxidized Au/TiO_2, where a slow increase in the O_2 pressure was observed at 273 K in the absence of evacuation. A similar increase of O_2 pressure was observed from oxidized TiO_2 but Au powder did not show any increase. The increase was ascribed to the desorption of weakly adsorbed O_2 on the support surface of Au/TiO_2. The rate of the reduction of preoxidized Au/TiO_2 with CO almost corresponded to the increase in the O_2 pressure and was far smaller than the rate of the catalytic oxidation of CO with O_2 on the catalyst, indicating that molecular oxygen weakly adsorbed on the support surface of Au/TiO_2 contributes only partly to the catalytic oxidation of CO. During the oxidation, O_2 in the gas phase may be directly activated on the surface of deposited gold particles and /or on the very narrow perimeter interface between the gold and the support (Iizuka *et al.,* 1999).

Furthermore, Boccuzzi and co-workers (2001a, 2001b) studied the effect of calcinations for three Au/TiO_2 catalysts prepared by the deposition-precipitation technique. The different calcination temperatures were 473, 573 and 873 K giving the mean diameters of Au particles of 2.4, 2.5 and 10.6 nm, respectively. The first two catalysts exhibited 100% conversion of CO at temperature below 240 K, whereas the third catalyst exhibited 100% conversion at temperature above 300 K. From the FT-IR data at 90 K, the large majority gold terrace sites did not adsorb CO.

2.4.3 Photocatalytic Reaction

Bamwenda and coworkers (1995) compared Au/TiO_2 and Pt/TiO_2 catalysts used for photo-assisted hydrogen production from a water-ethanol solution. They found that the activity of Au catalysts for H_2 production strongly depended on the method of catalyst preparation, but the activity of Pt catalysts was less sensitive to the preparation method. In addition, the yield of H_2 depended on the pretreatment conditions. Both gold and platinum catalysts calcined in air at 573 K had the highest activities towards H_2 generation. The maximum H_2 yield was observed for 0.3-1 wt% Pt and 1-2 wt% Au. The rate of H_2 production was strongly governed by the initial pH (4-7) of the suspension. The roles of Au and Pt on TiO_2 seemed to involve the attraction and trapping of photogenerated electrons, the reduction of protons and the formation and desorption of hydrogen. The higher overall activity of Pt catalysts

samples is probably a result of the more effective trapping and pooling of photogenerated electrons by Pt and/or because platinum sites have a higher capability for the reduction reaction.

CHAPTER III
EXPERIMENTAL

3.1 Materials

3.1.1 Chemicals for Catalyst Preparation

All chemicals used in catalyst preparation and analytical procedures were described as followed:

1. Aluminium oxide C (Al_2O_3) was obtained from Degussa AG.
2. Titanium oxide P25 (TiO_2) was obtained from Degussa AG.
3. Silver Nitrate ($AgNO_3$), assay 99.9%, was obtained from Carlo Erba.
4. Hydrogen tetrachloroaurate (III) trihydrate ($HAuCl_4.3H_2O$), ACS, 99.99%, was obtained Alfa Aesar A Johnson Matthey Company.
5. Titanium (IV) butoxide or Tetrabutyl orthotitanate ($C_{16}H_{36}O_4Ti$), AR grade, was obatined from Fluka Chemie A.G.
6. Methanol (CH_3OH), AR grade of 99.8%, was obtained from Labscan.
7. Nitric acid (HNO_3), AR grade of 65%, was obtained from Labscan.
8. Hydrochoric acid (HCl) was obtained from Labscan.

3.1.2 Reactant Gases for Reaction and TPD Experiment

All reactant gases were obtained from Thai Industrial Gas Co., Ltd. as shown below:

1. Helium (HP grade)
2. 30% Ethylene balance with Helium
3. 15% Oxygen balance with Helium
4. Oxygen 97%

TPD reactant gases were obtained from Air Product Co., Ltd. as followed:

1. Nitrogen (HP grade)
2. 8% Oxygen in Helium

3.2 Catalyst Preparation Procedures

3.2.1 Incipient Wetness Method

3.2.1.1 Silver catalysts

Silver catalysts were prepared by the incipient wetness method using aluminum oxide (fumed alumina, Degussa C, 85-115 m^2/g) with aqueous silver nitrate (Carlo Erba, 99.9%) solution to achieve nominal silver loadings of 10, 12, 14 and 16% wt. After impregnation, the catalyst precursors were dried at 110°C over night followed by calcination in air at 500°C for 5 h. After that, each catalyst was sieved in order to select grain sizes in the range of 212-425 μm for the activity studies.

With the above procedure, Ag on TiO_2 (Degussa P25, 60 m^2/g) was prepared with aqueous silver nitrate solution to achieve nominal silver loadings of 10, 12, 14, 16% wt.

3.2.1.2 Gold-silver catalysts

For the preparation of gold-silver on alumina catalyst, a silver catalyst with nominal 14% wt Ag loading was prepared and dried at 110°C for 2 h. Then, 18 g of this catalyst was divided into six aliquots. Five of these aliquots were impregnated with appropriate amounts of aqueous gold precursor ($HAuCl_4$, Alfa) solution, to achieve nominal gold loadings of 0.1, 0.3, 0.5, 0.7 and 1.0% wt. The sixth aliquot was impregnated with pure distilled water, without any precursor salts. After that, the six catalyst samples were dried at 110°C over night followed by calcination in air at 500°C for 5 h. The catalysts were sieved in order to select grain sizes in the range of 212-425 μm for the activity study.

3.2.1.3 Gold Catalysts

Au on TiO_2 (Degussa P25) was prepared with aqueous gold precursor ($HAuCl_4$, Alfa) solution with a nominal gold loading of 1% wt. Then, the

catalyst precursors were dried at 110°C over night followed by calcination in air at 500°C for 5 h. After that, each catalyst was sieved in order to select grain sizes in the range of 212-425 μm for the activity studies.

3.2.2 Deposition Precipitation Method

Au/TiO_2 catalysts were prepared by deposition-precipitation of $Au(OH)_3$ on titanium dioxide (Degussa P-25) in the aqueous solution at a constant pH of 8. An amount of $HAuCl_4$ with 1% wt Au was dissolved in distilled water under continuous stirring and heating at 70°C. This solution pH was maintained at 8 by gradually adding 1 M ammonium solution into the aqueous solution. Then the calculated amount of TiO_2 support was added into the mixed solution. The mixed solution was still maintained at pH 8 for 1 h. The resultant residue was washed several times until the conductivity was constant, then dried at 110°C over night, and finally calcined at 400°C for 5 h (Tsubota *et al*., 1995, and Uphade *et al*., 2000).

3.2.3 Sol Gel Method

The nominal 1% wt Au/TiO_2 with sol-gel technique was prepared under nitrogen atmosphere and at ambient temperature (297 K). Solutions were divided into two parts. A first solution was prepared by dissolving of 21.15 ml of tetrabutoxytitanium(IV)(TBOT) in 79.28 ml methanol (AR grade). A second solution was the mixture of 4.5 ml distilled water, 0.34 ml nitric acid (65 wt %) and 19.83 ml methanol. The second solution was added to the first solution with vigorous stirring and in a closed, initially nitrogen flushed system resulting in formation of gel. The resulting translucent gel was then aged for 2 h to increase the rigidity of the gel network by successive polycondensation reaction. After this first ageing process, the corresponding titania gel was redispersed with 46.92 ml methanol and homogenized for 10 min under vigorous stirring. The solution became opaque. Afterwards, the Au precursor solution containing 0.1 g $HAuCl_4 \cdot H_2O$, 0.58 ml water and 7.74 ml methanol was added and then the mixed solution was aged for 19 h under vigorous stirring. Finally, it was dried overnight and calcined at 500°C for 5 h at air atmosphere (Schneider *et al.,* 1994).

3.3 Catalyst Characterization

All catalysts were characterized by atomic adsorption spectrophotoscopy (AAS), diffuse reflection infrared Fourier transform spectroscopy (DRIFTS), X-ray diffraction (XRD) at The Petroleum and Petrochemical College (PPC) and scanning electron microscopy (SEM), scanning transmission electron microscopy (STEM), transmission electron microscopy (TEM), temperature programmed desorption (TPD), and X-ray photoelectron spectroscopy (XPS) at EMAL, The University of Michigan. The details were described as below:

3.3.1 Atomic Adsorption Spectroscopy (AAS)

A Varian Spectr AA-300 was employed to determine the compositions of gold and silver in the catalysts prepared. Figure 3.1 illustrates a photo of the AAS unit used in this work.

Figure 3.1 AAS Varian Spectr AA-300 at PPC.

3.3.2 Diffuse Reflection Infrared Fourier Transform Spectroscopy (DRIFTS)

The fresh catalysts were run on DRIFTS using O_2 and C_2H_4 reactant gases at a concentration ratio of 2%:2% in a Nicolet Avatar 360 Spectrometer equipped with a DTGS detector as shown in Figure 3.2. Experiments were performed using a diffuse reflectance cell from SpectraTech, Type 0030-103 with ZnSe windows. The catalyst was placed in this cell and pretreated with O_2 at 200°C for 1 h. Then, purge with helium for 30 min. For each FT-IR spectrum, 128 scans were taken at a resolution in situ of 8 cm^{-1}. Prior to recording each spectrum, a background spectrum of the sample pretreated in situ under helium flow was obtained. After that, introduced mixed gasses into the system and operated at temperature that provided the maximum yield for each catalyst from activity studies' result. The spectrum of each effluent gas on and over the catalyst was collected every 5 min until 40 min of reaction.

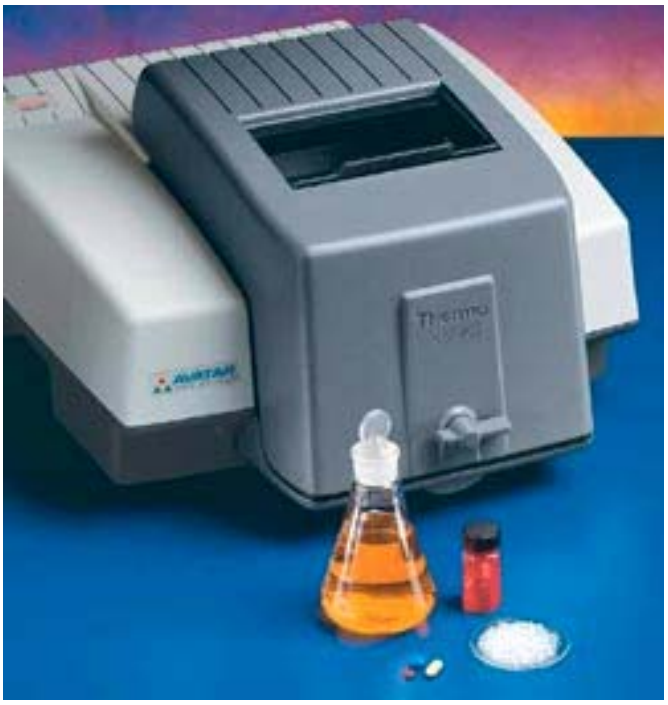

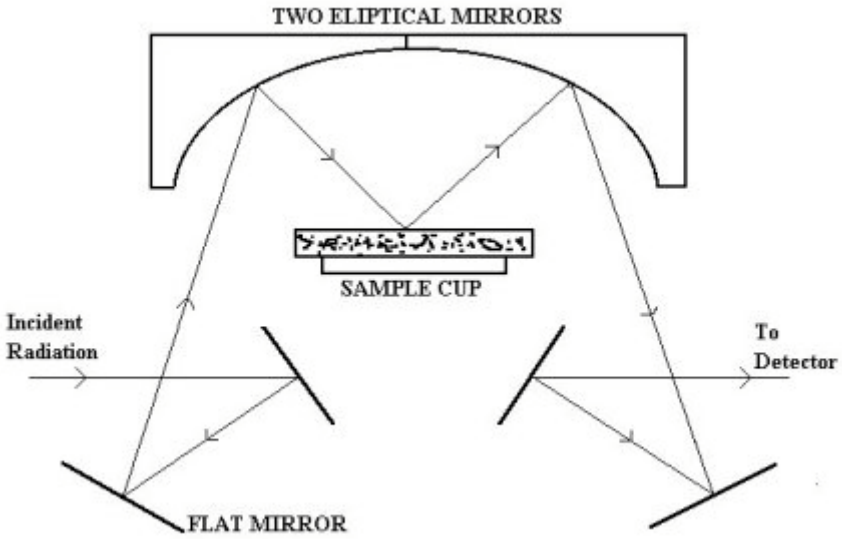

Figure 3.2 DRIFTS Nicolet Avatar 360 at PPC.

3.3.3 X-Ray Diffraction (XRD)

X-ray diffraction (XRD) profiles of the prepared catalysts were obtained by using a Rigaku RINT 2000 diffractometer equipped with a Ni filtered Cu Kα radiation source (λ= 1.542 Å) of 40 kV and 30 mA. A photo of XRD system is shown in Figure 3.3. A catalyst sample was pressed into a hollow of glass holder and held in place by a glass window. Then, it was scanned in the range of 2θ from 20^{o} to 90^{o} in the continuous mode with the rate of 5^{o} min^{-1}. The XRD results gave peak parameters, including the centroid 2θ, the full line width at half the maximum intensity (B), d-value and intensity. The mean crystallite size was calculated from the XRD data from X-ray line broadening, using the full line width at half maximum of intensity and the 2θ values and plugging them into the Scherrer equation (Cullity, 1956 and Matar *et al.,* 1989):

$$t = \frac{0.9\lambda}{B\cos\theta_B} \tag{3.1}$$

where t is crystallite size (Å)

λ is the X-ray wavelength (1.542 Å for Cu anode source)

B is the line broadening

θ_B is the Bragg angle

This equation works well for particle sizes of less than 1,000 Å. The broadening of diffraction lines measured at half the maximum intensity (B) is corrected by using Warren's method, which is

$$B^2 = B_M^2 - B_S^2. \quad (3.2)$$

where B_M is the breadth of the diffraction line and

B_S is the breadth of the line from a standard.

3.3.4 Scanning Electron Microscopy (SEM)

The surface morphology of all prepared catalysts was examined with a PHILIPS XL30FEG SEM. Each sample was prepared by dispersing the catalyst in isopropanol. The sample was vigorously shaken with hand or by a vortex mixer. Then, a drop of the suspension was placed on the SEM's stub and the solvent was allowed to evaporate at room temperature. Finally, this specimen was ready to load in the SEM's chamber for examination. A photo of the SEM system is shown in Figure 3.4.

Figure 3.3 XRD Rikagu RINT 2000 at PPC.

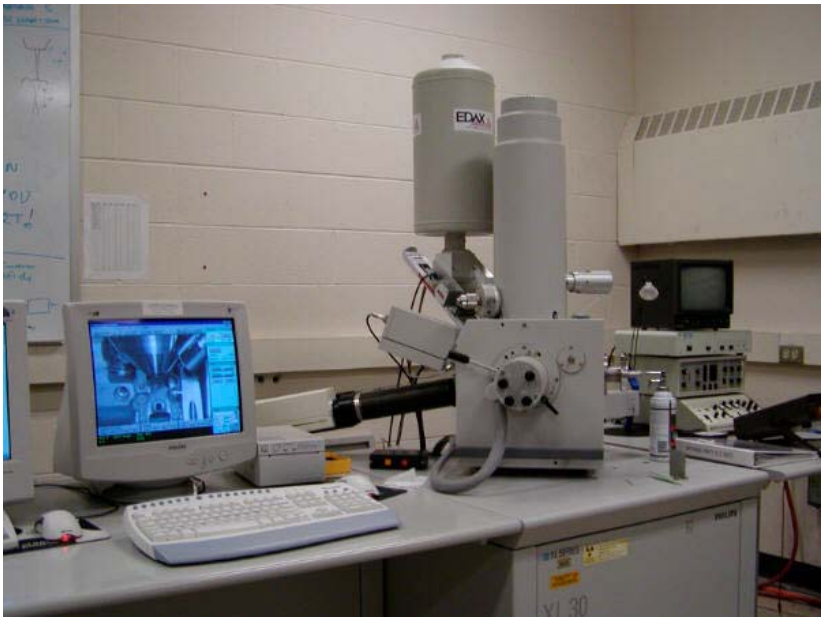

Figure 3.4 SEM PHILIPS XL30FLG at EMAL.

3.3.5 Scanning Transmission Electron Microscopy (STEM) and Transmission Electron Microscopy (TEM)

A JOEL 2010F transmission electron microscope operating at 200 kV equipped with energy dispersive spectroscope (EDS) was employed to identify the existence of Ag and Au particles on the catalyst surface. The catalyst samples were ground into fine powder and ultrasonically dispersed in isopropanol. A small droplet of the suspension was deposited on a honey carbon copper grid with 200 mesh sizes, and the solvent was evaporated prior to loading the sample into the microscope. Figure 3.5 shows a photograph of the TEM system.

Figure 3.5 TEM JOEL 2010 F at EMAL.

3.3.6 Temperature programmed desorption (TPD)

The experiments were carried out by placing 100 mg of catalyst into a U-tube quartz reactor. The catalyst was pretreated in a flow of O_2 (8% O_2/N_2) at 200°C for 1 h. In an attempt to better assess the role of gold on oxygen adsorption; two different experimental protocols were employed. In the first protocol "with cooling step", the catalyst was cooled from 200°C to room temperature under oxygen atmosphere. Then, the reactor was flushed with N_2 for 0.5 h in order to remove the gas phase of O_2. After that, the reactor temperature was ramped from room temperature to 600°C at a linear heating rate of 40°C min^{-1} in flowing N_2 (30 ml min^{-1}). In the second protocol "without cooling step", the oxygen pretreated catalyst was flushed with N_2 for 0.5 h at 200°C and then the reactor temperature was ramped linearly from 200°C to 600°C. The desorbing oxygen was detected with a thermal conductivity detector (TCD).

3.3.7 X-Ray Photoelectron Spectroscopy (XPS)

X-ray photoelectron spectroscopy (XPS) spectra of the studied catalysts were recorded by using a PHI 5400 XPS with Mg Kα radiation (1253.6 eV). Copper Cu $2p_3$ (934 eV) was used to calibrate the binding energies. The analyzer was operated at 89.45 eV pass energy for survey spectra and 17.90 eV pass energy during all high-resolution core level spectra. The base pressure of the spectrometer was $3x10^{-9}$ torr. A catalyst sample was pressed into a pellet and the pellet was then placed on the sample holder. Then, it was kept in the load lock for out-gassing under high vacuum condition for a period of time before it was introduced into the analyzer. The spectra of Ag $3d_3$ and Ag $3d_5$ were investigated, but it was hard to identify Au spectra because of the small gold concentration. In all catalyst samples, the characteristic O1s, Al 2s, Al 2p and C1s peaks were observed. Figure 3.6 illustrate a photo of XPS unit used in this work.

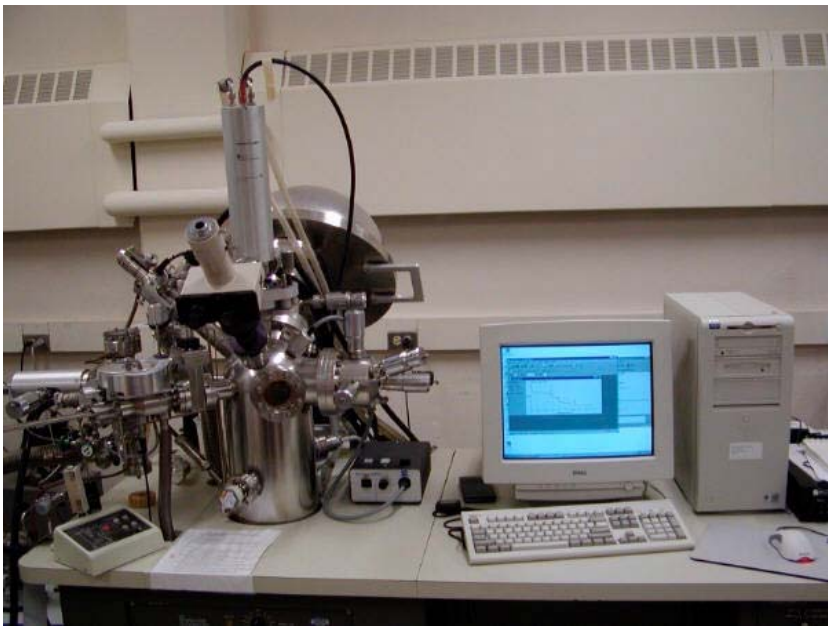

Figure 3.6 PHI 5400 XPS at EMAL.

3.4 Ethylene Epoxidation Reaction Experiment

The experimental study of ethylene oxidation was conducted in a differential reactor, which was operated at 24.7 psia. Catalyst powder of 300 mg was placed inside a Pyrex tube and secured by glass wool plugs. The tubular reactor being 10 mm in diameter was placed in a furnace equipped with a temperature controller. The catalyst was initially pretreated with oxygen at 200°C for 2 h in order to diminish some impurities and remove residual moisture from the catalyst. The feed gas was a mixture of 15% oxygen in helium, 30% ethylene in helium and pure helium (HP grade) obtained from Thai industrial gas (TIG). The flowrates of these three gas streams were regulated by mass flow controllers to obtain the feed gas composition of 6% oxygen and 6% ethylene with helium balance. The feed gas was passed through the reactor at a constant space velocity of 6,000 h^{-1} and the temperature was varied from 220 to 270°C. The compositions of the feed gases and effluent gases were analyzed by using an on-line gas chromatograph (HP5890 Series II) equipped with HaYeseb D 100/120-packed column, capable of separating carbon dioxide, ethylene and oxygen. The ethylene oxide product was calculated from the carbon material balance with 0.25% carbon atom error (Yeung *et al.,* 1998 and Lafarga *et al.,* 2000). The presence of acetaldehyde could be ignored because it was formed in very small amounts as a result of further oxidation of acetaldehyde to carbon dioxide and water under the studied conditions. The schematic diagram of experiment setup is shown in Figure 3.7 and the system of this experiment is illustrated in Figure 3.8.

Calculations for the ethylene conversion, ethylene oxide selectivity and yield are based on the following equations:

$$\textit{Ethylene conversion } (X) = [F_{C_2H_4\ in} - F_{C_2H_4\ out}] / [F_{C_2H_4\ in}]$$

$$\textit{Ethylene oxide selectivity } (S) = [F_{C_2H_4O\ out}] / [F_{C_2H_4\ in} - F_{C_2H_4\ out}]$$

$$\textit{Ethylene oxide yield } (Y) = X \cdot S = [F_{C_2H_4O\ out}] / [F_{C_2H_4\ in}]$$

where $F_{C_2H_4\ in}$ = Inlet mass flowrate of ethylene (mole/min)

$F_{C_2H_4\ out}$ = Outlet mass flowrate of ethylene (mole/min)

$F_{C_2H_4O\ out}$ = Outlet mass flowrate of ethylene oxide (mole/min)

In addition, outlet mass flowrates of ethylene oxide were determined from the carbon balance and calculated sample was shown in Appendix C. However, the presence of ethylene oxide over catalysts was identified by DRIFTS experiment.

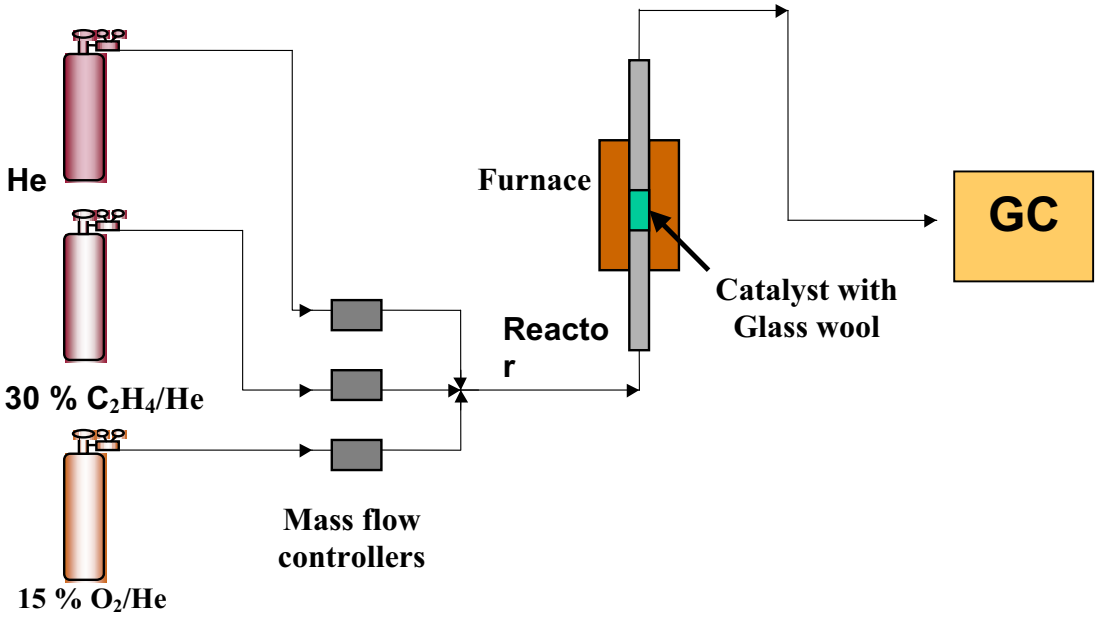

Figure 3.7 Schematic diagram of experimental setup for ethylene oxidation.

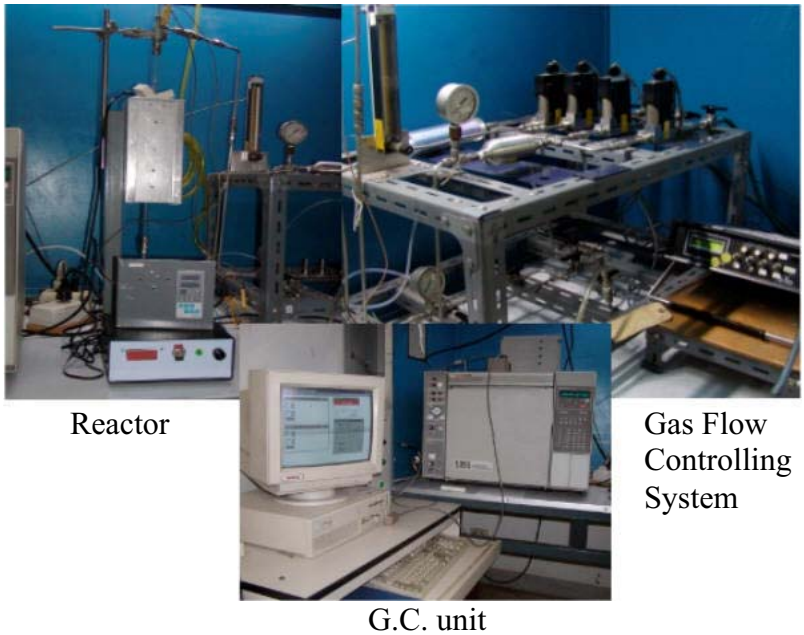

Figure 3.8 Experimental setup of ethylene oxidation at PPC

CHAPTER IV
RESULTS AND DISCUSSION

4.1 Selective Oxidation of Ethylene over Ag on High Surface Alumina Catalysts

4.1.1 Characterization results

Oxygen TPD profiles for various Ag loadings are shown in Figure 4.1 There was a sole desorption peak for each catalyst at around 250 – 300°C. The position of the TPD peak maximum shifted to slightly higher temperatures with increasing silver loading and reacheed a maximum value of 306°C for the 13.18% Ag/Al_2O_3 catalyst. The desorption curves show the onset of a broad additional desorption feature beyond 450°C. The first peak at around 250 – 300°C can be attributed to the decomposition of bulk Ag_2O to metallic Ag. The other peak starting at 450°C and extending to higher temperatures beyond 600°C may be due to the decomposition of the dispersed Ag_2O phase, which is more stable than bulk phase Ag_2O (Luo *et al.,* 1998). It was noticed that the amount of O_2 desorption for 13.18% Ag/Al_2O_3 was higher than for other silver loadings. This suggests 13.18% Ag/Al_2O_3 catalyst has the largest number of active silver surface sites capable to be adsorbed

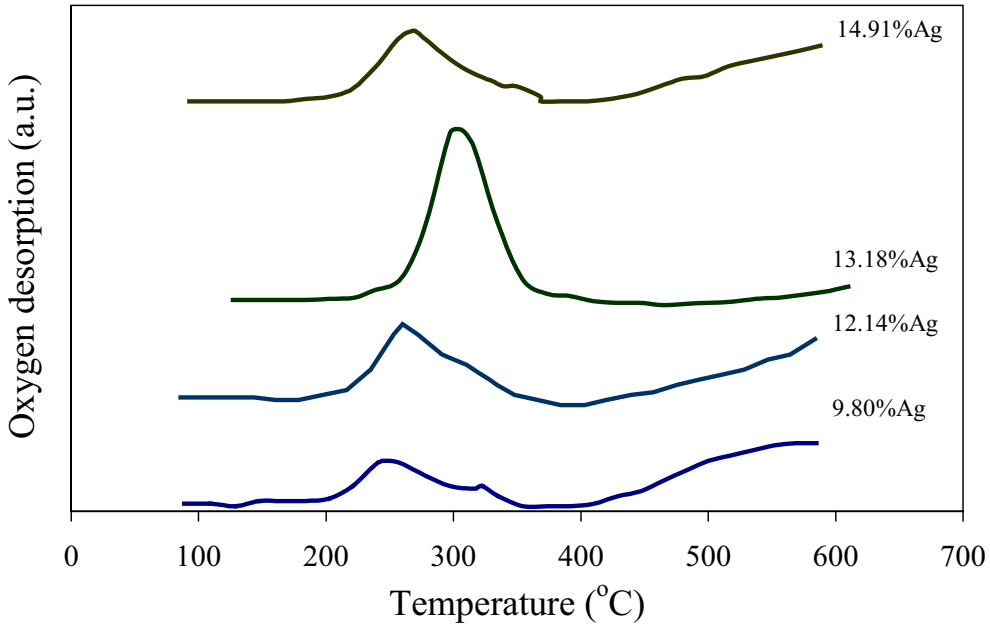

Figure 4.1 TPD profiles of O_2 of the Ag/Al_2O_3 at various silver loadings.

by oxygen. This is confirmed by XPS results as shown in Table 4.1 where the 13.18% Ag/Al_2O_3 has the highest AgO/Ag ratio obtained the highest ratio's value (1.83). However, for the starting condition of XPS, the catalyst sample was fresh, while the condition of TPD experiment was started by exposure with O_2, therefore; the AgO/Ag ratio after O_2 exposure should be higher. Thus, it showed the highest TPD profiles.

Table 4.1 The AgO/Ag ratios of Ag catalysts at different Ag loadings (from Ag $3d_5$ and $Ag3d_3$ of XPS)

Catalysts	AgO/Ag Ratio
9.80% Ag/Al_2O_3	1.51
12.14% Ag/Al_2O_3	1.62
13.18% Ag/Al_2O_3	1.83
14.91%Ag/Al_2O_3	1.34

Moreover, the XPS binding energy (BE) for each peak were nearly the same for the entire series of catalysts. The Ag $3d_3$ binding energy was in the range of 373.86 - 374.85 eV, corresponding to the characteristic for the metallic state of silver (374.2 eV). The Ag $3d_5$ binding energy of 367.78-368.61 eV can be attributed to AgO (367.7 eV),and Ag and Ag_2O (368.2 eV). The O 1s peak (530.87-531.74 eV) corresponds to O 1s (531.1 eV) in the alumina support, in agreement with the Al 2p peak position. (72.9 eV) corresponding to Al_2O_3 [www.xpsdata.com].

The XRD patterns of catalysts with various silver loadings (Figure 4.2) display 4 dominant peaks at $2\theta = 38°$ and 77° representing for metallic silver, and at $2\theta = 44°$,and 64° representing for silver oxide and metallic silver. These peaks reached higher intensity with increasing silver loading. The results indicate that all silver catalysts contain both metallic silver and silver oxide. The mean crystallite size was calculated from the Scherrer equation as shown in Table 4.2. As be seen in table, the calculated values of the mean crystallite sizes of the catalysts are in the range of 180-190 Å.

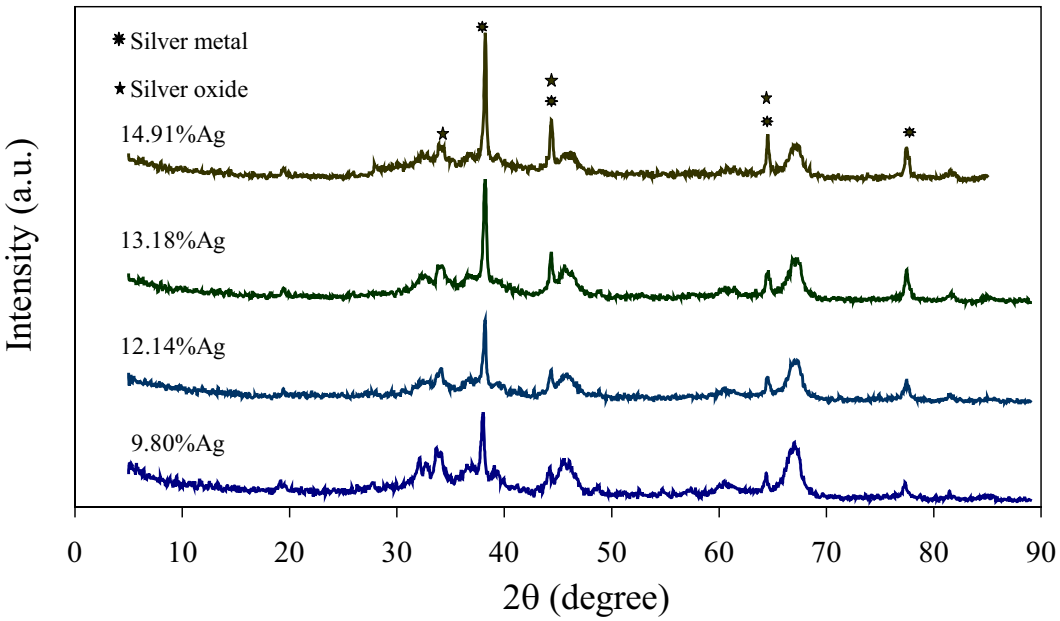

Figure 4.2 XRD patterns of the Ag/Al_2O_3 catalysts at various silver loadings.

Table 4.2 Mean crystallite sizes of silver catalysts at various silver loadings

Catalysts	Mean crystallite size, Å
9.80% Ag/Al_2O_3	180
12.14% Ag/Al_2O_3	189
13.18% Ag/Al_2O_3	192
14.91%Ag/Al_2O_3	183

STEM equipped with EDS can be used to identify the elemental composition of individual particles of a catalyst. Figure 4.3 shows transmission electron micrographs of the 13.18% Ag/Al_2O_3 catalyst. Figure 4.3 (a) shows many high contrast particles, and many of them are agglomerated into aggregated particles. Figure 4.3 (b) shows a close-up image of an area containing particles of both silver as well as silver oxide dispersed on the support. For example, when the electron

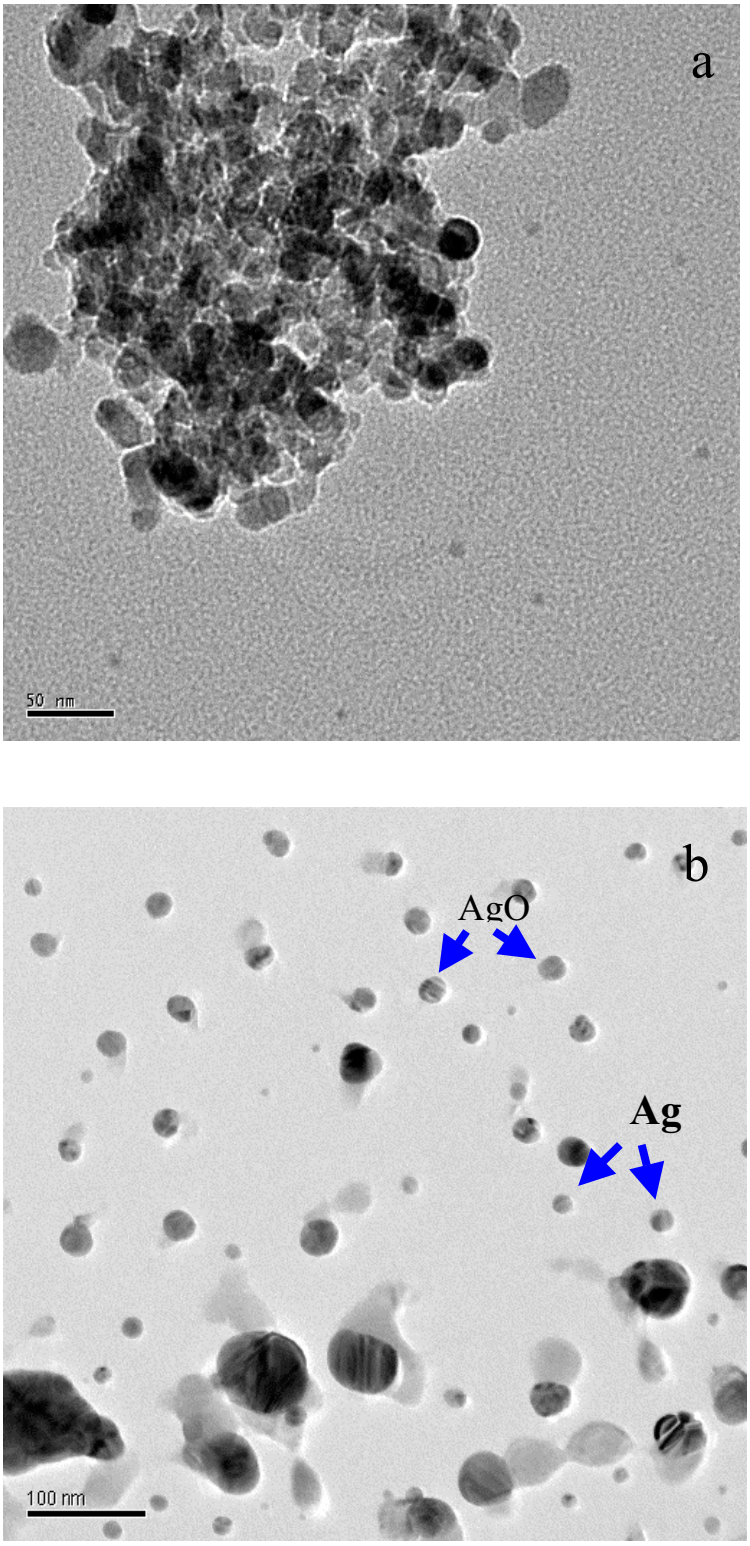

Figure 4.3 STEM micrographs of 13.18% Ag/Al_2O_3: (a) aggregates of silver and silver oxide; (b) individual Ag and AgO particles.

beam was stopped over one individual particle whose particle size was around 210 Å, the EDS analysis revealed that this particle contained only metallic silver. A somewhat larger particle with about 300 Å in diameter, on the other hand, gave EDS signals for both silver as well as oxygen, indicating that this particle consists of AgO. From the micrographs, it is apparent that there is a wide range of particle sizes. Some of the very large particles observed are significantly larger than the average particle size calculated from XRD line broadening. The reason for this discrepancy is that XRD actually measures the size of microcrystalline domains; while the regions of high contrast visible in a STEM micrograph may encompass particles containing several microcrystalline domains.

4.1.2 Catalyst activity for epoxidation of ethylene

The ethylene epoxidation experiments were carried out at different temperatures. For each operational temperature, the reaction was allowed to continue until it came to steady state before taking data. Figure 4.4 shows ethylene conversion increases with increasing temperature, while selectivity of ethylene oxide decreases drastically with increasing temperature (Figure 4.5). It can be simply concluded that a higher temperatures favor the complete oxidation over the partial oxidation. Within the Ag loading range studied, it was noticed that at any given temperature, the ethylene oxide selectivity increased with increasing Ag loadings and reached a maximum at 13.18% Ag/Al_2O_3. From the characterization results, it also appears that this catalyst has the largest crystallite size (Table 4.2) and AgO/Ag ratio (from XPS, Table 4.1). Therefore, this fumed alumina support can facilitate the formation of large Ag particles which are according to STEM either metallic Ag with average size of 210 Å , or AgO with average size of 300Å. Wu *et al.* (Wu and Harriott, 1975) found that catalysts with Ag particle size less than 20 Å showed nearly zero ethylene oxide selectivity, and the selectivity improved with increasing particle size up to 1000 Å. Thus, it can be stated that ethylene epoxidation depends more on the particle size than on the interaction between Ag and the Al_2O_3 support. Moreover, a high ratio of AgO/Ag of catalyst showed better performance because in the presence of AgO can suppress the dissociation of molecular oxygen on silver surface. The reason is that if no vacant neighboring adsorption sites are available,

molecularly adsorbed oxygen will not dissociate and may remain molecularly adsorbed to high temperatures (Ertl *et al.*, 1997). From the TPD result, the 13.18% Ag/Al_2O_3 catalyst provides the maximum oxygen coverage than others; therefore, ethylene epoxidation is maximized. van Santen and his group (Ertl *et al.*, 1997) demonstrated that maximum oxygen coverage obtainable had a stoichiometry of one oxygen adatom to one surface silver, as in AgO, located in subsurface position. The presence of subsurface oxygen atoms will reduce the electron density on neighboring silver atoms. When contact with an alkene, the interaction between ethylene π electrons and oxygen electrons will lead to a flow of oxygen electrons to the positive charged surface metal atoms. Surface oxygen adatoms then behave as electrophilic oxygen atoms that preferentially react with high electron density part of molecule, as the π bond of ethylene as shown in Figure 4.7. Based on the results show in Figure 4.5 and 4.6, the optimum temperature is around 240°C giving around 80% for the ethylene oxide selectivity and around 2% for the ethylene oxide yield. Mao and his groups (Mao and Vannice, 1995a and Mao and Vannice, 1995b) studied the high surface area $\alpha-Al_2O_3$ and found that it gave non ethylene oxide selectivity. The reason is that their catalysts contained very small Ag particles with around 2-3 nm, which are considerably too small to promote ethylene epoxidation.

The effects of concentration ratio of C_2H_4:O_2 on the ethylene oxide selectivity and yield are shown in Figures 4.8-4.9. Due to a very low conversion of ethylene, oxygen material balance was applied to calculate ethylene oxide product. Figure 4.8 shows that the concentration ratio of C_2H_4:O_2 is 6%:6% provides the highest ethylene oxide selectivity, while the concentration ratio of C_2H_4:O_2 is 10%:10% exhibits the highest yield (Figure 4.9). As be known, the ethylene oxide reaction requires a high oxygen surface coverage on the silver surface (Ertl *et al.*, 1997); therefore, the 10% to 10% ratio provides the highest oxygen coverage resulting in the highest yield as compared to the other concentration ratios having lower oxygen concentration.

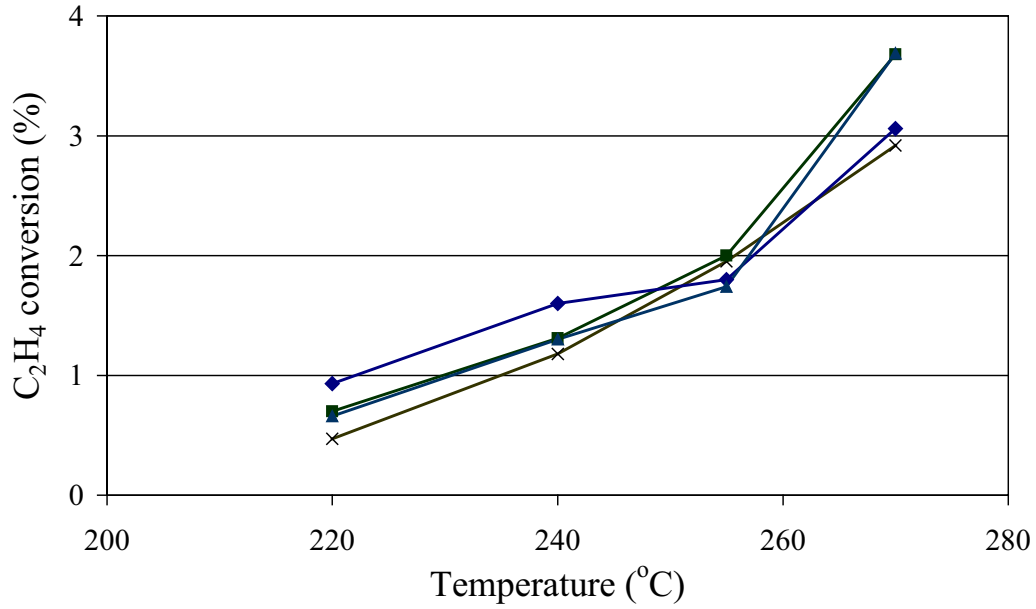

Figure 4.4 Ethylene conversion at various silver loadings at space velocity of 6,000 h^{-1}, P = 10 psig and 6% O_2 and 6% C_2H_4 balance with He: (✕) 9.80% Ag; (■) 12.14% Ag; (◆) 13.18% Ag; (▲) 14.91% Ag.

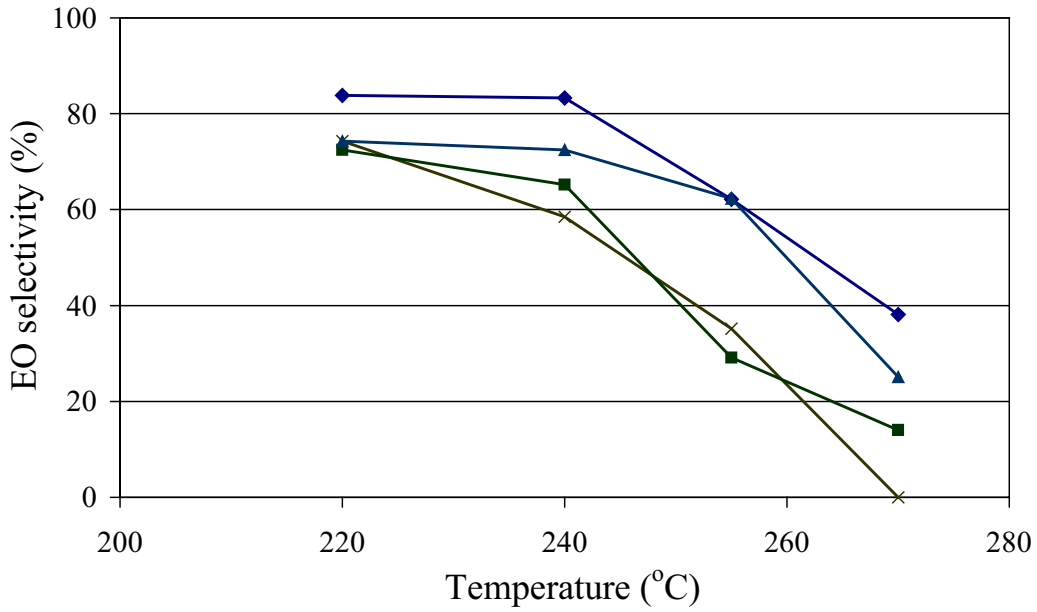

Figure 4.5 Ethylene oxide selectivity at various silver loadings at space velocity of

6,000 h^{-1}, P = 10 psig and 6% O_2 and 6% C_2H_4 balance with He:
(×) 9.80% Ag; (■) 12.14% Ag; (◆) 13.18% Ag; (▲) 14.91% Ag.

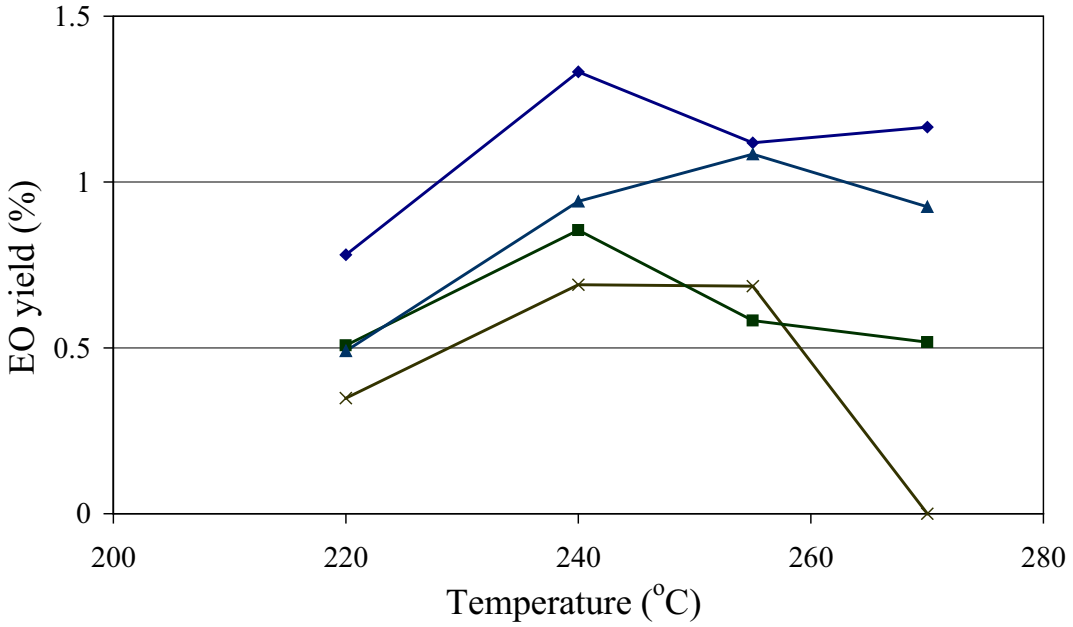

Figure 4.6 Ethylene oxide yield at various silver loadings at space velocity of 6,000 h^{-1}, P = 10 psig and 6% O_2 and 6% C_2H_4 balance with He:
(×) 9.80% Ag; (■) 12.14% Ag; (◆) 13.18% Ag; (▲) 14.91% Ag.

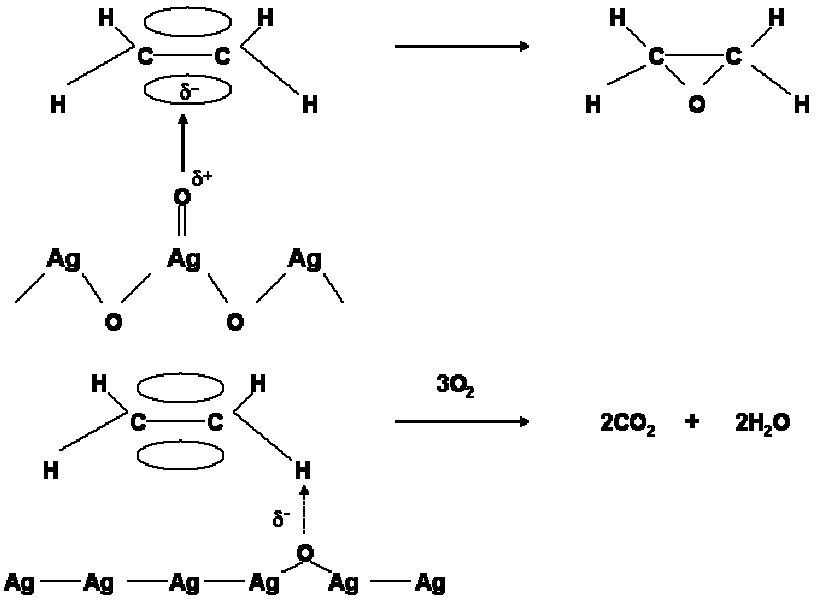

Figure 4.7 Schematic representation of the surface conditions that lead to epoxidation.

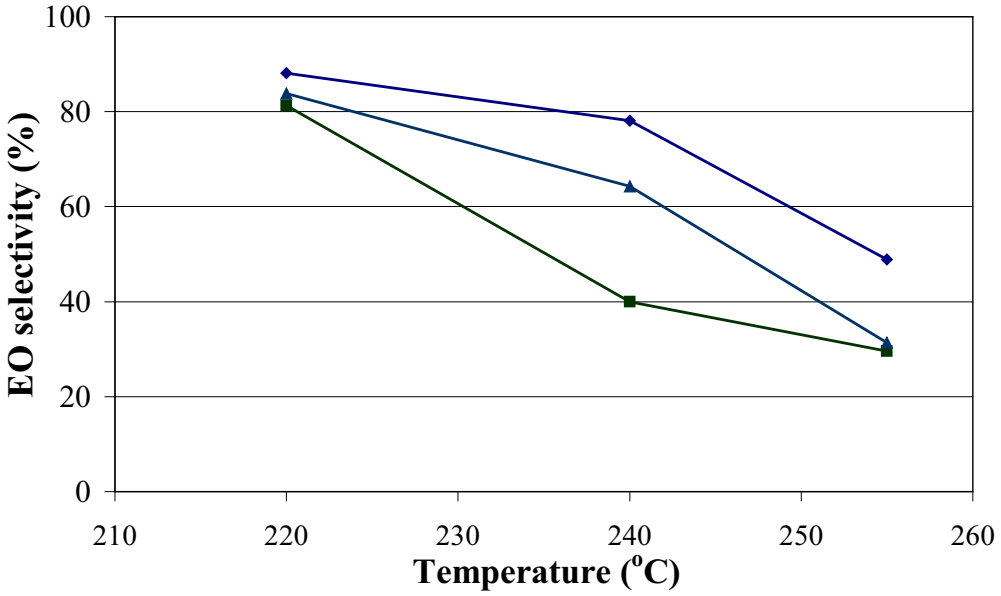

Figure 4.8 Ethylene oxide selectivity at 13.18% Ag/Al_2O_3 with space velocity of 6,000 h^{-1}, P = 10 psig for various ratio of C_2H_4:O_2: (■) 12%:6%; (◆) 6%:6%; (▲) 10%:10%.

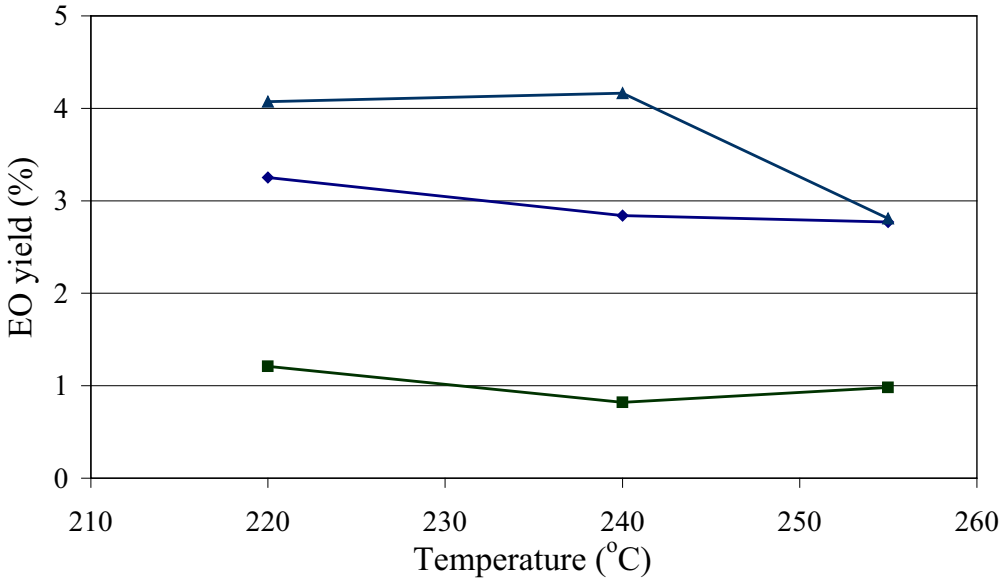

Figure 4.9 Ethylene oxide yield at 13.18% Ag/Al_2O_3 with space velocity of

6,000 h^{-1}, P = 10 psig for various ratio of C_2H_4:O_2: (■) 12%:6%; (◆) 6%:6%; (▲) 10%:10%.

The presence of ethylene oxide was confirmed by the subsequence reaction detected with mass spectrometry (as shown in Appendix A, Figure A.1). With this technique, the result showed the trend of ethylene oxide presence, but it did not clear. Therefore, DRIFTS reaction was another technique to prove ethylene oxide occurred over the catalyst. The procedure of DRIFTS experiment has already discussed in chapter III. The reaction of 13.18% Ag on Al_2O_3 catalyst was done at 220°C. The FT-IR spectrum was presented only the spectrum collected after 30 min on stream under steady state reaction. As can be seen from Figure 4.10, it is noticed some bands in the range 1000-2000 cm^{-1} that are wavenumbers at 1020, 1336, 1408, 1453, 1582 and 1625 cm^{-1}. Comparing to a library's information, this spectrum was attributed to epoxy ring (800-1300 cm^{-1}) and CH-bend (1300-1600 cm^{-1}) functional group (Skoog *et al.*, 1998). In addition, there are bands of CO_2 at 2317 and 2360 cm^{-1} (does not present on graph). Therefore, it confirms that ethylene oxide can be produced over monometallic Ag catalysts.

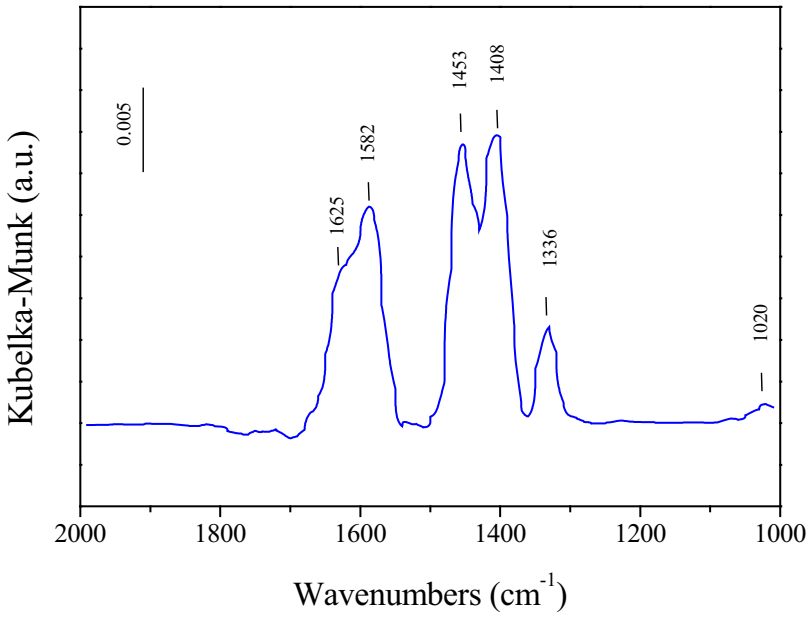

Figure 4.10 DRIFTS spectrum of 13.18% Ag/Al_2O_3 samples recorded after 30 min exposure of gases mixture with concentration ratio

of C_2H_4:O_2 = 2%:2%.

4.1.3 Conclusions

The TPD profiles of oxygen showed a slight shift of the maximum deposition peak towards higher temperatures with increasing silver loadings. The corresponding temperature for the TPD peak maximum reached the highest value for the 13.18% Ag/Al_2O_3, followed by a decrease to lower peak temperatures with further increase in Ag loading. The desorption peaks can be ascribed to the decomposition of Ag_2O to metallic Ag. The catalyst that showed the highest selectivity and yield of ethylene oxide gave the highest desorption peak temperature, suggesting that in this catalyst the AgO phase is more stable. There is no clear trend in particle size as a function of silver loading. Analytical electron microscopy revealed the presence of both metallic Ag and AgO particles. In general, the AgO particles tend to be larger than the metallic Ag particles. The average particle size calculated from XRD is smaller than the STEM derived average particle size. This may indicate that some of the particles contain more than one microcrystalline domain. From the experimental reaction results, it was found that 13.18% Ag/Al_2O_3, which provided the largest crystallite size, gave the highest conversion of ethylene and selectivity and yield of ethylene oxide. It was a good correlation between crystallite size and the activity study that this high surface alumina provided suitable Ag particle size enhanced the ethylene epoxidation. Moreover, silver on high surface alumina prevented sintering effect due to high dispersion of silver. In addition, the effect of oxygen coverage on silver active site showed that high oxygen coverage as C_2H_4:O_2 = 10%:10% enhanced the ethylene oxide production.

4.2 Selective Oxidation of Ethylene over Alumina supported Bimetallic Ag-Au Catalysts

Gold is unique among metallic elements because of its resistance to oxidation and corrosion. In addition to its inert character, gold has very low affinity for gas adsorption. However, there is evidence that under certain conditions oxygen can adsorb on gold. For example (MacDonald and Hayes, 1970), when gold powder was exposed to molecular oxygen, oxygen uptake was observed over a wide temperature range with two distinct maxima at -50°C and 200°C, respectively. Adding gold into silver catalysts was found three adsorbed oxygen of atomic oxygen, molecular oxygen and subsurface oxygen at elevated temperatures and showed that alloying Ag with Au influenced the bond strengths with silver surface and modified the relative population of the adsorbed species (Kondarides *et al.*, 1996). In this work, a small amount of gold was added as a promoter in sequence on silver catalyst and to study the effect of gold on the ethylene epoxidation.

4.2.1 Characterization results

The effects of gold loading on TPD of O_2 were observed for the two experimental protocols, which are with and without a cooling step prior to TPD. Figure 4.11 shows TPD of O_2 after cooling to room temperature. There were no significant differences in the oxygen desorption temperature for catalysts with different gold loadings. There was no maximum desorption peak observed for blank alumina and the 0.79% Au/Al_2O_3 catalyst. This indicates that there are no measurable amounts of oxygen adsorbed on the alumina support and on pure gold supported on alumina. This was in marked contrast to the results of the desorption experiment without a cooling step. As shown in Figure 4.12, there is now a slight shift of the TPD peak maximum toward lower temperatures with increasing gold loading. For example, TPD of O_2 was shifted from 327°C (0.0% Au-13.18% Ag/Al_2O_3) to 308°C (0.93% Au-13.18% Ag/Al_2O_3). This indicates that the interaction between silver and oxygen is weakened in the presence of gold. This is in agreement with the observation of Kondarides and Verykios (1996) who reported a decrease of the heat of adsorption of oxygen with increasing Au content of supported

Ag-Au alloy catalysts. Toreis and Verykios (1987) and Kondarides and Verykios, (1996) explained their results in terms of electronic effects, where the electronic structure of silver atoms has been affected by nearest-neighbor gold atoms. They suggested that d-electrons of gold are transferred to silver and that this transfer is partially compensated by transfer of conducting s, p-electrons in the opposite direction, whereas the dissociative adsorption of oxygen on silver also requires transfer of electrons from silver to oxygen. It is expected that the electron deficiency due to neighbor interaction of gold atoms results in weakening of Ag-O bonds. Thus, the adsorbed species tend to desorb at lower temperatures. When comparing the two cases with and without a cooling step preceding desorption, it becomes apparent that desorption without a cooling step gives peak temperatures 10-20°C lower than in experiments with a cooling step. In TPD of O_2 of 0.79% Au/Al_2O_3 without a cooling step, small oxygen desorption peak is observed. It can be concluded that a small amount of oxygen can adsorb on supported gold at 200°C, but these adsorbed species are unstable when the sample is cooled to room temperature, as there was no TPD peak observed after the cooling step. This observation is in agreement with prior reports of oxygen adsorption on supported Au (Schwank, 1983 and references cited therein).

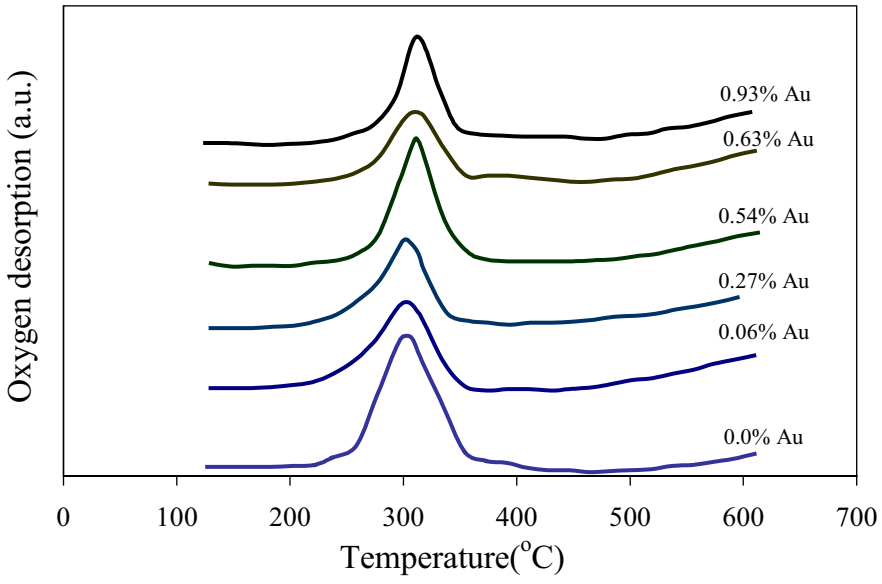

Figure 4.11 TPD profiles of O_2 with cooling step at room temperature of 13.18% Ag/Al_2O_3 at various gold loadings.

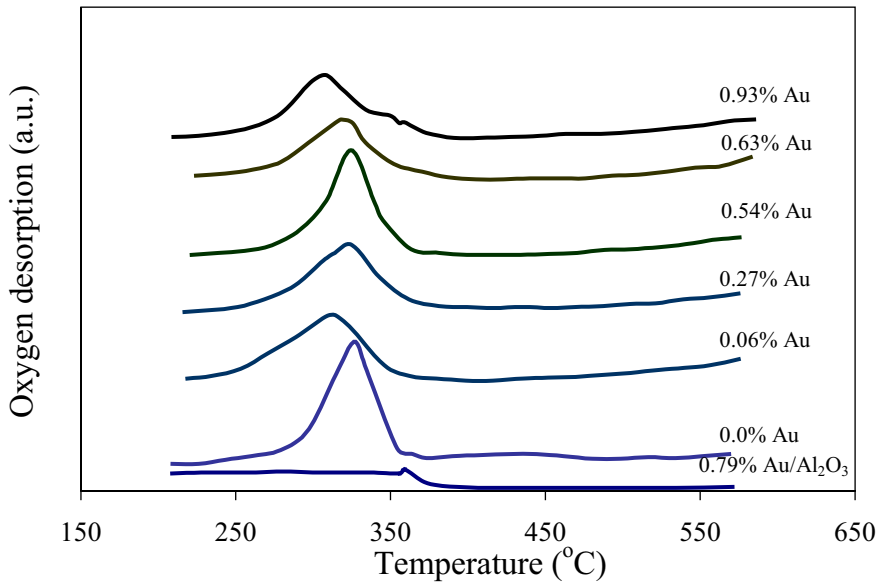

Figure 4.12 TPD profiles of O_2 without cooling step at room temperature of 13.18% Ag/Al_2O_3 at various gold loadings and 0.79% Au/Al_2O_3.

Figure 4.13 (a) shows XRD patterns of 13.18% Ag/Al_2O_3 with various gold loadings of 0.06, 0.27, 0.54, 0.63, and 0.93%. Silver and gold both are face-centered cubic metals and the atomic radii of the two elements are quite similar (1.444 Å for silver and 1.441 Å for gold). Given the relatively small amount of gold, the gold peaks cannot be clearly resolved from the silver peaks. The effect of gold on XRD patterns become more pronounced at higher gold loadings. Figure 4.13 (b) shows a closeup of the (111) peak region. In two of the catalysts, namely the 0.54%wt Au, and the 0.93 %wt Au samples, the (111) peaks are noticeably shifted to higher values. These shifts in XRD peak position indicate an interaction between Ag and Au, resulting in a quite significant decrease in lattice constant to a value of 4.0795 Å, compared to 4.0884 Å for the monometallic Ag sample. The theoretical lattice constants calculated form the atomic radius of silver and gold at room temperature are 4.085438 Å for Ag and 4.08453Å for gold. The (311) peak region (Figure 4.13 (c)) shows significant differences in both peak shape and position not only for the 0.54%wt Au and the 0.93 %wt Au samples, but also for the 0.63%wt Au sample. This lends further support to the notion that there is an interaction between Ag and Au, causing the lattice to contract. Figure 4.13 (d) shows how the lattice

constants determined from the peak positions for the (111) and (311) planes change as a function of gold content.

The mean crystallite size was calculated from XRD data by using the Scherrer equation. Due to the overlapping of the silver and gold peaks, we cannot calculate crystallite sizes of gold and silver separately. The mean crystallite size of the Ag-Au catalysts was in the range of 180-186 Å (Table 4.3). Gold addition did not appear to significantly affect the particle size.

a

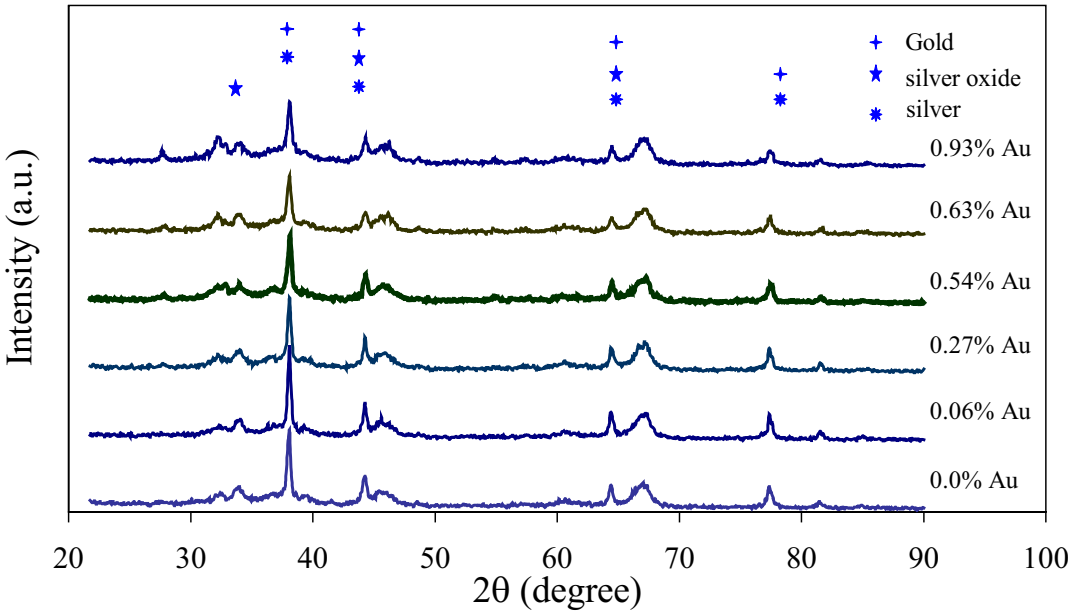

Figure 4.13 XRD patterns of 13.18% Ag/Al_2O_3 at various gold loadings: (a) overview patterns;

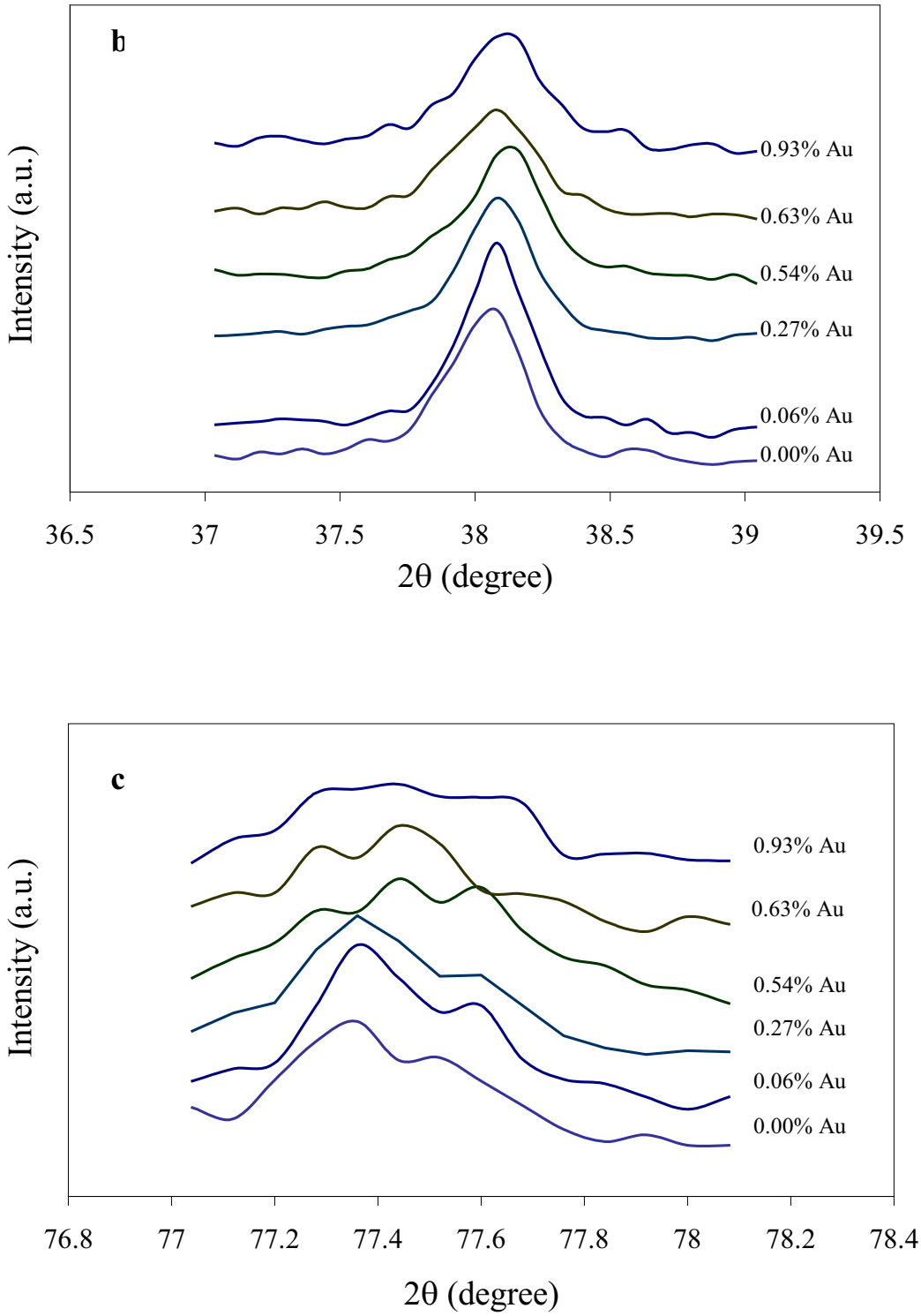

Figure 4.13 (cont'd) XRD patterns of 13.18% Ag/Al_2O_3 at various gold loadings: (b) (111) region; (c) (311) region;

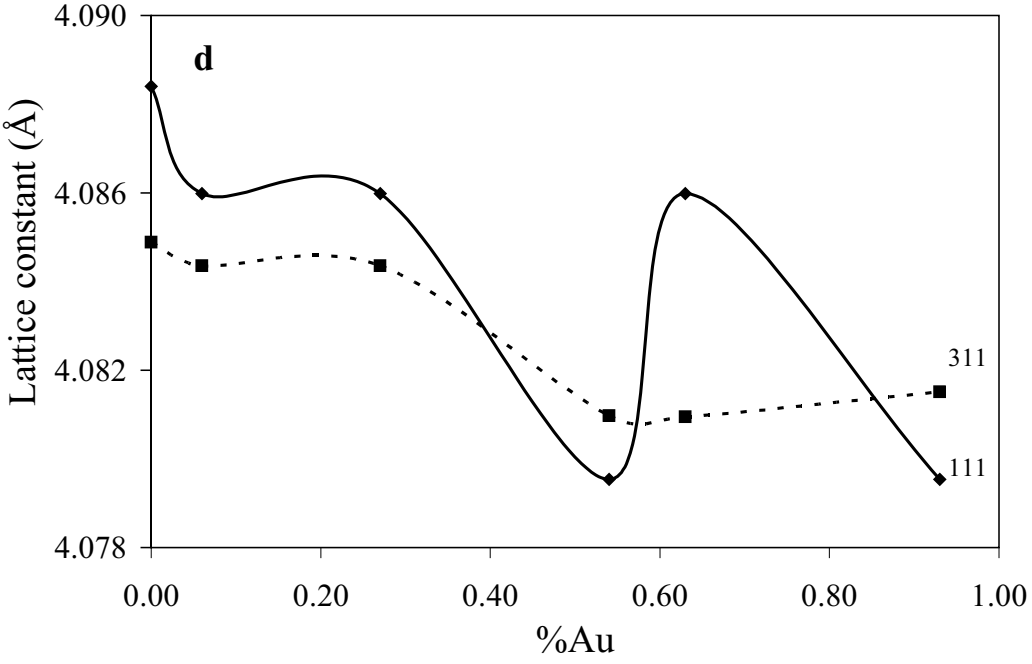

Figure 4.13 (cont'd) XRD patterns of 13.18% Ag/Al_2O_3 at various gold loadings: (d) lattice constant.

Table 4.3 Mean crystallite sizes of silver-gold catalysts for 13.18% Ag/Al_2O_3 at various gold loadings

Catalysts	Mean crystallite size, Å
0.06% Au-13.18% Ag/Al_2O_3	181
0.27% Au-13.18% Ag/Al_2O_3	186
0.54% Au-13.18% Ag/Al_2O_3	183
0.63% Au-13.18% Ag/Al_2O_3	186
0.93% Au-13.18% Ag/Al_2O_3	180

Scanning transmission electron microscopy with EDS was used to examine the size of particles and to identify the type of metal in individual particles. Figure 4.14 (a) and (b) show transmission electron micrographs of the 0.93% Au - 13.18% Ag/Al_2O_3 catalyst. Figure 4.14 (a) displays a region of the catalyst, containing many particles of high contrast. EDS indicated that these high contrast particles contained either metallic silver or silver oxide, but no gold signal was detected. However, in other regions of the catalyst, as shown on Figure 4.14 (b), EDS detected both gold and silver within individual particles as shown in Figure 4.14 (c). Among the catalyst regions investigated, no monometallic Au particles were found. It appears that the sequential impregnation resulted in a catalyst where some of the silver particles were covered with gold. However, from X-ray diffraction it can be implied that gold and silver do not form large Au-Ag alloy particles, but gold is most likely deposited on top of Ag particles. We cannot rule out the possibility that on some particles a thin Ag-Au alloy over layer has formed.

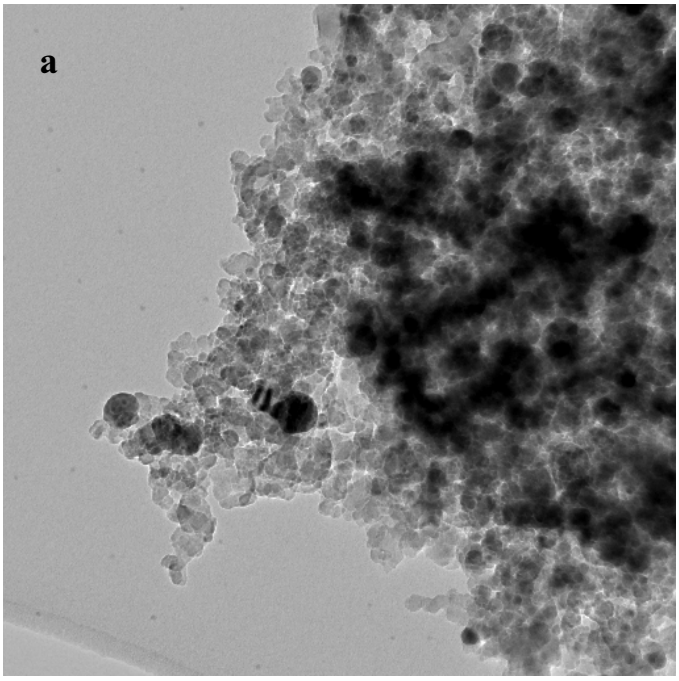

Figure 4.14 STEM micrographs of 0.93% Au-13.18% Ag/Al_2O_3:
(a) aggregates of silver and silver oxide without Au;

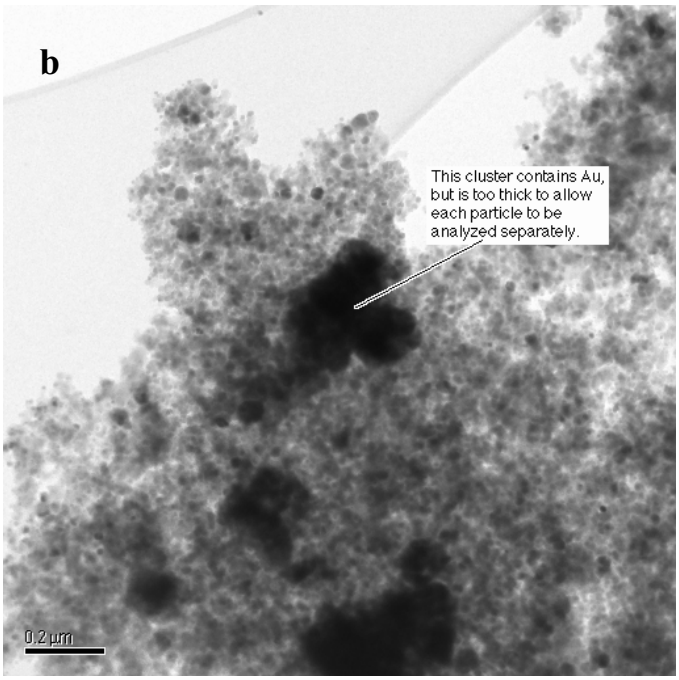

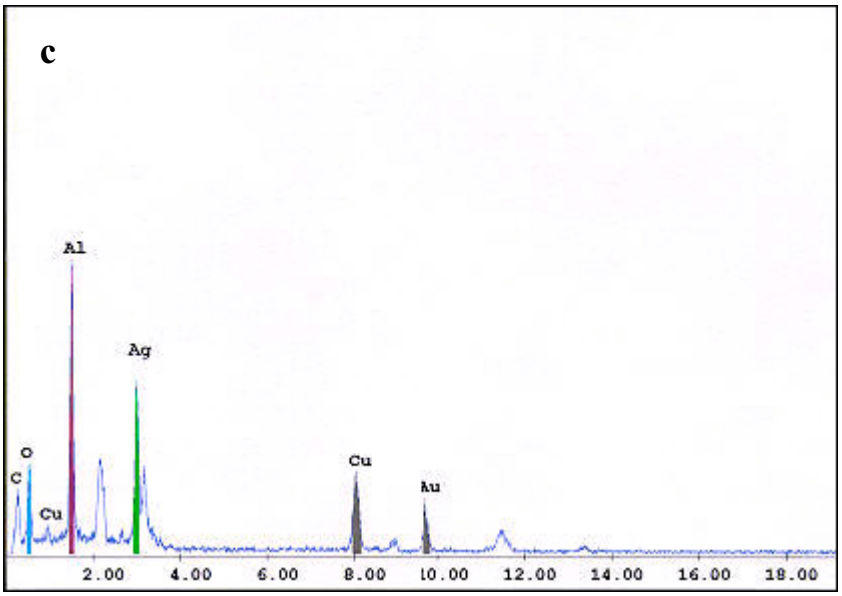

Figure 4.14 (cont'd) STEM micrographs of 0.93% Au-13.18% Ag/Al_2O_3: (b) aggregates with Au; (c) EDS profile.

4.2.2 Catalyst activity for epoxidation of ethylene

Form the previous work, 13.18% Ag/Al_2O_3 loading and space velocity of 6,000 h^{-1} were identified as the optimum conditions. Therefore, the effect of gold was studied under these conditions. Gold was added in the range of 0.06, 0.27, 0.54, 0.63, and 0.93% wt, to the catalyst with optimal silver loading (13.18% Ag/Al_2O_3). An addition of gold can improve significantly ethylene oxide activity as shown in Figures 4.15-4.16. The highest ethylene oxide selectivity of 90% is obtained on the catalysts containing 0.63% wt Au, but the highest ethylene oxide yield is obtained on the sample with 0.54% wt Au at 240°C (Figure 4.17). It is interesting to note that the catalyst with the highest yield showed a significant shift of the XRD peak. The reason why adding gold gives good ethylene oxide selectivity can be explained that gold acts as a diluting agent on the silver surface and creates new single silver sites, which favor molecular oxygen adsorption (Kondarides and Verykios, 1996). This molecular oxygen reacts with ethylene into ethylene oxide according to the mechanism proposed by Campbell (Campbell, 1985) and in agree with the TPD results. For the blank Au/Al_2O_3, a small of desorbed O_2 was found by

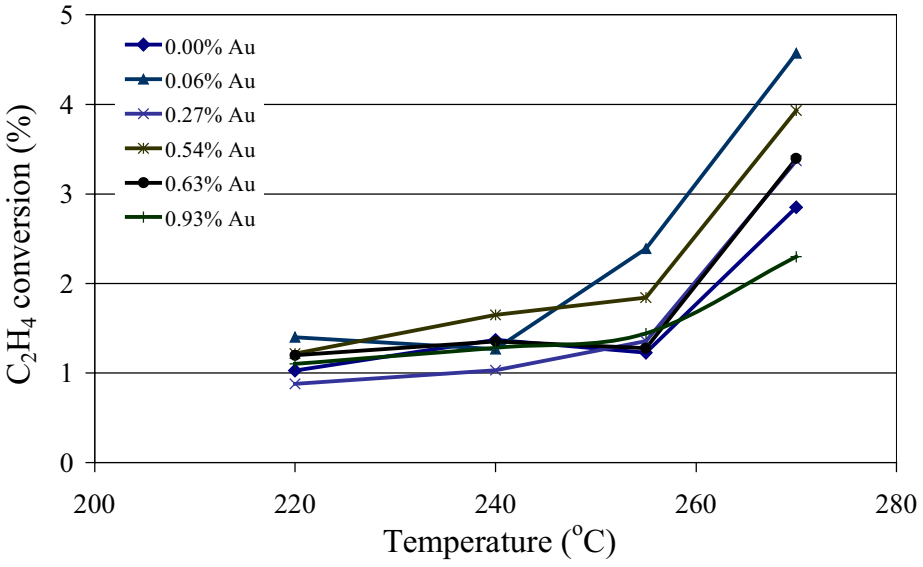

Figure 4.15 Ethylene conversion for 13.18% Ag/Al_2O_3 at various gold loadings at space velocity of 6,000 h^{-1}, P = 10 psig and 6% O_2 and 6% C_2H_4 balance with He.

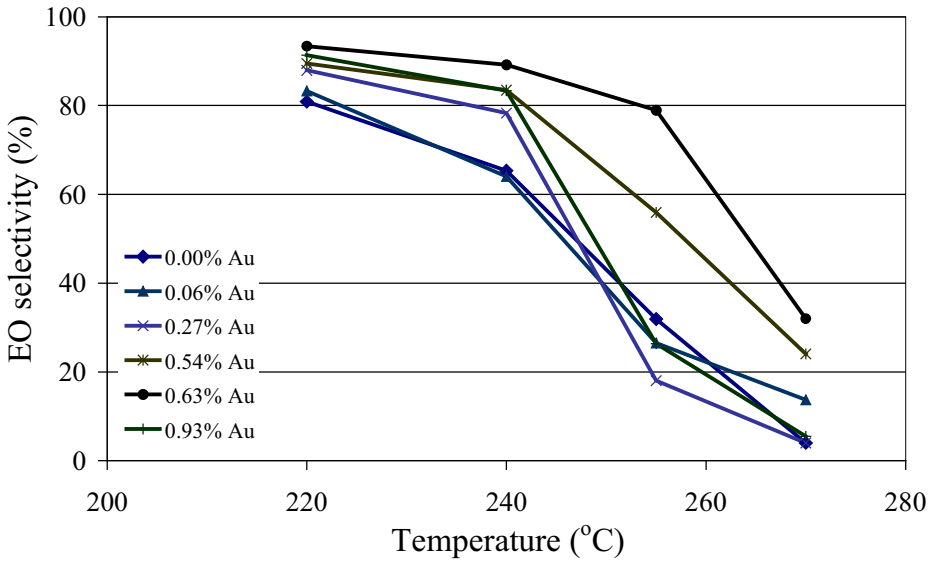

Figure 4.16 Ethylene oxide selectivity for 13.18%Ag/Al_2O_3 at various gold loadings at space velocity of 6,000 h^{-1}, P = 10 psig and 6% O_2 and 6% C_2H_4 balance with He.

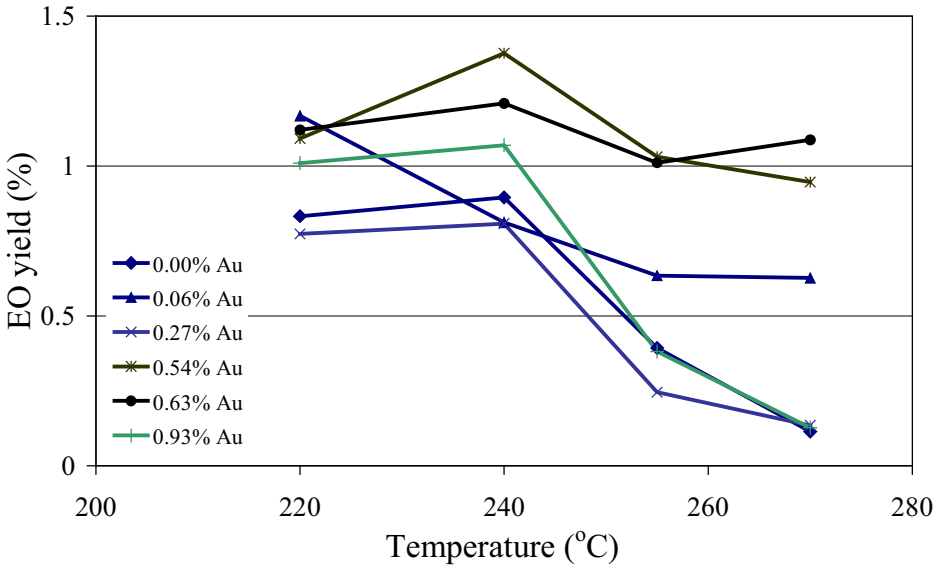

Figure 4.17 Ethylene oxide yield for 13.18% Ag/Al_2O_3 at various gold loadings at space velocity of 6,000 h^{-1}, P = 10 psig and 6% O_2 and 6% C_2H_4 balance with He.

TPD, However, no enhance of ethylene oxidation was observed on this catalysts. Therefore, one can neglect the effect of residual chorine from the use of auric acid in catalyst preparation, as the promoter effect of halogen is noticeable here. It is noteworthy that adding a small amount of Au to Ag supported on amorphous Al_2O_3 improves the ethylene oxide selectivity and yield. Therefore, Au represents a promising promoter for the epoxidation reaction of ethylene.

FTS

expe st as

shov l the

FT-I eam

unde ange

100(and

163 d to

epox oups

(Skc cm^{-1}.

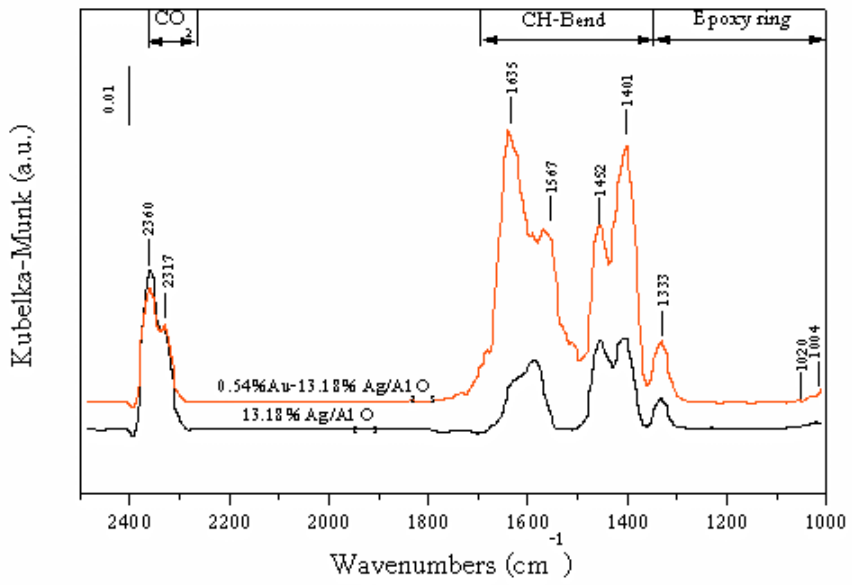

Figure 4.18 DRIFTS spectra of 0.54%Au-13.18% Ag/Al_2O_3 compare to13.18% Ag/Al_2O_3 samples recorded after 30 min exposure of gas mixture with concentration ratio of C_2H_4:O_2 = 2%:2%.

From the FT-IR results, it can be verified that ethylene oxide can be produced over these catalysts. Moreover, it was observed that bimetallic Au- Ag catalyst is more active than monometallic Ag catalyst as well as the activity study results. By the way, it is noteworthy that adding a small amount of Au to Ag support on amorphous Al_2O_3 improves the ethylene oxide selectivity and yield.

4.2.3 Conclusions

Based on the STEM-EDS results, it can be concluded that the gold-silver catalysts contain an inhomogeneous distribution of gold. Some particles are metallic silver and silver oxide, while some other particles contain both silver and gold. No evidence was found for separate gold particles. The mean particle size of the bimetallic silver-gold catalysts was around 180-186 Å compared with 180-190 Å for the monometallic Ag catalyst. Impregnation of the silver catalyst with gold did not appear to change the particle size. The TPD of oxygen showed a slight shift towards lower temperature with increasing gold loading. This indicates that there must be an interaction between Ag and Au causing a weakening of the adsorption bond strength between silver and oxygen. Within the range of gold loadings investigated, the catalyst containing 0.54 %wt Au on 13.18 %wt Ag/Al_2O_3 gave the highest activity and yield of ethylene oxide. In agreement with previous suggestions in the literature, the effect of gold is attributed to a geometric effect where the silver surface is diluted, creating single silver sites that favor molecular oxygen adsorption, which react with ethylene to produce ethylene oxide.

4.3 Ethylene epoxidation on TiO_2 supported Au catalysts

The study of well-known strong metal-support interaction (SMSIs) when the support is a reducible oxide has deserved an extensive attention. The migration of oxygen from reduced support particles onto metallic particles can induce formation of a suboxide of the support, the reduction being induced by the metallic particles (Holgado *et al.*, 1998). That group VIII noble metals supported on TiO_2 exhibits a strong metal-support interaction effect is well known. Schwank *et al.* (Shastri *et al.*, 1984) compared the behavior of gold supported on TiO_2 with other typical catalyst support materials. TiO_2 could stabilize as well as provide high dispersion of Au up to 700°C. It was suggested that this phenomenon did not appear to be due to the SMSI effect. Though a temperature of 700°C was sufficient to accomplish complete phase transformation of anatase to rutile in blank TiO_2, but no transformation occurred under identical conditions when TiO_2 impregnated was with Au. Au/TiO_2 is well known that it is good for low temperature, water-gas shift and propylene epoxidation; therefore, it should also be applicable for ethylene epoxidation.

4.3.1 Characterization results

TPD of oxygen experiments of Au/TiO_2 catalysts prepared by different methods were carried out with and without cooling step as described in previous results studying the effect of gold presence (chapter 4.2). As be seen from Figures 4.19-4.20, the desorption temperatures of oxygen with and without cooling step have the similar trend, Interestingly for three prepared catalysts and blank TiO_2, large desorption peaks were observed at around 400°C (with cooling step) and 460°C (without cooling step). These broad desorption peaks are assigned to desorbing of oxygen from TiO_2 support due to the removal of lattice oxygen from subsurface regions causing the creation of oxygen vacancies (Walton *et al.,* 1997). Typically, molecular oxygen desorbs from oxide surfaces between 27 to 127°C (Bielanski and Haber, 1991). As expected, 0.96% Au/TiO_2 sol gel gave the largest amount of desorption peak. The reason is that Au particle size of this catalyst is the smallest and better distribution on the support as compared to those with the other two preparation

methods according to the TEM results. Therefore, there are more active sites that O_2 can be absorbed and the interaction between Au and O_2 is weak and oxygen can easily be desorbed (Hayashi *et al.,* 1998). In addition, it is noticeable that an addition of gold on TiO_2 support affected to shift oxygen desorption peaks to lower temperature for all preparation methods as compared to blank TiO_2. It can explain in term of electronic effect that there are electrons transfer between gold atom and TiO_2 support while adsorbed oxygen also requires transfer of electrons between TiO_2 support and oxygen. Therefore, it is expected that the electron deficiency due to the neighbor interaction between gold atom result in weakening of Ti-O bond.

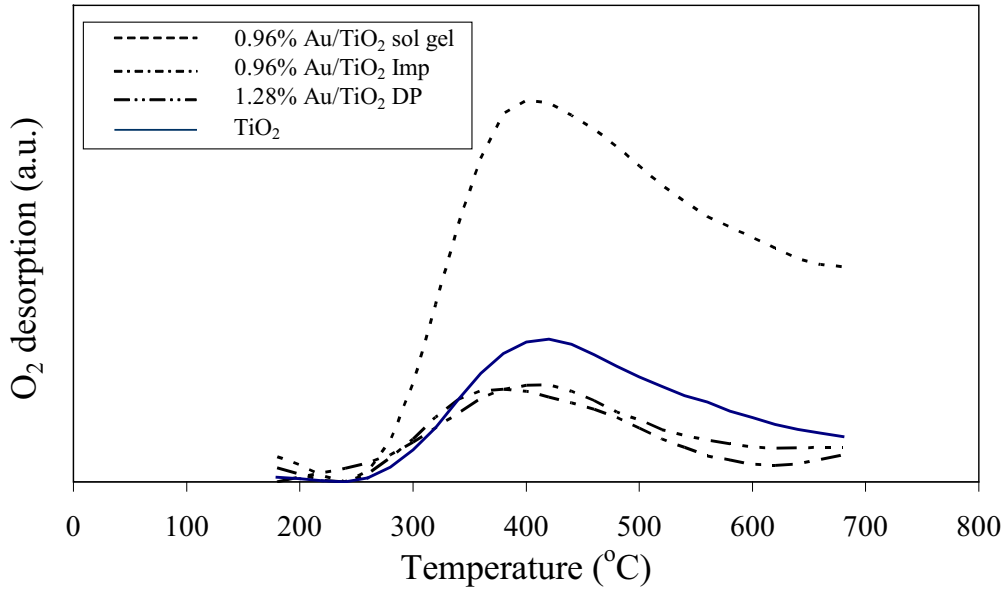

Figure 4.19 TPD profiles of O_2 with cooling step on Au/TiO_2 sample.

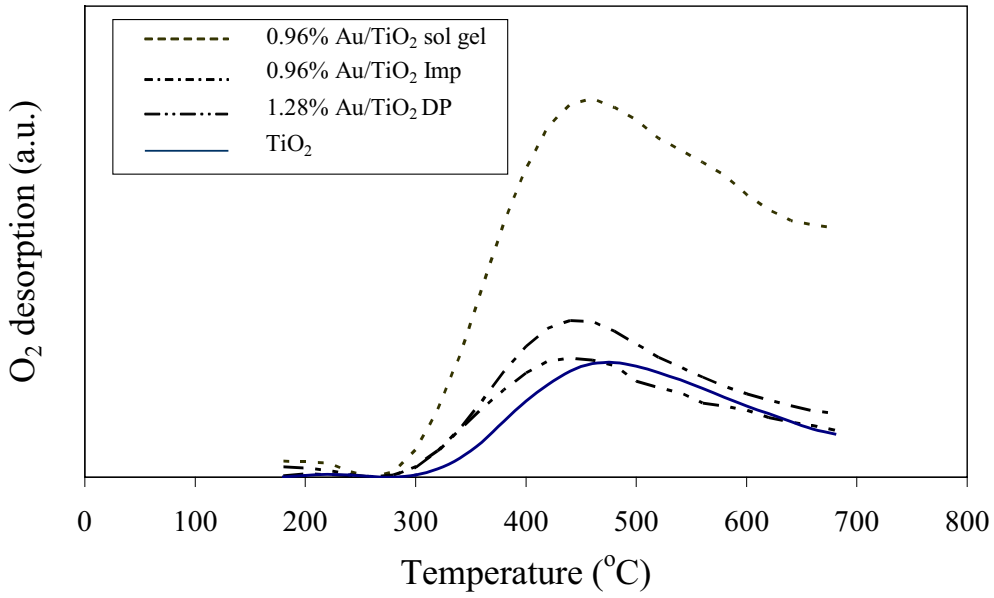

Figure 4.20 TPD profiles of O_2 without cooling step on Au/TiO_2 sample.

Figure 4.21 shows the oxygen desorption with and without cooling step of different Au/TiO_2 catalysts. It has been known that the oxygen desorption in the range 227-527°C may be ascribed to one or combination of the following effects; spill over oxygen (Bielanski and Haber, 1991), surface and sub-surface lattice oxygen (Komuro, 1975) and oxygen from Au sites (Walton *et al.*, 1998a). As can be seen from Figure 4.21, there is some oxygen desorption below 200°C due to the molecular oxygen on Au active site (Schwank, 1983). The highest desorption peaks at around 300-400°C are assigned to oxygen that adsorbs on the surface or subsurface on TiO_2. Furthermore, the oxygen desorption from the TiO_2 support is confirmed by using He as a exposure gas instead of O_2 as shown in Figure 4.22. The result insists that the oxygen desorbs out from the TiO_2 support at higher temperature range of 300-400°C. It is observed from the TPD results that oxygen desorption peak with He exposure gives higher amount of desorbed oxygen than that with O_2 exposure. It can be explained that TiO_2 is a nonstoichiometric material. There are two main defects for titania known as oxygen vacancies and interstitial Ti^{3+} ions. When the catalyst is exposed with O_2, it will anneal oxygen vacancies with oxygen absorption into the surface and sub-surface region of the lattice (Komuro, 1975 and

Walton *et al.*, 1998b). This results in higher stability of the lattice causing desorption of O_2 at higher temperature than exposure with He. When the catalyst is exposed to He at higher temperatures, it will produce the defect of lattice causing the unstable support. Therefore, the oxygen on the surface or sub-surface desorbs out more easily.

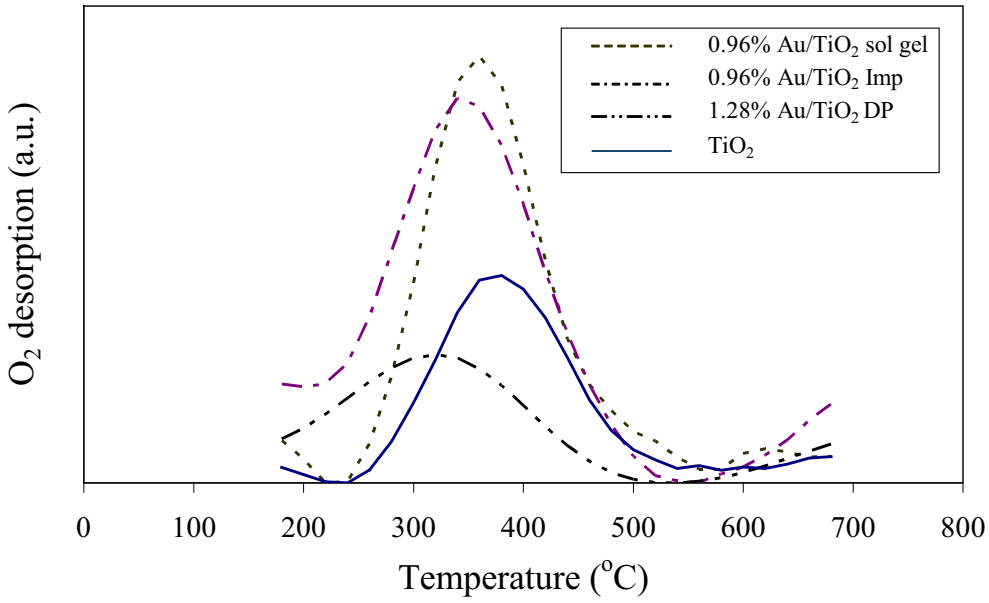

Figure 4.21 O_2 desorption difference between TPD runs with and without cooling step.

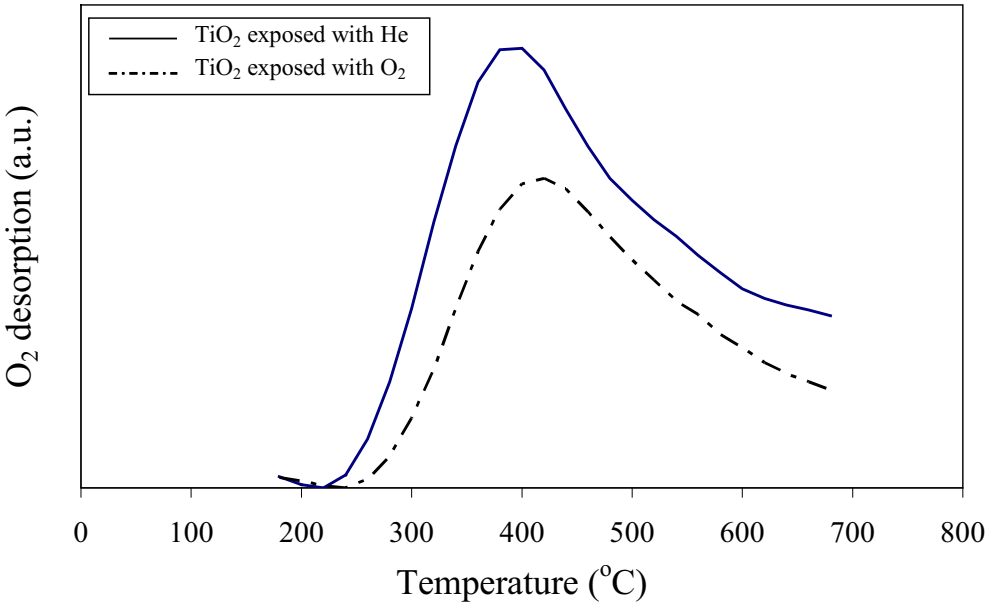

Figure 4.22 Comparison between TiO_2 (P25) exposed to He and O_2.

The XRD results of Au on TiO_2 catalyst prepared with different techniques are compared with pure TiO_2 and shown in Figure 4.23. The results show that 0.96% Au/TiO_2 with impregnation (Imp) and 1.28% Au/TiO_2 deposition-precipitation (DP), prepared by TiO_2 P25 from Degussa, are composed of both anatase (A) and rutile (R) phase but 0.96% Au/TiO_2 (sol gel) shows only anatase phase. All three catalysts have similar BET surface areas around 60 m^2/g.

As expected, the gold peaks are not clearly discernible from these XRD patterns, however very small peaks at 38.27°, 44.65° and 77.58° could be seen. The gold catalysts prepared have nanosize gold particles which are undetectable by XRD equipment. However, the average crystallite sizes of Au/TiO_2 catalyst prepared by impregnation, deposition-precipitation and sol gel were 23, 19 and 37 nm, respectively , calculated using the Scherer equation.

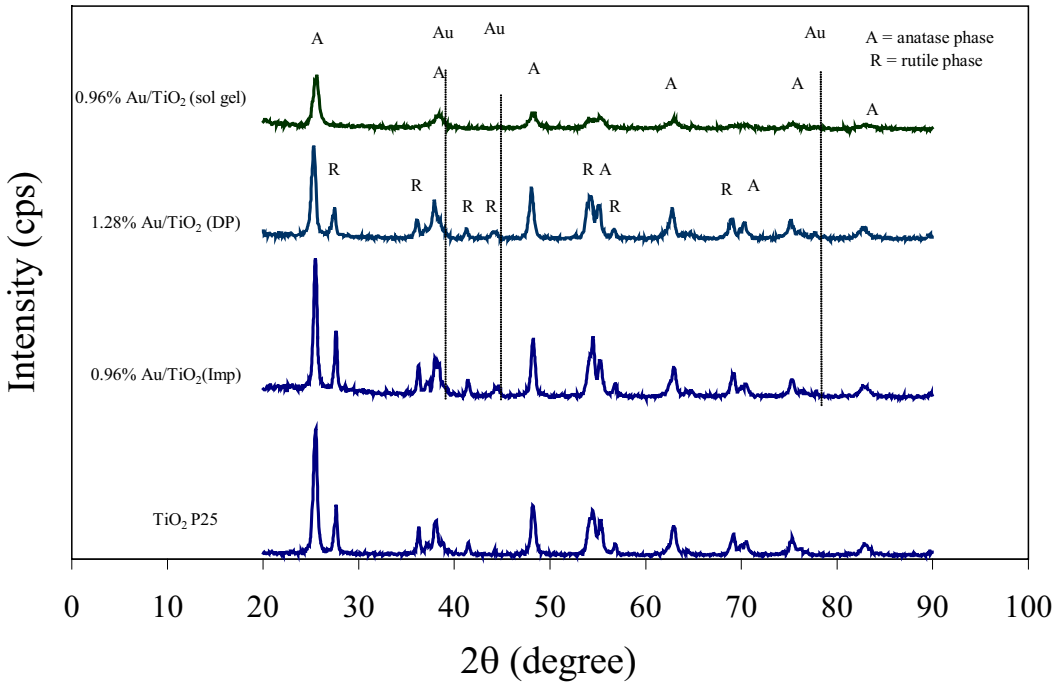

Figure 4.23 XRD patterns of Au/TiO_2 catalysts prepared with three different methods compared to XRD patterns for commercial TiO_2.

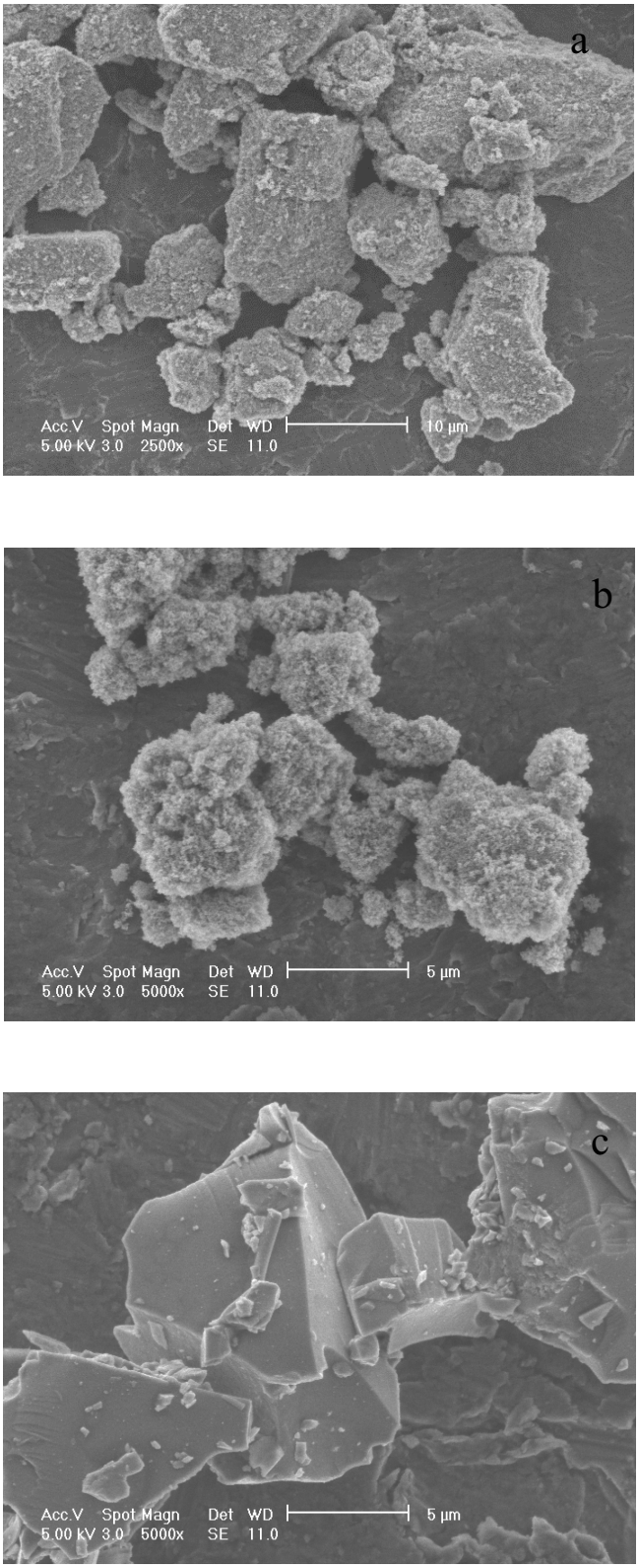

Figure 4.24 SEM surface morphology of gold catalysts prepared by different methods: (a) impregnation; (b) deposition-precipitation; (c) sol gel.

The SEM morphology of 0.96% Au/TiO_2 (Imp)(Figure 4.24 (a)) and 1.28% Au/TiO_2 (DP) (Figure 4.24 (b)) are found the deposition of gold atoms on the the surface supports, where as, 0.96% Au/TiO_2 (sol gel) has smooth clusters (Figure 4.24 (c)) because Au and Ti are formed into network structure.

The TEM micrographs shown in Figures 4.25-4.27 reveal the presence of the gold particles as dark spots in the catalyst clusters. The existence of gold particles on TiO_2 support was verified by using EDS focusing on the regions containing highly contrasting spots using transmission electron microscope. For 0.96% Au/TiO_2 (Imp), the gold particles are seen as highly contrasting spots with an average particle size of 3.2 ± 0.7 nm (Figure 4.25). Interestingly, the 1.28% Au/ TiO_2 (DP) catalyst apparently had a smaller Au particle size of 2.5 ± 0.6 nm (Figure 4.26). Figure 4.27 is a TEM micrograph of 0.96% Au/TiO_2 (sol gel) which reveal a better distribution of Au compare with those of the other two methods and the Au particle size is much smaller, 1.2 ± 0.3 nm. Therefore, Au deposited on TiO2 by the three preparative methods have nanoparticle sizes in the order sol gel <deposition-precipitation< impregnation.

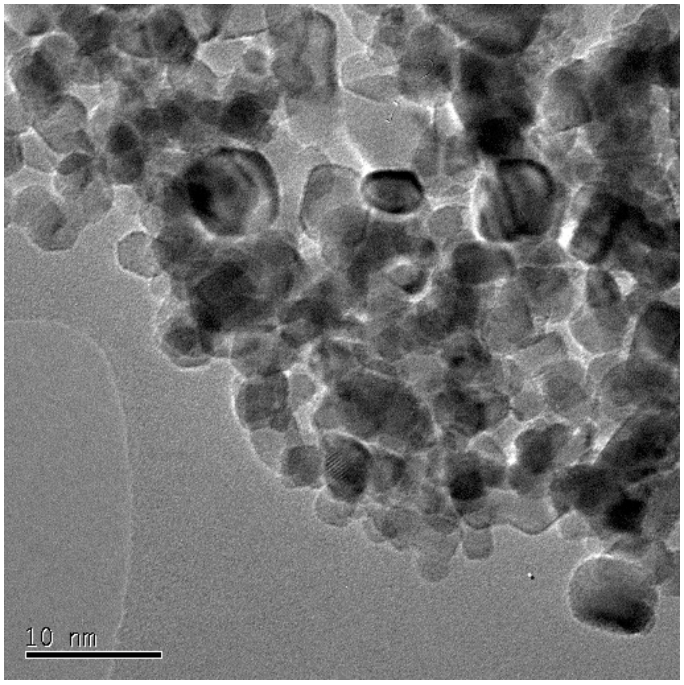

Figure 4.25 Gold particles (dark spots) on the TiO_2 surface for 0.96% Au/TiO_2 catalyst prepared by impregnation method.

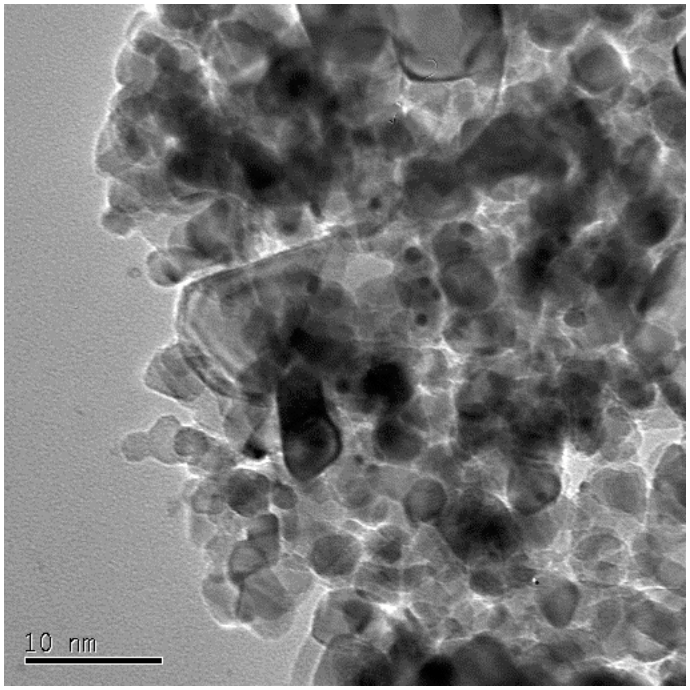

Figure 4.26 Gold particles (dark spots) on the TiO_2 surface for 1.28% Au/TiO_2 catalyst prepared by deposition-precipitate.

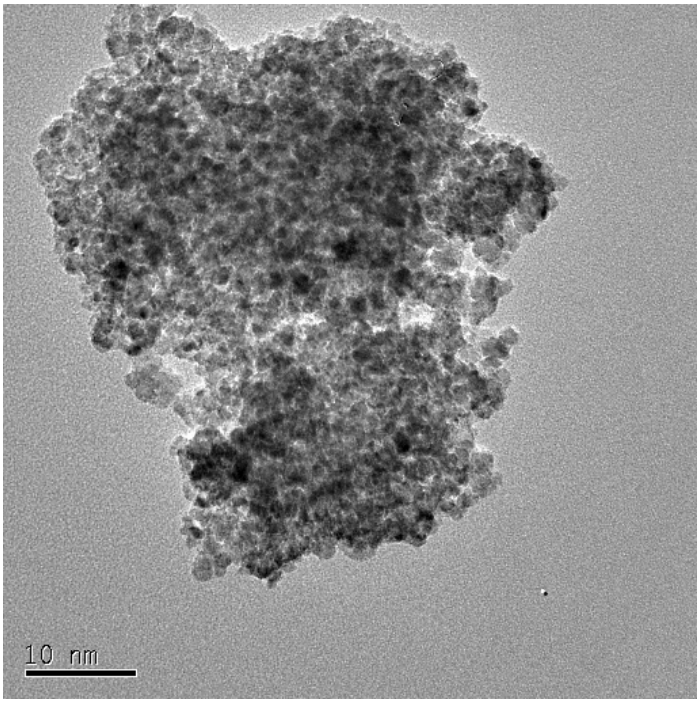

Figure 4.27 Gold particles (dark spots) on the TiO_2 surface for 0.96% Au/TiO_2 catalyst prepared by sol gel.

4.3.2 Catalyst activity of ethylene epoxidation

Figure 4.28 and 4.29 illustrates the effect of temperature on the ethylene epoxidation activity of Au/TiO_2 catalysts prepared by three different methods. For all studied catalysts, the ethylene conversion increased with increasing the reaction temperature, while the selectivity of ethylene oxide decreased with increasing reaction temperature, as a result of the two competitive reactions, partial oxidation and deep oxidation. For the deep oxidation reaction, both ethylene and ethylene oxide react with oxygen from the support to produce carbon dioxide and water. As is well known, a higher temperature leads to a higher rate of deep oxidation reaction resulting in lower ethylene oxide selectivity. Furthermore, 0.96% Au on TiO_2 prepared by impregnation gives a highest ethylene oxide selectivity and yield than the other two preparation methods of deposition-precipitation and sol gel (Figures 4.28-4.30). From the results of the present study, it is clearly seen that there is a good correlation between the particle size of gold and the ethylene epoxidation reaction. It has been reported that oxygen species are formed at the perimeter interface between the gold particles and the TiO_2 support when the particle size is greater than 2 nm (Hayashi *et al.,* 1998) . These oxygen species located at the perimeter interface are mostly molecular oxygen (Schwank, 1983 and Haruta and Date, 2001) which may react directly with ethylene in gas phase to produce the ethylene oxide. The results shows that the maximum yield is at 255°C somewhere in the region of 1% for 0.96% Au/TiO_2 with impregnation and around 0.8% for 1.28% Au/TiO_2 deposition-precipitation. On the other hand, 0.96% Au/ TiO_2 sol gel gives the maximum 0.6% ethylene oxide yield at 240°C. Moreover, the TPD results confirm that the interaction between oxygen molecule and Au are weak leading to the promotion on ethylene oxide. Regarding to the gold particle size, the impregnation method gives the largest gold particle size (~ 3 nm) compare to the other methods; therefore, ethylene oxide selectivity depended on the particle size of gold and the interaction between gold and support.

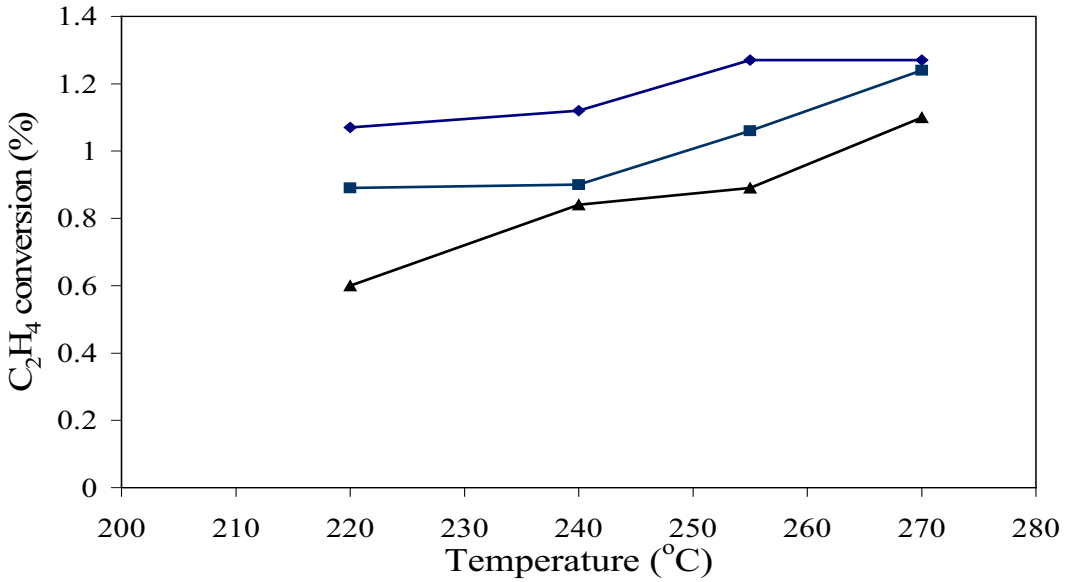

Figure 4.28 Ethylene conversion for different catalyst preparations at space velocity of 6,000 h^{-1}, P = 10 psig and 6% O_2 and 6% C_2H_4 balance with He: (◆) 0.96% Au/TiO_2 with impregnation; (■) 1.28% Au/TiO_2 deposition-precipitate; (▲) 0.96% Au/TiO_2 sol gel.

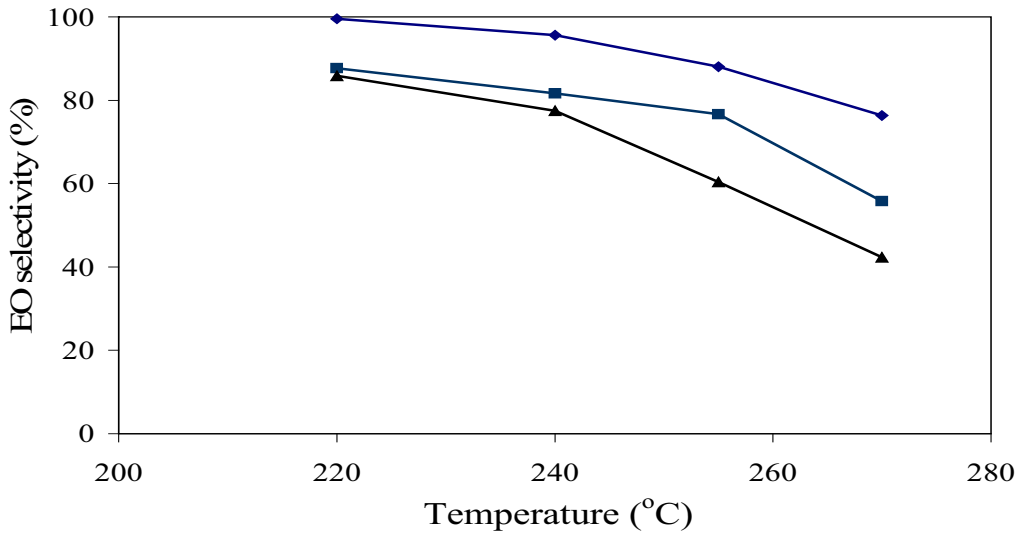

Figure 4.29 Ethylene oxide selectivity for different catalyst preparations at space velocity of 6,000 h^{-1}, P = 10 psig and 6% O_2 and 6% C_2H_4 balance with He: (◆) 0.96% Au/TiO_2 with impregnation; (■) 1.28%

Au/TiO_2 deposition-precipitate; (▲) 0.96% Au/TiO_2 sol gel.

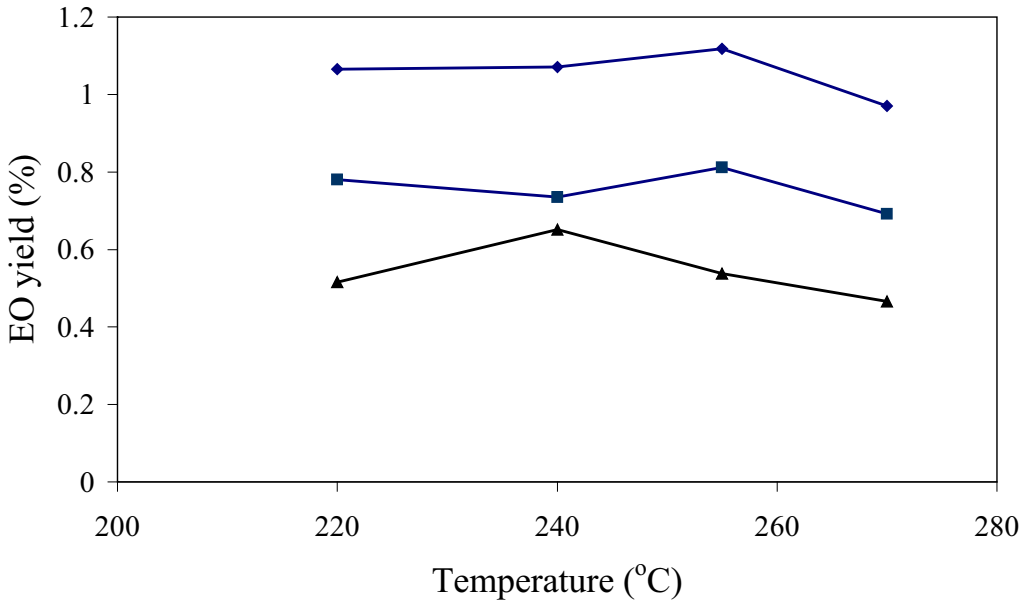

Figure 4.30 Ethylene oxide yield for different catalyst preparations at space velocity Of 6,000 h^{-1}, P = 10 psig and 6% O_2 and 6% C_2H_4 balance with He: (◆) 0.96% Au/TiO_2 with impregnation; (■) 1.28% Au/TiO_2 deposition-precipitate; (▲) 0.96% Au/TiO_2 sol gel.

The FT-IR results of the catalytic oxidation of ethylene are shown in the Figures 4.31-4.33, recorded at increasing exposure times at a reaction temperature of 220°C. The reaction was carried out at 220°C in the gas phase and the FT-IR spectra collected after 1, 5, 10, 15, 20, 25 and 30 min reaction times. These bands are compared with spectra containing CH-bending (1300-1700 cm^{-1}), epoxy functional groups (800-1300 cm^{-1}) and CO_2 functional groups (2300-2400 cm^{-1}). For 0.96% Au/TiO_2 (Imp), The dominant spectra of 1065, 1330, 1445 and 1717 cm^{-1} increase with increasing exposure time (Figure 4.31, curves b-g) compared with the curve of ethylene exposed for 30 min at 220°C (Figure 4.31, curve a). Figure 4.32 shows that for 1.28% Au/TiO_2 (DP) the intensity of bands (1015, 1347, 1445 and 1534 cm^{-1}) increases progressively with time. Similarly, the same behavior occurs for 0.96% Au/TiO_2 (sol gel) at spectra 1067, 1342, 1447 and 1530 cm^{-1} as shown in Figure 4.33, curves a-f. For the spectra of each catalyst the epoxy ring and CH-bending modes can be assigned (Skoog *et al.*, 1998). Thus, it was concluded that the

reaction over each catalyst in DRIFTS was ethylene epoxidation. Moreover, a comparison of Figures 4.31-4.33 for FT-IR spectra of ethylene epoxidation over each catalyst shows that 1.23% Au/TiO_2 (DP) is the most activity than others. Incidentally, spectra bands for CO_2 at 2330 and 2360 cm^{-1} were observed for each catalyst (not shown on the figures). From the results, it can be stated that there is a good relation between the particle size of gold deposited and activity of ethylene epoxidation reaction. It has been reported that oxygen species are formed at the perimeter interface between the gold particles and the TiO_2 support when the particle size of gold is greater than 2 nm (Hayashi *et al.*, 1998). These oxygen species are mostly molecular oxygen (Schwank, 1983 and Haruta and Date, 2001) which is believed to be responsible for reacting directly with ethylene in the gas phase to produce ethylene oxide.

4.3.3 Conclusions

Au/TiO_2 is used as a catalyst not only for CO oxidation, but also for epoxidation as well. This gold on TiO_2 was previously used for propylene epoxidation and found that the particle size had a significant effect on the epoxidation activity. Based on results of present studies, it is suggested that the reaction of ethylene epoxidation depends on the size of gold which is governed by a catalyst preparation method. The optimum size of gold particles was approximately 3 nm for the epoxidation reaction of ethylene. If the particle size was less than 2 nm, the reaction was difficult to occur that why the ethylene oxide yield of Au/TiO_2 (sol gel) was found to be low (0.6%). Moreover, support also has effect on the reaction because oxygen on support directly promotes complete combustion noticeably from TPD. Nevertheless, these gold catalysts still give the lower activity comparing to Au-Ag/Al_2O_3 catalysts of the previous study(Roatluechai *et al.*, 2002).

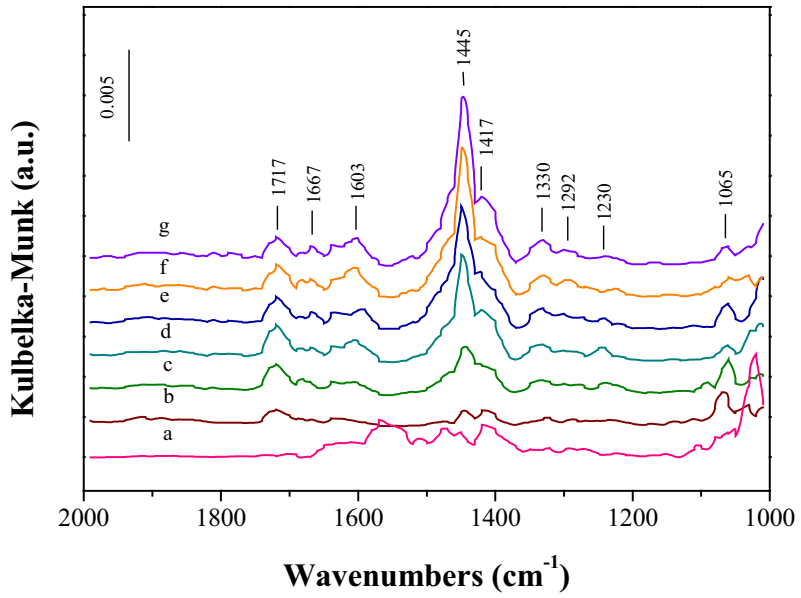

Figure 4.31 FT-IR spectra over Au/TiO_2 (Imp) of (a) ethylene and ethylene oxidation recorded after (b) 1 min; (c) 5 min; (d) 15 min; (e) 20 min; (f) 25 min; (g) 30 min.

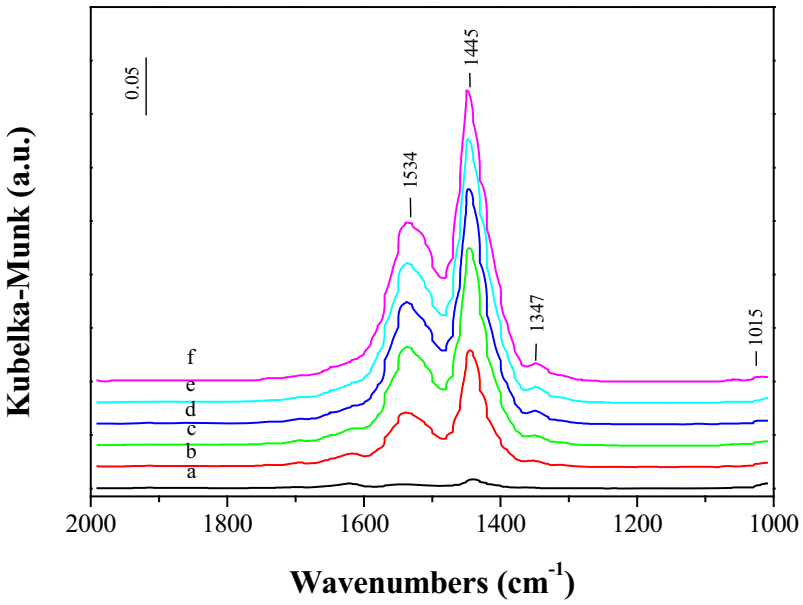

Figure 4.32 FT-IR spectra of ethylene oxidation over Au/TiO_2 (DP) recorded after (a) 1 min; (b) 10 min; (c) 15 min; (d) 20 min; (e) 25 min; (f) 30 min.

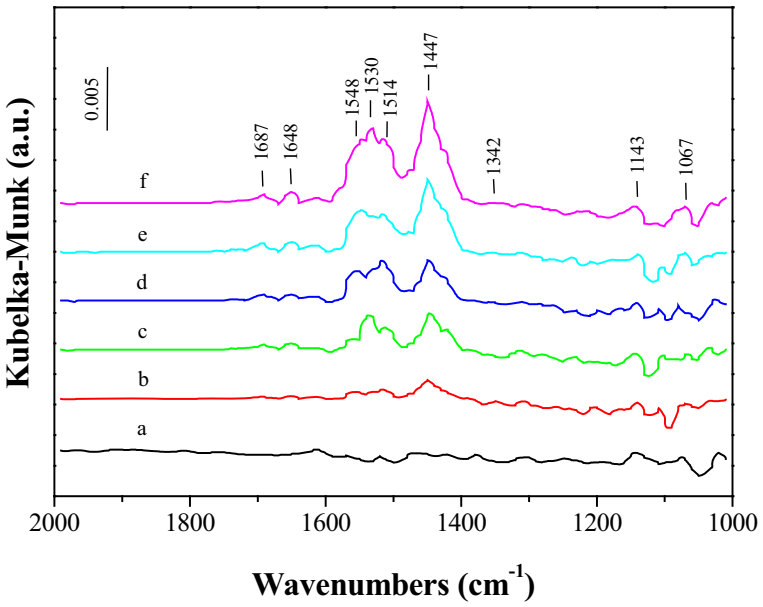

Figure 4.33 FT-IR spectra of ethylene oxidation over Au/TiO_2 (sol gel) recorded after (a) 1 min; (b) 10 min; (c) 15 min; (d) 20 min; (e) 25 min; (f) 30 min.

Bielanski, A. and Haber, J. (1991) Oxygen in catalysis. New York: M. Dekker.

Haruta, M. and Date, M. (2001) Advances in the catalysis of Au nanoparticles. Applied Catalysis A: General, 222, 427-437.

Hayashi, T., Tanaka, K. and Haruta, M. (1998) Selective vapor-phase epoxidation of propylene over Au/TiO_2 catalysts in the presence of oxygen and hydrogen. Journal of Catalysis, 178(2), 566-575.

Holgado, M. J., Inigo, A. C. and Rives, V. (1998) Effect of preparation conditions on the properties of highly reduced Rh/TiO2 (anatase and rutile) catalysts. Applied Catalysis A: General, 175(1-2), 33-41.

Komuro, M. (1975) Kinetic Studies of Oxygen Chemisorption on Rutile Single-Crystal Surface by Means of Electrical-Conductivity. Bulletin of the Chemical Society of Japan, 48(3), 756-761.

Roatluechai, S., Chavadej, S. and Schwank, J. (2002) Selective Oxidation of Ethylene over Alumina Supported Bimetallic Ag-Au catalysts. submitted to Appl. Catal.

Schwank, J. (1983) Catalytic gold: Application of element gold in heterogeneous catalysis. Gold bulletin, 16(4), 103-109.

Shastri, A. G., Datye, A. K. and Schwank, J. (1984) Gold Titania Interactions - Temperature-Dependence of Surface-Area and Crystallinity of Tio2 and Gold Dispersion. Journal of Catalysis, 87(1), 265-275.

Skoog, D. A., Holler, J. F. and Nieman, T. A. (1998) Principles of Instrumental Analysis. United State of America: Thomson Learning, Inc.

Walton, R. M., Gland, J. L. and Schwank, J. W. (1997) Gas sensing characteristics of ultrathin TiO2-x films investigated with XPS, TPD and in situ resistance measurements. Surface and Interface Analysis, 25(2), 76-80.

Walton, R. M., Dwyer, D. J., Schwank, J. W. and Gland, J. L. (1998a) Gas sensing based on surface oxidation reduction of platinum-titania thin films I. Sensing film activation and characterization. Applied Surface Science, 125(2), 187-198.

Walton, R. M., Dwyer, D. J., Schwank, J. W. and Gland, J. L. (1998b) Gas sensing based on surface oxidation reduction of platinum-titania thin films II. The role of chemisorbed oxygen in film sensitization. Applied Surface Science, 125(2), 199-207.

CHAPTER V
CONCLUSIONS AND RECOMMENDATIONS

Many researchers have claimed that only low surface area Al_2O_3 can enhance the ethylene epoxidation reaction. Several attempts were made unsuccessfully to use high surface area Al_2O_3 as support for Ag to produce ethylene oxide. In this research work, high surface area fumed Degussa C alumina support was investigated because of its non porous property that was believed to give large Ag particles and a good distribution of Ag particle sizes. It was found that this non porous support material could give large Ag particles, around 21 nm for metallic Ag, and 30 nm for silver oxide and could enhance the ethylene epoxidation reaction confirmed by DRIFTS experiment. Therefore, it can be stated that Ag on high surface area alumina can promote ethylene epoxidation provided that the Ag particle size is large. Moreover, high oxygen coverage on silver catalyst increases ethylene oxide activity.

Addition of gold as promoter enhanced the ethylene oxide selectivity. It is believed that gold can create single silver sites that favor molecular oxygen adsorption. In other words, gold can reduce the dissociation of molecular oxygen on Ag sites, lowering the concentration of atomic oxygen. In addition, the interaction between Ag and Au causes a weakening of the adsorption bond strength between silver and oxygen. In this work, 0.54% Au on 13.18% Ag/Al_2O_3 gave the highest ethylene epoxidation activity.

It has been known that gold catalyst is good for low temperature CO oxidation, propylene epoxidation and photocatalytic reaction. Thus, Au/TiO_2 with different methods of preparation were studied. From the results, the gold particle size of Au/TiO_2 influenced the ethylene epoxidation and the suitable gold particle was found to be around 4 nm. It is known that oxygen species located at the perimeter interface are mostly molecular oxygen which favors to ethylene epoxidation. If the particle size of Au was less than 2 nm, the epoxidation reaction would not occur. The different methods of catalyst preparation gave different gold particle sizes. Au/TiO_2 with impregnation gave the highest activity due to its optimum particle size.

The mechanism of adsorbed oxygen should be studied by using isotope O^{18} and O^{16}. Thus, the evidence of atomic and/or molecular oxygen adsorbed on this high surface area supports such as Al_2O_3 and TiO_2 can be verified. Moreover, the reaction mechanism of ethylene with the adsorbed oxygen species can be clarified.

Both Ag and Au particle sizes influence significantly on ethylene epoxidation. Therefore, catalysts with a wide range of particle sizes should be prepared by varying the calcination temperature. As is known, a high temperature can induce the agglomeration of the metal particle to form a bigger size.

REFERENCES

Al-Juaied, M. A., Lafarga, D. and Varma, A. (2001) Ethylene Epoxidation in a Catalytic Packed-Bed Membrane Reactor: Experiments and Model. Chemical Engineering Science, 56, 395-402.

Bamwenda, G. R., Tsubota, S., Nakamura, T. and Haruta, M. (1995) Photoassisted Hydrogen Production from A Water-Ethanol Solution: A Comparison of Activities of Au-TiO_2 and Pt-TiO_2. Journal of Photochemistry and Photobiology A: Chemistry, 89, 177-189.

Bielanski, A. and Haber, J. (1991) Oxygen in catalysis. New York: M. Dekker.

Boccuzzi, F., Chiorino, A. and Manzoli, M. (2001a) Au/TiO_2 nanostructured catalyst: effects of gold particle sizes on CO oxidation at 90 K. Materials Science & Engineering C-Biomimetic and Supramolecular Systems, 15(1-2), 215-217.

Boccuzzi, F., Chiorino, A., Manzoli, M., Lu, P., Akita, T., Ichikawa, S. and Haruta, M. (2001b) Au/TiO_2 nanosized samples: A catalytic, TEM, and FTIR study of the effect of calcination temperature on the CO oxidation. Journal of Catalysis, 202(2), 256-267.

Bukhtiyarov, V. I. and Kaichev, V. V. (2000) The Combined Application of XPS and TPD to Study of Oxygen Adsorption on Graphite-Supported Silver Clusters. Journal of Molecular Catalysis A-Chemical, 158, 167-172.

Bukhtiyarov, V. I., Boronin, A. I., Prosvirin, I. P. and Savchenko, V. I. (1994) Stages in the modification of silver surface for catalysis of the partial oxidation of

ethylene: II Action of the reaction medium. Journal of Catalysis, 150, 268-273.

Campbell, C. T. (1985) The selective epoxidation of ethylene catalyzed by Ag(111): A comparison with Ag(110). Journal of Catalysis, 94, 436-444.

Campbell, C. T. and Koel, B. E. (1985) Chlorine Promotion of Selective Ehylene Oxidation over Ag(110): Kinetics and Mechanism. Journal of Catalysis, 92, 272-283.

Carterand, E. A. and Goddard III, W. A. (1988) The surface atomic oxyradical mechanism for Ag-catalyzed olefin epoxidation. Journal of Catalysis, 112, 80-92.

Cullity, B. D. (1956) Elements of X-ray diffraction. Reading, Mass.: Addison-Wesley Pub. Co.

Dumas, T. and Bulani, W. (1974) Oxidation of Petrochemicals: Chemistry and Technology. London: Applied Science Publishers.

Ertl, G., Knٮ zinger, H. and Weitkamp, J. (1997) Handbook of heterogeneous catalysis. Weinheim: Vch.

Geenen, P. V., Boss, H. J. and Pott, G. T. (1982) A Study of the Vapor-Phase Epoxidation of Propylene and Ethylene on Silver and Silver Gold Alloy Catalysts. Journal of Catalysis, 77(2), 499-510.

Goncharova, S. N., Paukshtis, B. S. and Bal'Zhinnimaev, B. S. (1995) Size effects in ethylene oxidation on silver catalysts. Influence of support and Cs promoter. Applied Catalysis A: General, 126, 67-84.

Grant, R. B. and Lambert, R. M. (1985) A Single-Crystal Study of the Silver-Catalyzed Selective Oxidation and Total Oxidation of Ethylene. Journal of Catalysis, 92(2), 364-375.

Haruta, M. and Date, M. (2001) Advances in the catalysis of Au nanoparticles. Applied Catalysis A: General, 222, 427-437.

Haruta, M., Tsubota, S., Kobayashi, T., Kageyama, H., Genet, M. J. and Delmon, B. (1993) Low-Temperature Oxidation of CO over Gold Supported on TiO_2, α-Fe_2O_3, and Co_3O_4. Journal of Catalysis, 144(1), 175-192.

Hayashi, T., Tanaka, K. and Haruta, M. (1998) Selective vapor-phase epoxidation of propylene over Au/TiO_2 catalysts in the presence of oxygen and hydrogen. Journal of Catalysis, 178(2), 566-575.

Holgado, M. J., Inigo, A. C. and Rives, V. (1998) Effect of preparation conditions on the properties of highly reduced Rh/TiO2 (anatase and rutile) catalysts. Applied Catalysis A: General, 175(1-2), 33-41.

Iizuka, Y., Fujiki, H., Yamauchi, N., Chijiiwa, T., Arai, S., Tsubota, S. and Haruta, M. (1997) Adsorption of CO gold supported on TiO_2. Catalysis Today, 36, 115-123.

Iizuka, Y., Tode, T., Takao, T., Yatsu, K., Takeuchi, T., Tsubota, S. and Haruta, M. (1999) A kinetic and adsorption study of CO oxidation over unsupported fine gold powder and over gold supported on titanium dioxide. Journal of Catalysis, 187(1), 50-58.

Jun, Y., Jingfa, D., Xiaohong, Y. and Shi, Z. (1992) Rhenium as a promoter ethylene epoxidation. Applied Catalysis A: General, 92, 73-80.

Karavasilis, C., Bebelis, S. and Vayenas, C. G. (1996) In situ controlled promotion of catalyst surfaces via NEMCA: The effect of Na on the Ag-catalyzed ethylene epoxidation in the presence of chlorine moderators. Journal of Catalysis, 160, 205-213.

Komuro, M. (1975) Kinetic Studies of Oxygen Chemisorption on Rutile Single-Crystal Surface by Means of Electrical-Conductivity. Bulletin of the Chemical Society of Japan, 48(3), 756-761.

Kondarides, D. I. and Verykios, X. E. (1993) Oxygen Adsorption on Supported Silver Catalysts Investigated by Microgravimetric and Transient Techniques. Journal of Catalysis, 143, 481-491.

Kondarides, D. I. and Verykios, X. E. (1996) Interaction of oxygen with supported Ag-Au alloy catalysts. Journal of Catalysis, 158, 363-377.

Lafarga, D. and Varma, A. (2000) Ethylene epoxidation in a catalytic packed-bed membrane reactor: effects of reactor configuration and 1,2-dichloroethane addition. Chemical engineering science, 55, 749-758.

Lafarga, D., Al-Juaied, M. A., Bondy, C. A. and Varma, A. (2000) Ethylene epoxidation on Ag-Cs/α-Al_2O_3 catalyst: Experimental results and strategy for kinetic parameter determination. Industrial and Engineering Chemistry Research, 39, 2148-2156.

Lee, J. K., Verikios, X. E. and Pitchai, R. (1989) Support and Crystallite Size Effects in Ethylene Oxidation Catalysis. Applied Catalysis, 50, 171-188.

Luo, M.-f., Yuan, X.-x. and Zheng, X.-m. (1998) Catalyst characterization and activity of Ag-Mn,Ag-Co and Ag-Ce composite oxide for oxidation of volatile organic compounds. Applied Catalysis A: General, 175, 121-129.

Mao, C.-F. and Vannice, M. A. (1995a) High surface area α-aluminas III. Oxidation of ethylene, ethylene oxide, and acetaldehyde over silver dispersed on high surface area α-alumina. Applied Catalysis A: General, 122, 61-76.

Mao, C.-F. and Vannice, M. A. (1995b) High surface area α-aluminas II. Adsorption of oxygen, ethylene, carbon dioxide and carbon monoxide on silver dispersed on HSA α-alumina. Applied Catalysis A: General, 122, 41-59.

Matar, S., Mirbach, M. J. and Tayim, H. A. (1989) Catalysis in petrochemical processes. Dordrecht ; Boston: Kluwer Academic Publishers.

Minahan, D. M. and Hoflund, G. B. (1996a) Study of Cs-promoted, α-alumina-supported silver ethylene-epoxidation catalysts: I. Characterization of the support and Cs-prepared catalyst. Journal of Catalysis, 158, 109-115.

Minahan, D. M. and Hoflund, G. B. (1996b) Study of Cs-promoted, α-alumina-supported silver ethylene-epoxidation catalysts: II. Effects of aging. Journal of Catalysis, 162, 48-53.

Minahan, D. M. and Hoflund, G. B. (1996c) Ion-beam characterization of alumina-supported silver catalysts used for ethylene epoxidation. Neclear Instruments and Methods in Physics Research B, 118, 517-521.

Mul, G., Zwijenburg, A., Linder, B. v. d., Makkee, M. and Moulijin, J. A. (2001) Stability and Selectivity of Au/TiO_2 and $Au/TiO_2/SiO_2$ Catalysts in Propene Epoxidation: An in situ FT-IR study. Journal of Catalysis, 201, 128-137.

Nakatsuji, H., Nakai, H., Ikeda, K. and Yamamoto, Y. (1997) Mehcanism of partial oxidation of ethylene on Ag surface: dipped adcluster model study. Surface Science, 384, 315-333.

Nijhuis, T. A., Huizinga, B. J., Makkee, M. and Moulijn, J. A. (1999) Direct epoxidation of propene using gold dispersed on TS-1 and other titanium-containing supports. Industrial & Engineering Chemistry Research, 38(3), 884-891.

Pena, M. A., Carr, D. M., Yeung, K. L. and Varma, A. (1998) Ethylene epoxidation in a catalytic packed-bed membrane reactor. Chemical engineering science, 53(22), 3821-3834.

Podgornov, E. A., Prosvirin, I. P. and Bukhtiyarov, V. I. (2000) XPS, TPD and TPR studies of Cs-O complexes on silver: their role in ethylene epoxidation. Journal of Molecular Catalysis a-Chemical, 158(1), 337-343.

Roatluechai, S., Chavadej, S. and Schwank, J. (2002) Selective Oxidation of Ethylene over Alumina Supported Bimetallic Ag-Au catalysts. submitted to Appl. Catal.

Schneider, M., Duff, D. G., Mallat, T., Wildberger, M. and Baiker, A. (1994) High-Surface-Area Platinum-Titania Aerogels - Preparation, Structural-Properties, and Hydrogenation Activity. Journal of Catalysis, 147(2), 500-514.

Schwank, J. (1983) Catalytic gold: Application of element gold in heterogeneous catalysis. Gold bulletin, 16(4), 103-109.

Seyedmonir, S. R., Plischke, J. K., Vannice, M. A. and Young, H. W. (1990) Ehtylene oxidation over small silver crystallites. Journal of Catalysis, 123, 534-549.

Shastri, A. G., Datye, A. K. and Schwank, J. (1984) Gold Titania Interactions - Temperature-Dependence of Surface-Area and Crystallinity of TiO_2 and Gold Dispersion. Journal of Catalysis, 87(1), 265-275.

Skoog, D. A., Holler, J. F. and Nieman, T. A. (1998) Principles of Instrumental Analysis. United State of America: Thomson Learning, Inc.

Smeltzer, W. W., Tollefson, E. L. and Cambron, A. (1956) Adsorption of Oxygen by a Silver Catalyst. Canadian Journal of Chemistry-Revue Canadienne De Chimie, 34(8), 1046-1060.

Stangland, E. E., Stavens, K. B., Andres, R. P. and Delgass, W. N. (2000) Characterization of gold-titania catalysts via oxidation of propylene to propylene oxide. Journal of Catalysis, 191(2), 332-347.

Tories, N. and Verikios, X. E. (1987) The oxidation of ethylene over silver-based alloy catalysts: 3.Silver-gold alloys. Journal of Catalysis, 108, 161-174.

Uphade, B. S., Okumura, M., Tsubota, S. and Haruta, M. (2000) Effect of physical mixing of CsCl with Au/Ti-MCM-41 on the gas-phase epoxidation of propene using H-2 and O-2: Drastic depression of H-2 consumption. Applied Catalysis A: General, 190(1-2), 43-50.

van Santen, R. A. and de Groot, P. M. (1986) The mechanism of ethylene epoxidation. Journal of Catalysis, 98, 530-539.

Verikios, X. E., Stein, F. P. and Coughlin, R. W. (1980) Influence of Metal Crystallite Size and Morphology on Selectivity and Activity of Ethylene Oxidation Catalyzed by Supported Silver. Journal of Catalysis, 66, 368-382.

Walton, R. M., Gland, J. L. and Schwank, J. W. (1997) Gas sensing characteristics of ultrathin TiO_2-x films investigated with XPS, TPD and in situ resistance measurements. Surface and Interface Analysis, 25(2), 76-80.

Walton, R. M., Dwyer, D. J., Schwank, J. W. and Gland, J. L. (1998a) Gas sensing based on surface oxidation reduction of platinum-titania thin films I. Sensing film activation and characterization. Applied Surface Science, 125 (2), 187-198.

Walton, R. M., Dwyer, D. J., Schwank, J. W. and Gland, J. L. (1998b) Gas sensing based on surface oxidation reduction of platinum-titania thin films II. The role of chemisorbed oxygen in film sensitization. Applied Surface Science, 125(2), 199-207.

Wells, G. M. (1991) Handbook of petrochemicals and processes. Aldershot, Hants, England ; Brookfield, Vt., USA: Gower.

Wu, J. C. and Harriott, P. (1975) The Effect of Crystallite Size on the Activity and Selectivity of Silver Catalysts. Journal of Catalysis, 39, 395-402.

Yeung, K. L., Gavriilidis, A., Varma, A. and Bhasin, M., M. (1998) Effects of 1,2 dichloroethane addition on the optimal silver catalyst distribution in pellets for epoxidation of ethylene. Journal of Catalysis, 174, 1-12.

Yong, Y. S. and Cant, N. W. (1989) Comparative Study of Nitrous Oxide and Oxygen as Oxidants for the Conversion of Ethylene to Ethylene Oxide over Silver. Applied Catalysis, 48, 37-50.

Yong, Y. S. and Cant, N. W. (1990) Ethene Epoxidation over Silver Catalysts in the Presence of Carbon-Monoxide and Hydrogen. Applied Catalysis, 62(2), 189-203.

Zwijenburg, A., Saleh, M., Makkee, M. and Moulijin, J. A. (2002) Direct Gas-Phase Epoxidation of Propene over Bimetallic Au Catalysts. Catalysis Today, 72, 59-62.

Output จากโครงการวิจัยที่ได้รับทุนจาก สกว.

Publications:

1. Rojluechai S., Chavadej S.,Schwank J. W. and Vissanu Meeyoo (2005) “Effect of Gold on Activity of Ethylene Epoxidation over High Surface Area Alumina Support Ag-Au Catalysts” summitted to Catalysis Communication.

Proceedings:

1. Roatluechai S., Chavadej S. and Schwank J. W. (2000) “Selective Oxidation of Ethylene over Supported Ag and Bimetallic Ag-Au Catalysts”, Proceedings of Regional Symposium on Chemical Engineering 2000, Singapore, A-46.
2. Roatluechai S., Chavadej S. and Schwank J. W. (2001) “The Promoted Effect of Au on Ag Catalysts: Selective Oxidation of Ethylene”, Proceedings of the 6th World Congress in Chemical Engineering, Melbourne, Australia.
3. Roatluechai S., Chavadej S. and Schwank J. W. (2002) “Selective oxidation of ethylene over Au/TiO2 Catalysts”, Proceedings of the 9th APCChE Congress, APCChE 2002, Christchurch, New Zealand.

Presentations:

1. Roatluechai S., Chavadej S. and Schwank J. W. (2001) “Selective Oxidation of Ethylene over Supported Ag and Bimetallic Ag-Au Catalysts” , the presentation of RGJ-Ph.D. Congress II, Chonburi, Thailand.
2. Roatluechai S., Chavadej S. and Schwank J. W. (2001) “Selective Oxidation of Ethylene over Supported Ag and Bimetallic Ag-Au Catalysts”, the presentation of the 17th North American Catalysis Society Meeting, Toronto, Canada.
3. Roatluechai S., Chavadej S. and Schwank J. W. (2002) “Nanosized Au/TiO_2 Catalysts for Ethylene Epoxidation”, *Oral Presentation of the 17th Canadian Symposium on Catalysis*, Vancouver, Canada.

APPENDICES

Effect of Gold on Activity of Ethylene Epoxidation over High Surface Area Alumina Support Ag-Au Catalysts

Siriphong Rojluechai[a], Sumaeth Chavadej[a,*], Johannes W. Schwank[b], Vissanu Meeyoo[c]

[a]The Petroleum and Petrochemical College, Chulalongkorn University, Bangkok 10330, Thailand.
[b]Department of Chemical Engineering, The University of Michigan, Ann Arbor, MI 48109, U.S.A.
[c]Department of Chemical Engineering, Mahanakorn University, Bangkok, Thailand.

Abstract

In this study, the effect of gold on the ethylene epoxidation activity of Ag/Al_2O_3 catalysts was investigated. It was found that by forming Ag-Au bimetallic resulted in a weakening Ag-O bond. Gold was found to act as a diluting agent on silver surface and created new single silver sites which favor molecular oxygen adsorption leading to better ethylene oxide selectivity. The optimum Ag to Au ratio was reported a 13.18:0.63. The formation of Ag/Au alloy was found to decrease the reaction selectivity.

Keywords:

Silver catalyst, Ag-Au bimetallic, ethylene oxide, ethylene epoxidation

* Corresponding author:
E-mail : sumaeth.c@chula.ac.th
Fax : 662-215-4459

1. Introduction

Typically, silver on low surface area inert supports was used for the ethylene epoxidation for decades but yield provide low selectivity and activity. By introducing electronegative moderators to the catalyst, selectivity of ethylene oxide was improved. The moderators, which are known to improve the selectivity of silver are Cl, Br, I, S, Se, Te, P and Bi. Chlorine is the most commonly used moderator added in the form of organic chlorides such as 1, 2-ethylene dichloride with a low concentration of a few parts per million. The role of the moderator is thought to change not only the relative concentrations of atomic and molecular oxygen, but also to increase the probability of molecular oxygen to react with ethylene to form ethylene oxide. Moreover, the role of promoters is also significant to stabilize silver against sintering [1].

Rhenium and Cesium are other alternative promoters for epoxidation reaction. The effect of Rhenium is to weaken the silver-oxygen bond, and to reduce the electron density of the adsorbed oxygen, which could be the reason for the enhancement of the selectivity of ethylene oxide [2]. Moreover, it has been found that for high surface area α-alumina, addition of Cesium contributes to the neutralization of surface acidity which promotes complete combustion [3]. Cesium adding likely stabilizes the defects on the Ag surface, where electrophilic oxygen is probably localized. On the other hand, it can decrease the concentration of nucleophilic oxygen (surface Ag_2O), which is responsible for the deep oxidation of C_2H_4 [4].

With Regard to the role of gold, Kondarides and Verykios [5] concluded that alloying Ag with Au influenced the bond strengths of oxygen with the silver surface.

which resulted in modifying the relative population of the adsorbed species. The results confirmed the presence of three adsorbed species of oxygen at elevated temperatures, namely molecular, atomic and subsurface. In the oxidation of ethylene, Geenen *et al.* [6] reported that the selectivity to ethylene oxide decreased sharply with increasing gold content of Ag-Au alloy on α-alumina support. On gold rich alloys no ethylene oxide was formed, the only products being carbon dioxide and water. The reason is that the reaction of ethylene with O_2^- results only in ethylene oxide if the adsorbed complex is sterically hindered by adjacent adsorbed species, such as O^{2-} or Cl^-, such that abstraction of hydrogen from the ethylene molecule in the way depicted above cannot occur. In the case of the alloys, the O_2^- species are separated from one another and hence the adsorbed ethylene complex will react to form carbon dioxide and water.

In this paper, we investigated the role of gold on the catalytic activity of silver catalysts over ethylene epoxidation. High surface area alumina was used as a support aiming to clearly investigate the interaction between Au and Ag.

2. Experimetal

2.1 Catalyst preparation

In this work, silver catalysts were prepared by the incipient wetness method using aluminum oxide (fumed alumina, Degussa C, 85-115 m^2/g) with silver nitrate solution to achieve a nominal silver loading of 14 wt%. Then, the Ag catalyst was impregnated with different amounts of chloauric acid ($HAuCl_4$, Aldrich) solution having different

concentrations to achieve nominal gold loadings of 0.3, 0.5, 0.7 and 1.0 wt%. Then, the catalyst samples were dried overnight in an oven at 110°C followed by calcination in air at 500°C for 5 h.

2.2 *Catalyst characterization*

Specific surface areas of catalyst sample prepared were determined by N_2 adsorption at 77 K (BET method) using a surface area analyzer (Quantachrome, Autosorb 1). Prior to the analysis, the samples were outgased at 250°C for 3 h. Metal contents in the samples were analyzed by an atomic adsorption spectrophotometer (Varian, Spectr AA-300).

The structure of samples were examined by X-ray diffraction (XRD) on a Rigaku RINT 2000 diffractometer equipped with a Ni filtered Cu Kα radiation source (λ= 1.542 Å) of 40 kV and 30 mA. Then, the catalyst samples were scanned in the range of 2θ from 20° to 90° in the continuous mode with a rate of 5° min^{-1}.

The morphology of the samples was also investigated under a transmission electron microscope (TEM) (JEOL, 2010) operating at 200 kV.

Temperature programmed desorption (TPD) experiments were carried out by placing 100 mg of catalyst into a U-tube quartz reactor. The catalyst was pretreated in a flow of O_2 (8% O_2/N_2) at 200°C for 1 h. Then, it was flushed with N_2 for 0.5 h in order to remove the gas phase of O_2. After that, the reactor temperature was ramped from 200°C to 600°C with a linear heating rate of 40°C min^{-1} in flowing of N_2 (30 ml min^{-1}). The desorbing oxygen was detected by a thermal conductivity detector.

2.3 Ethylene oxidation reaction experiment

The ethylene oxidation reaction was conducted in a differential flow reactor, which was operated at 24.7 psia. Typically, 30 mg of catalyst was placed inside a Pyrex tube and secured with Pyrex glass wool plugs. The tubular reactor having 10 mm in diameter was placed in a furnace equipped with a temperature controller. The catalyst was initially pretreated with oxygen at 200°C for 2 h in order to diminish all impurities and remove residual moisture from the catalyst. The feed gas was a mixture of 15% oxygen in helium, 30% ethylene in helium and pure helium (HP grade) obtained from Thai Industrial Gas (TIG). The flowrates of these three gas streams were regulated by mass flow controllers to obtain a feed gas composition of 6% oxygen and 6% ethylene with helium balance. The feed gas was passed through the reactor at a constant space velocity of 6,000 h^{-1} and the temperature was varied from 220 to 270°C. Exit gases were analyzed by using an on-line gas chromatograph (HP, 5890 Series II) equipped with a HaYeseb D 100/120-packed column, capable of separating carbon dioxide, ethylene and oxygen. The ethylene oxide product was calculated from the carbon material balance with 0.25% carbon atom error [7, 8]. Moreover, the calculated values of ethylene oxide produced were confirmed by performing O_2 mass balance with 0.3% oxygen atom error.

3. Results and discussion

3.1 BET, XRD and TEM Characterization

The BET surface areas of the catalysts are shown in Table 1. It was found that the surface areas of the catalysts are similar to that of the blank support and in the range of 90 to 100 m^2/g. This may imply that both Ag and Au are evenly dispersed on the surface of support. The use of high surface area alumina in this study aims to clearly investigate the interaction between Ag and Au under electron microscope.

The results from TEM analysis show that Ag particles are highly dispersed on the alumina support with the average particle size of ca 40 nm as shown in Fig. 1a. The addition of Au on the Ag/Al_2O_3 catalysts resulted in formation of small particles of Au on the Ag particles with a particle size of 2-3 nm for low Au loadings (Fig. 1b-1c). At the Au loading above 0.54:13.18 wt%, there was an evidence of large Au particles (about 40 nm) formed adjunct to Ag particles. This leads to a speculation that high Au loading may cause alloy formation between Au and Ag (Fig. 1d-1e). [5] reported an evidence of alloy formation at an Au:Ag ratio 1:10, as in our case around 1:9.

XRD patterns of the studied catalysts (Fig. 2) showed a typical fcc phase of Ag showing visible tailing at about 29. 33, 48 and 60° (2θ) which represent the indices of (111), (200), (220) and (311). The presence of Au does not alter the typical XRD pattern. Only a slight change in 2θ of 29° was found in the case of high Au loading. This seems to

indicate an alloy formation between Au and Ag, agreeing with the results from TEM analysis.

The mean measured crystallite sizes of the Au-Ag catalysts are in the range of 18-18.6 nm (Table 2) indicating that gold addition does not significantly affect the crystallite size of Au-Ag catalysts.

3.2 Temperature programmed desorption (TPD) results

Temperature programmed desorption was carried out to investigate the interaction between oxygen and the catalyst surface. Doping Ag with a small amount of Au results in decreasing desorption temperature from 350°C to 300°C as shown in Fig. 3. This indicates that the interaction between silver and oxygen is weakened in the presence of gold. The presence of Au atoms has been found to affect the electronic properties of Ag [5, 9]. In general, the dissociative adsorption of oxygen on Ag requires a charge transfer from Ag to oxygen. Hence, it is not unexpected that the electron deficiency induced on Ag atoms by the presence of neighboring Au atoms would result in weakening the Ag-O bond. Thus, it is more likely that oxygen adsorption on the Ag catalyst is as molecular oxygen when a small amount of Au present. As shown in Table 3, the amount of oxygen adsorbed on the catalysts decreases with increasing Au content. The result confirms that under the presence of small amounts of Au on Ag the catalyst, the interaction between gold and silver affects significantly the oxygen adsorption. The added Au simply weakens the bond strength between silver and oxygen [5].

3.3 Catalyst activity for epoxidation of ethylene

The catalytic epoxidation of ethylene was carried out over Ag/Al_2O_3 and Au doped Ag/Al_2O_3 catalysts at the temperature range of 200-300°C. The results showed that the catalytic activity of the Ag/Al_2O_3 catalyst increases with increasing Au loading. As shown in Fig. 4, for any given Au loading on Ag/Al_2O_3 catalyst, the ethylene conversion is low at the temperature between 220-255°C but increases drastically when the reaction temperature increases above 255°C. On the contrary, the ethylene oxide selectivity decreases with increasing reaction temperature and is very pronounced when the temperature is above 240°C. This might be due to the fact that total oxidation of ethylene is favor at high temperatures, owing to more accessible dissociated oxygen. Fig. 5 illustrates the effect of Au loading on the Ag/Al_2O_3 catalyst on ethylene epoxidation reaction. The ethylene oxide selectivity slightly increased with increasing Au loading up to 0.63 wt% and it decreased with increasing Au loading above 0.63 wt%. The results indicate that an addition of gold on Ag catalyst can promote the ethylene epoxidation reaction by weakening Ag-O bond and the optimum Au loading is ca. 0.63 wt% on 13.18 wt% Ag/Al_2O_3. Above this point a decrease in oxygen adsorption capacity results in a decreasing activity.

4. Conclusions

In conclusion, it was found that gold acts as a diluting agent on the silver surface and creates new single silver sites which favor molecular oxygen adsorption leading to

enhancement of epoxidation reaction. Adding a small amount of gold on silver catalyst is to form a bimetallic species which has a lower electron density at the surface resulting increasing its capacity for chemisorption of electron acceptor species. Au-Ag alloy was found to be less active than bimetallic catalysts.

Acknowledgements

The authors would like to gratefully acknowledge The Royal Golden Jubilee Ph.D. Program and Basic Research Grant for Royal Golden Jubilee Program, The Thailand Research Fund for supporting both partial research expense and scholarship for Mr.Siriphong Rojluechai. The Research Unit of Petrochemical and Environmental Catalysis under the Ratchadapisakesompok Fund, Chulalongkorn University and The petroleum and Petrochemical Consortium under The Ministry of Education are also acknowledged for partially financial support and providing all analytical instruments. The microscopy work carried out at the National Metal and Materials Technology Center is also acknowledged.

References

[1] S. Matar, M. J. Mirbach, H. A. Tayim, Catalysis in petrochemical processes, Kluwer Academic Publishers, Dordrecht ; Boston, 1989, p. 85.

[2] Y. Jun, D. Jingfa, Y. Xiaohong, Z. Shi, Appl. Catal. A 92 (1992) 73.

[3] C.-F. Mao, M. A. Vannice, Appl. Catal. A 122 (1995) 61.

[4] S. N. Goncharova, B. S. Paukshtis, B. S. Bal'Zhinnimaev, Appl. Catal. A 126 (1995) 67.

[5] D. I. Kondarides, X. E. Verykios, J. Catal. 158 (1996) 363.

[6] P. V. Geenen, H. J. Boss, G. T. Pott, J. Catal. 77(2) (1982) 499.

[7] D. Lafarga, M. A. Al-Juaied, C. A. Bondy, A. Varma, Ind. Eng. Chem. Res. 39 (2000) 2148.

[8] K. L. Yeung, A. Gavriilidis, A. Varma, M. Bhasin, M., J. Catal. 174 (1998) 1.

[9] N. Tories, X. E. Verikios, J. Catal. 108 (1987) 161.

Fig. 1. TEM micrographs of 13.18% Ag/Al_2O_3 at various gold loadings: (a) 0%Au; (b) 0.27%Au; (c) 0.54%Au; (d) 0.63%Au; (e) 0.93%Au.

Fig. 2. XRD patterns of the Ag/Al_2O_3 catalysts at various gold loadings.

Fig. 3. TPD profiles of O_2 of 13.18% Ag/Al_2O_3 at various gold loadings and 0.79% Au/Al_2O_3.

Fig. 4. Ethylene conversion and Ethylene oxide selectivity for 13.18%Ag/Al_2O_3 at various gold loadings at space velocity of 6,000 h^{-1}, P = 10 psig and 6% O_2 and 6% C_2H_4 balance with He.

Fig. 5. Turnover number of ethylene epoxidation at various gold loadings on 13.18% Ag/Al_2O_3 (reaction rate obtained with various gold (R_1) over obtained at 13.18% Ag/Al_2O_3 (R_0)) at space velocity of 6,000 h^{-1}, P = 10 psig, T = 240°C and 6% O_2 and 6% C_2H_4 balance with He.

Table 1. BET surface area of Ag and Au-Ag catalysts.

Table 2. Mean crystallite sizes of Ag and Au-Ag catalysts.

Table 3. Amount of total oxygen desorption and oxygen desorption in the range of 200-300°C for Ag and Au-Ag catalysts.

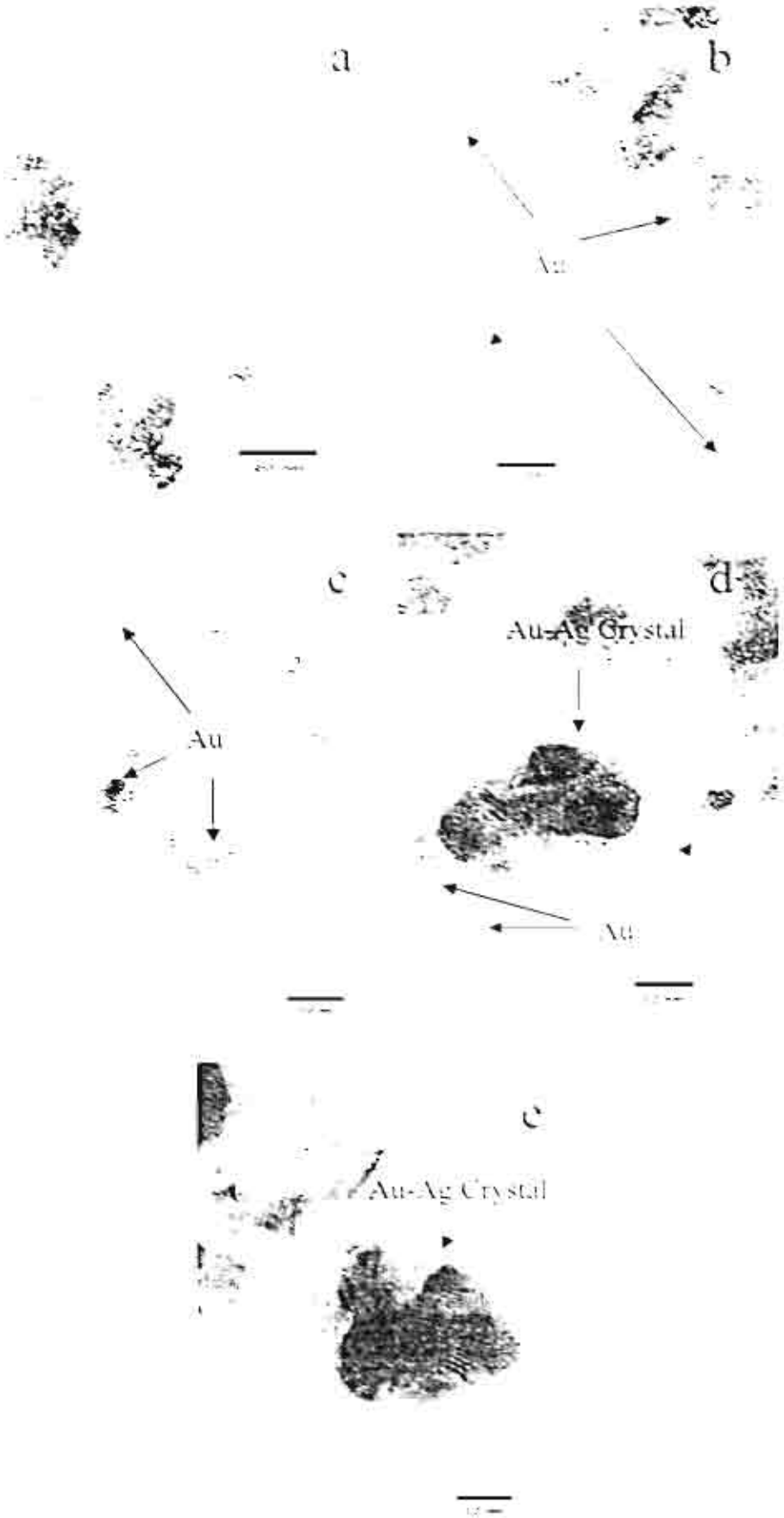
a
b
Au
c
d
Au-Ag Crystal
Au
Au
e
Au-Ag Crystal

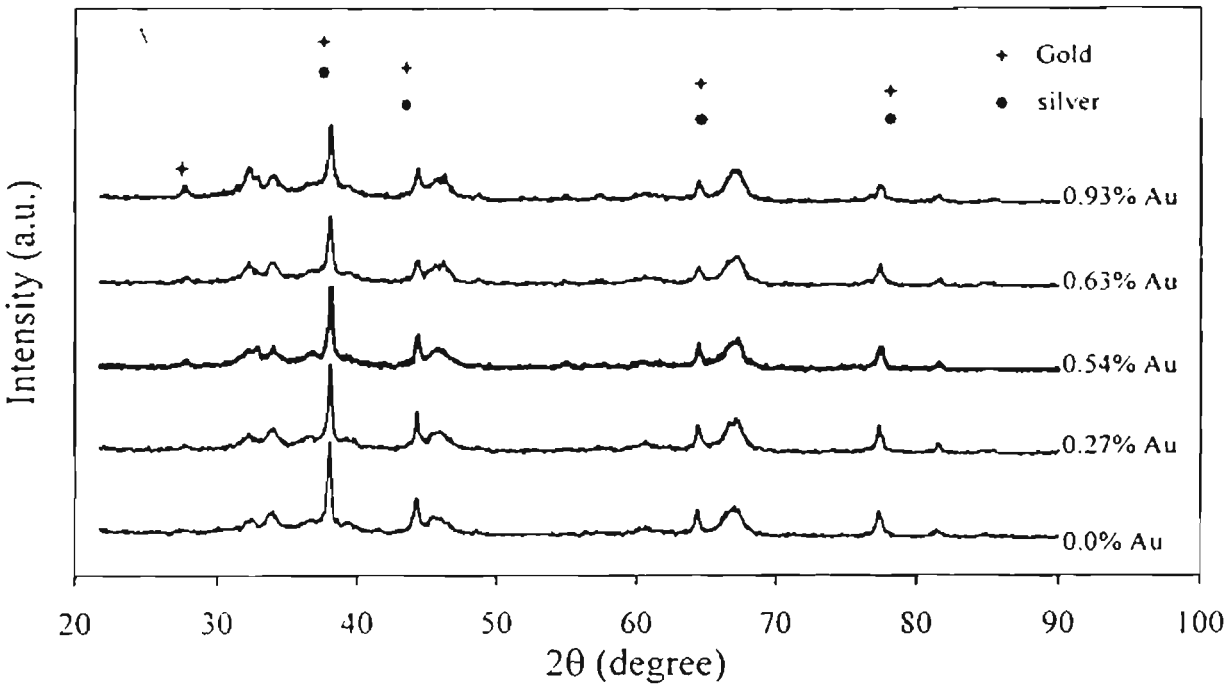
Gold
silver
0.93% Au
0.63% Au
0.54% Au
0.27% Au
0.0% Au
Intensity (a.u.)
20
30
40
50
60
70
80
90
100
2θ (degree)

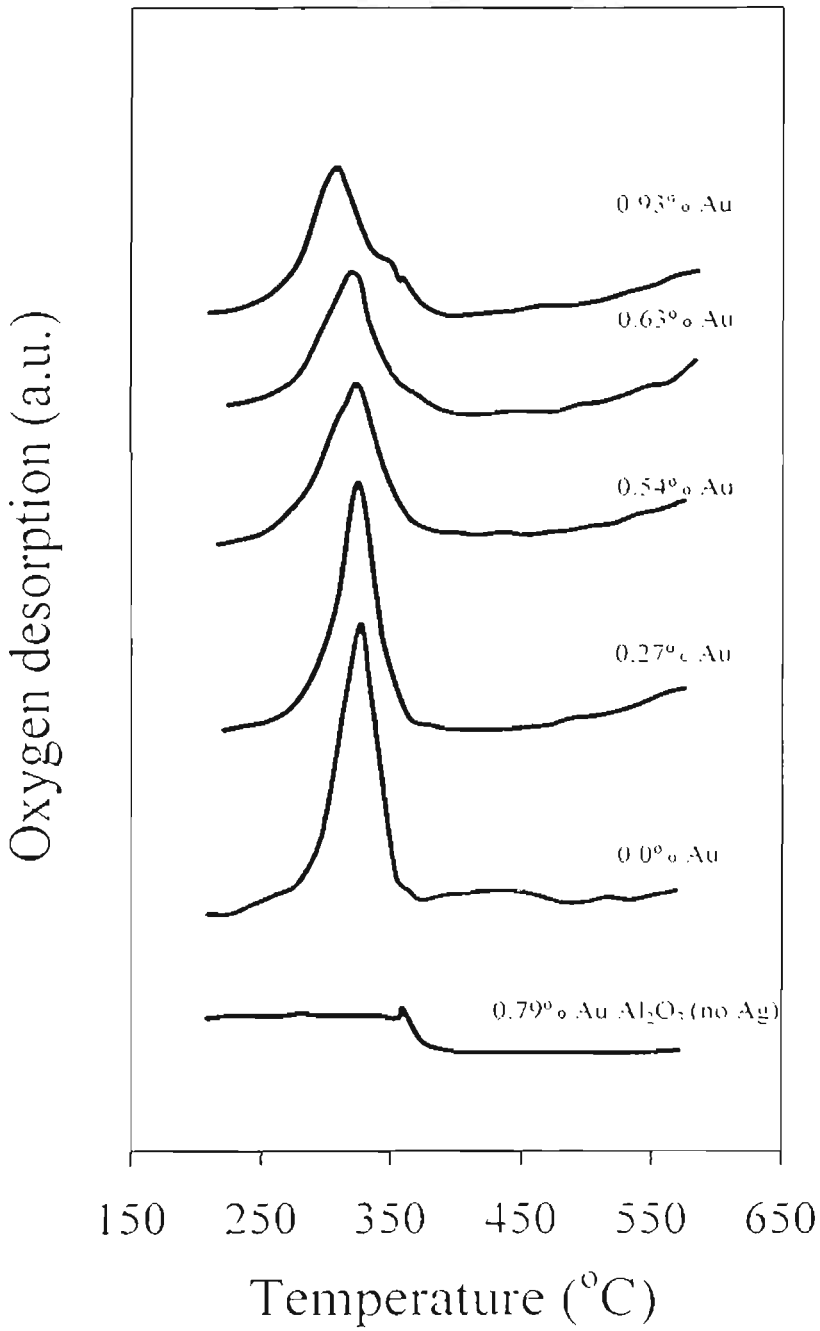
0.93% Au
0.63% Au
0.54% Au
0.27% Au
0.0% Au
0.79% Au Al2O3 (no Ag)
Oxygen desorption (a.u.)
150
250
350
450
550
650
Temperature (°C)

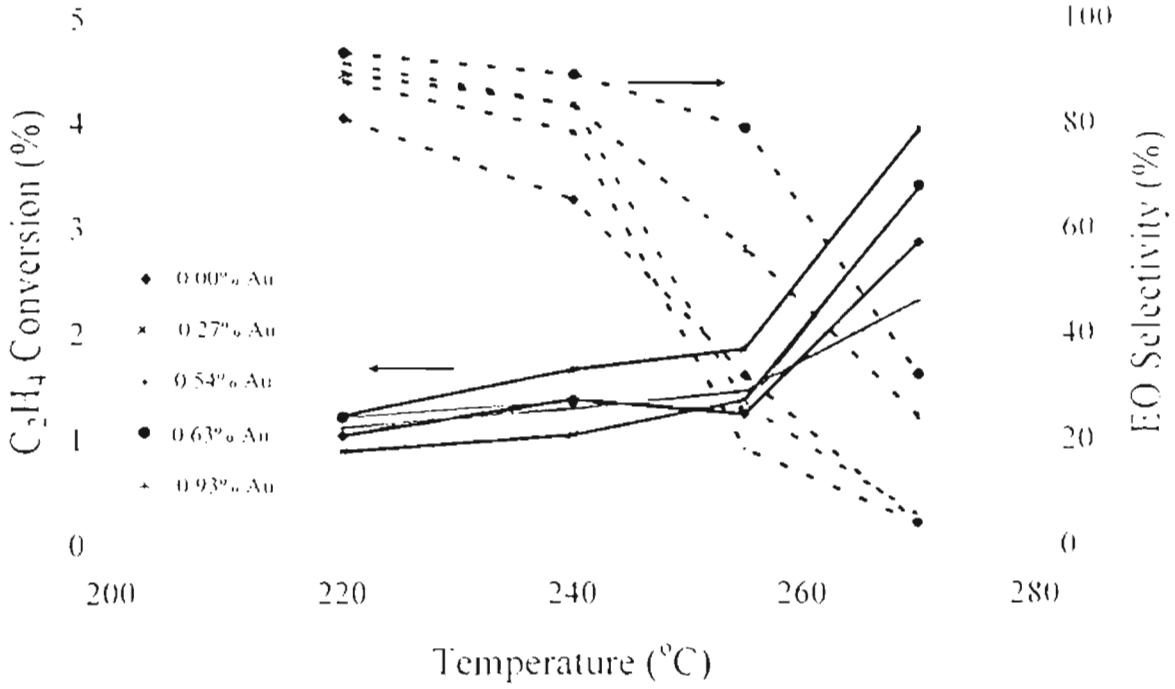
C_2H_4 Conversion (%)
EO Selectivity (%)
0.00% Au
0.27% Au
0.54% Au
0.63% Au
0.93% Au
0
1
2
3
4
5
0
20
40
60
80
100
200
220
240
260
280
Temperature (°C)

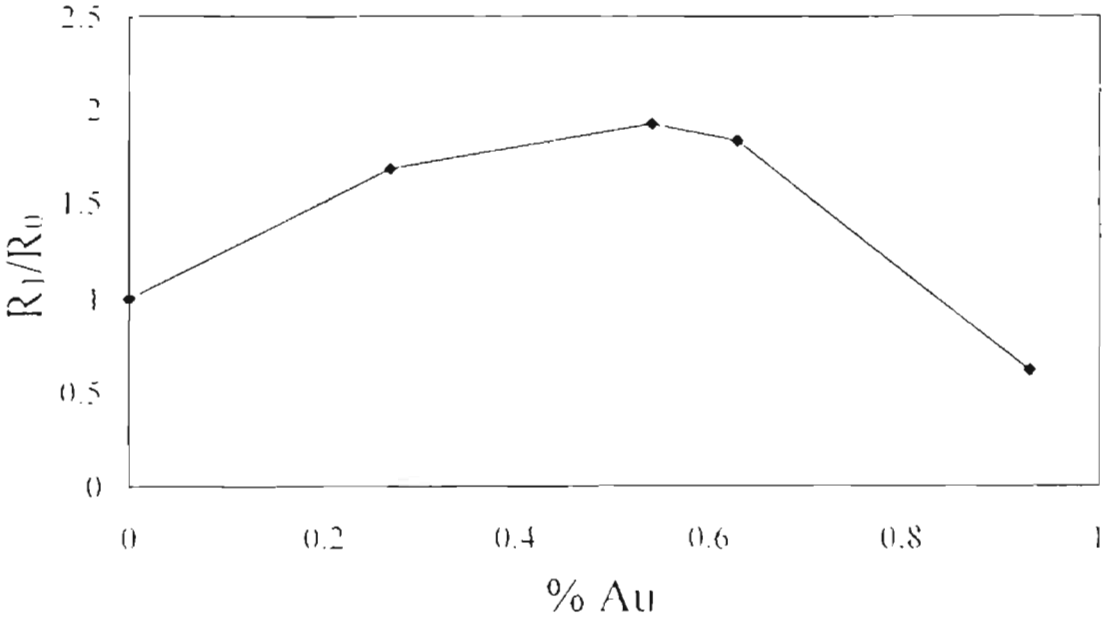
2.5
2
1.5
1
0.5
0
R_1/R_0
0
0.2
0.4
0.6
0.8
1
% Au

Catalyst	BET Surface Area, m^2/g
Degussa-Al_2O_3	98
13.18% Ag/Al_2O_3	90
0.27% Au-13.18% Ag/Al_2O_3	90
0.54% Au-13.18% Ag/Al_2O_3	89
0.63% Au-13.18% Ag/Al_2O_3	101
0.93% Au-13.18% Ag/Al_2O_3	99

Catalyst	Mean crystallite size, nm
13.18% Ag/Al_2O_3	19.2
0.27% Au-13.18% Ag/Al_2O_3	18.6
0.54% Au-13.18% Ag/Al_2O_3	18.3
0.63% Au-13.18% Ag/Al_2O_3	18.6
0.93% Au-13.18% Ag/Al_2O_3	18.0

Catalysts	Total oxygen desorption ($x10^{-7}$ mole/g catalyst)
0.00% Au-13.18% Ag/Al_2O_3	2200
0.27% Au-13.18% Ag/Al_2O_3	2017
0.54% Au-13.18%Ag/Al_2O_3	1943
0.63% Au-13.18%Ag/Al_2O_3	1870
0.93% Au-13.18%Ag/Al_2O_3	1393